

## ABSTRACT

Investigations of the effects of insulin on skeletogenesis in the embryonic chick have been carried out. A single injection of insulin early in development leads to dwarfism and disproportionate shortening of hindlimb bones. The growth rate of the tibiotarsus is reduced, the number of hypertrophic chondrocytes is increased, and there is significantly less matrix per cartilage cell. Insulin-treated tibiotarsi are frequently bent and develop cartilaginous necroses. Chondrocyte glycogen is not affected, but there is evidence of loss of cartilage matrix sulphate immediately prior to full degeneration and cell death. Alkaline phosphatase and cartilage calcification occur precociously and more extensively in insulin-treated tibiotarsi. Subperiosteal ossification and marrow cavity formation become accelerated. The relationship of insulin-induced pathologies to other skeletal disturbances is discussed. The alterations of cartilage from insulin-treated tibiotarsi are postulated to be the result of augmented lysosome activity and alterations in the Golgi complex.

Author: ALBERT RABINOVITCH

Thesis Title: ANATOMICAL, HISTOLOGICAL AND HISTOCHEMICAL STUDIES OF  
NORMAL AND INSULIN-INDUCED ABNORMAL DEVELOPMENT OF THE  
EMBRYONIC TIBIOTARSUS IN GALLUS DOMESTICUS.

Department: ZOOLOGY

Degree: MASTER OF SCIENCE

Date: JULY 1969

## ABSTRAIT

Les recherches des effets de l'insuline ont été faites sur la squeletogénèse chez l'embryon du poulet. Une seule injection d'insuline dans les débuts du développement produit le nanisme et un écourtement disproportionné des os des pattes postérieures. La vitesse du développement du tibia est réduite, le nombre des cellules gonflées du cartilage est accru, et, les statistiques montrent moins de matrice par cellule cartilagineuse. Les tibias traités à l'insuline sont fréquemment courbés et développent des nécroses cartilagineuses. Le glycogène des cellules du cartilage n'est pas altéré, mais il y a évidence de perte des sulphates de la matrice cartilagineuse immédiatement avant la dégénération complète et la mort des cellules. La phosphatase alcaline et la calcification du cartilage se rencontrent précocément et de façon plus extensive dans les tibias traités à l'insuline. L'ossification sous périostée et la formation de la cavité de la moelle s'accélèrent. Les relations de l'état pathologique produit par l'insuline, à d'autres désordres du squelette sont discutées. Les altérations du cartilage des tibias traités à l'insuline sont postulées d'être le résultat de l'activité augmentée des lysosomes et des altérations du complexe de Golgi.

Auteur: ALBERT RABINOVITCH

Titre de la thèse: ETUDE ANATOMIQUE, HISTOLOGIQUE ET HISTOCHIMIQUE DU DEVELOPPEMENT NORMAL ET ANORMAL PAR LE TRAITEMENT A L'INSULINE, DES TIBIAS CHEZ LES EMBRYONS DU POULET DOMESTIQUE.

Département: ZOOLOGIE, UNIVERSITE MCGILL.

Dégré: MAITRISE EN SCIENCES.

Date: JUILLET 1969.

**SHORT TITLE**

NORMAL AND INSULIN-INDUCED ABNORMAL TIBIOTARSAL HISTOGENESIS

Name: ALBERT RABINOVITCH

Department: ZOOLOGY

Degree: MASTER OF SCIENCE

Date: JULY 1969

ANATOMICAL, HISTOLOGICAL AND HISTOCHEMICAL STUDIES  
OF NORMAL AND INSULIN-INDUCED ABNORMAL DEVELOPMENT  
OF THE EMERYONIC TIBIOTARSUS IN GALLUS DOMESTICUS

by

ALBERT RABINOVITCH, B. SC.

A thesis submitted to the Faculty of Graduate  
Studies and Research in partial fulfillment of  
the requirements for the degree of Master of Science

Department of Zoology

McGill University

July 1969



## ACKNOWLEDGEMENTS

The author wishes to express his appreciation to Dr. D.M. Steven and Dr. J.R. Marsden, former and present Chairman of the Department of Zoology, respectively, for provision of study and research space, as well as for access to the materials required for this research project.

The author also thanks his academic supervisor, Dr. M.A. Gibson, presently of the Department of Biology, Acadia University, for suggesting this project and for allowing the author full freedom in the approaches used. His kindness in reading the manuscript prior to submission is also gratefully acknowledged.

A special note of thanks to Dr. N. Wolfson and Dr. C. Vowinckel of the McGill Zoology Department and Mrs. M. Clark for assistance with translations of Italian and German publications relevant to this work.

Financial indebtedness is due to the National Research Council of Canada for support with a Student Bursary and through Operating Grants to Dr. Gibson. In addition, a Phillip Carpenter Fellowship in Zoology was held for one summer of this study.

Finally, but of prime importance, is the unending assistance given to me by my wife Shelly. In addition to the more mundane tasks of trimming and pasting photographs, she provided much of the stimulus behind the project and served as a continuing source of encouragement and support.

## TABLE OF CONTENTS

ACKNOWLEDGEMENTS . . . . .	ii
INTRODUCTION AND LITERATURE SURVEY . . . . .	1
MATERIALS AND METHODS . . . . .	17
Introduction . . . . .	17
Injection Protocol . . . . .	17
Anatomical Preparations . . . . .	19
Histological and Histochemical Preparations . . . . .	20
Photography . . . . .	25
Tibiotarsal Lengths . . . . .	25
Hypertrophic Cell Size and Matrix/Cell Studies . . . . .	26
RESULTS AND DISCUSSION . . . . .	28
I - OBSERVATIONS AND ANALYSIS . . . . .	28
Dosage and Timing of Injection Studies . . . . .	28
Results of Injection at Preferred Dose and Time . . . . .	30
Non-Skeletal Deformities Among Insulin-Treated Embryos . . . . .	31
Non-Micromelic Skeletal Anomalies . . . . .	32
Gross Anatomy and Calcification . . . . .	33
Figures . . . . .	36
Tibiotarsus Lengths . . . . .	44
Cell Diameters, Areas and Amount of Matrix/Cell . . . . .	46
Histology and Cartilage Matrix Histochemistry . . . . .	48
Growth plate and epiphyseal cartilage . . . . .	48
Cartilage resorption and marrow cavity formation . . . . .	52

Joint formation . . . . .	53
Tibiotarsal angulations . . . . .	54
Figures . . . . .	56
Glycogen . . . . .	71
Figures . . . . .	75
Microscopic Calcification and Ossification . . . . .	81
Figures . . . . .	86
Alkaline Phosphatase . . . . .	95
Figures . . . . .	99
II - RELATIONSHIP TO OTHER PATHOLOGIES . . . . .	103
III - NATURE OF THE CARTILAGE DEGENERATION . . . . .	109
SUMMARY . . . . .	114
APPENDICES . . . . .	117
TABLES . . . . .	129
BIBLIOGRAPHY . . . . .	147

## INTRODUCTION AND LITERATURE SURVEY

The development of the embryonic chick hindlimb has been eloquently described as early as 1883 (Johnson), but this particular study was largely on the macroscopic level, and included only the 4th to 8th days of incubation.

A highly extensive and comprehensive consideration of the histological and cytological events during long bone formation in chicks was given by one of the pioneers in the field of bone and cartilage research, Dame Honor B. Fell (1925). Considering the limitations in the equipment of that day, it is truly remarkable to consider that many of her cytological observations have been "re-discovered" and confirmed by electron microscopic studies in recent years. Her work formed much of the foundation of present knowledge of avian endochondral ossification.

As Pappas (1968) has pointed out:

Virtually all known drugs, chemicals and physical measures, if administered in the proper dosage to the appropriate animal at a susceptible developmental stage, have the potential of inducing changes in the developmental pattern of the embryo. Congenital malformations are most likely to occur if teratogenic agents are introduced during the critical developmental period of rapid chemical and morphologic differentiation. The teratogen interrupts the morphologic development by inhibiting specific preprogrammed embryonic potential.

The discovery that insulin, a hormone produced by the beta cells of the pancreatic islets of Langerhans, could serve as a teratogen with respect to avian skeletogenesis must be credited to Walter Landauer who, in a vivid and detailed series of studies extending over the past two decades has contributed the bulk of current

knowledge on the subject.

In a first report (Landauer, 1945), he injected White Leghorn and Creeper eggs with 2 units of a commercial insulin preparation prior to incubation, and obtained relatively high incidences of rumplessness (41.6% and 17.1% respectively, indicating a differential response of stocks). In his own words, "This appears to be the first recorded instance of a morphogenetic effect of insulin", and suggested its cause to lie with an interference of embryonic carbohydrate metabolism. He also tested the effects of cystine and glutamic acid, two amino acids present in high concentrations in the insulin molecule (West et al, 1966), and excluded them from any major role in the genesis of this deformity of caudal vertebrae.

In a subsequent paper (Landauer and Lang, 1946), experiments were performed with inactivated and reactivated insulin, and the effects of injection at various embryonal stages was examined. Oxidation of the disulphide bonds of insulin with iodine (irreversibly inactivated) abolished its rumplessness-inducing properties, while treatment with acid alcohol (reversible inactivation) led to a higher deformity frequency, possibly due to reactivation of the insulin within the yolk. Alkali reactivation of the reversibly inactivated insulin yielded a rumplessness frequency slightly higher than untreated active insulin. These results stressed the importance of integrity of the insulin disulphide bonds and of the insulin molecule as a whole for teratogenic purposes. A series of dosages from 0.05 to 5 International Units, given within the period of 0-72 hours of incubation (Landauer and Bliss, 1946) showed that the teratogenic response of rumplessness increased with dosage,

and reached a frequency peak at 31 hours\*.

Caudal defects, however, were not the only abnormalities that could be elicited from insulin treatment. A later study (Landauer, 1947a) demonstrated that injection of the insulin into the yolk between 64 and 168 hours led to significant incidences of micromelia of all limbs, buphthalmia (eye enlargement), polydactyly, and beak defects (shortened, arched upper beak). The micromelic response was stronger in the legs than in the wings, and all limbs were maximally deformed after injection between 120 and 135 hours.

Later that same year, Landauer (1947b) studied the effects of adrenal cortical extract on insulin teratogenicity, and found that the extract did not alter rumplessness frequency from insulin, but did potentiate the micromelic response to insulin injection at 120 hours. Adrenal cortical extract, given alone, produced a generalized dwarfism without specific skeletal malformations. Landauer also noted that epinephrin (adrenalin) did not appear to be a teratogen itself, nor did it affect embryonal development when given together with insulin.

It is appropriate at this point to mention that beta cells of the islets of Langerhans cannot be histologically demonstrated in the chick embryo before the 11th or 12th day of incubation, and bioassays reveal the presence of pancreatic insulin from the 12th day onwards. Also, there is no insulin in the egg yolk (Grillo, 1961).

Zwilling (1948b) examined the relationship between micromelic and hypoglycemic responses to insulin. He found that a single injection of insulin at 120 hours led to a pronounced hypoglycemia lasting until about day 14 of incubation, and further, that as the depth and

\* "hours" will always refer to hours of incubation, unless otherwise specified.

duration of the hypoglycemia increased, so did the severity of the disproportionate limb shortness. At that time, he stated: "Whether the micromelia is caused by the drop in blood sugar, whether the reverse is true or whether these are merely parallel events still remains to be clarified". In an ensuing report (Zwilling, 1951), he determined that the hypoglycemic effect of insulin in this system is mediated via an inhibition of glycogenolysis in the yolk-sac membrane (the avian yolk-sac membrane is known to function as a sort of "transitory liver" during early embryonic development).

Landauer (1948) examined the interactions of nicotinamide and alpha-ketoglutaric acid with insulin in producing skeletal malformations. He observed that simultaneous injection of nicotinamide and insulin led to a reduction in incidence of both micromelia and rumplessness. Alpha-ketoglutaric acid protected against micromelia to a somewhat lesser extent, yet did not reduce rumplessness resulting from an early exposure to insulin. Neither of these two compounds is teratogenic.

Zwilling (1949), continuing analysis of the relationship of hypoglycemia to observed deformities, found that nicotinamide and alpha-ketoglutaric acid, in addition to alleviating micromelia (Landauer, 1948), also reduced the hypoglycemia caused by insulin, nicotinamide being the more effective in this regard. Whether the beneficial effects of these two compounds lies in restoration of normal blood sugar levels, or whether the effect is a more direct one on the enzyme systems of the affected tissue was still uncertain. At any rate, these results underlined his premise that "carbohydrate metabolism is of considerable importance for normal limb formation in chick embryos".

Treatment with sulfanilamide (Zwilling and DeBell, 1950) led to a micromelia macroscopically similar to the insulin syndrome, and this effect of both substances could be reversed with nicotinamide. Since sulfanilamide does not alter embryonic blood sugar levels, it was suggested that the insulin-induced hypoglycemia is probably not a direct cause of the micromelia, but rather that decreased glucose availability leads to an increased requirement for nicotinamide adenine dinucleotide (NAD, DPN, coenzyme I). Thus, supplementary treatment with nicotinamide can presumably offset the NAD deficiency created by treatment with either sulfanilamide or insulin, since nicotinamide could be used towards the synthesis of new NAD and NADP (NAD-phosphate, TPN, coenzyme II).

The first histological comparisons of normal bones and insulin-induced micromelic bones were those of Duraiswami (1950). Using Brown Leghorn eggs, and dosages of 0.05 to 6 units of crystalline insulin in distilled water, he described (in surviving 20-day embryos) pathological fractures, stunted growth, and lack of subperichondral ossification. These observations led him to conclude that the disturbance was a type of osteogenesis imperfecta. A further feature of the insulin-treated tibiotarsi was an apparently reduced chondroitin sulphuric acid content of the cartilage, as indicated by metachromatic staining with toluidine blue. He concluded that " unchecked insulin hypoglycaemia during the early stages of development may adversely affect the development of the cartilaginous skeleton . . . by depriving them of their essential constituent mucoprotein ".

Somewhat later (Duraiswami, 1952) he confirmed his earlier findings and, in addition, reported areas of "muroid degeneration" in the



cartilages of femur, tibiotarsus and acetabulum. These degenerative areas were also seen to extend across the tibiofemoral joint space, so that normal joint formation was impaired. Associated with the lack of subperiosteal ossification was a thickening of the periosteum, a condition seen in human osteogenesis imperfecta. Although his staining techniques included toluidine blue for mucopolysaccharides and periodic acid-Schiff (PAS) for polysaccharides and glycogen, he neither discussed nor presented micrographs of PAS-stained tissues.

Tests with a variety of substances (Landauer and Rhodes, 1952) including nicotinamide, glucose-1-phosphate, pyruvic acid, oxalacetic acid, lactic acid, citric and isocitric acids, sodium succinate, 1-glutamic acid hydrochloride, 3-hydroxy-anthranilic acid, and various inhibitors of anaerobic glycolysis suggested that "the teratogenic effects of insulin are produced by rendering coenzyme unavailable to the embryo", and that the effects of other drugs or chemicals given in association with insulin is determined by their effect on coenzyme availability. For example, pyruvic acid, administered at early stages with insulin, promotes reoxidation of NAD and NADP, thereby reducing both insulin mortality and insulin rumplessness. These findings are in agreement with those of Zwilling and DeBell (1950), discussed above.

Despite gross morphological similarities of micromelia from insulin and sulfanilamide (already discussed), or from boric acid (Landauer, 1952) or pilocarpine (Landauer, 1953), differences do exist in terms of which particular hindlimb long bone is principally affected.

Insulin, sulfanilamide and eserine produce a proportionately greater shortening of tibiotarsus than either femur or tarsometatarsus, while pilocarpine and boric acid exert a stronger micromelic effect on the tarsometatarsus than either of the more proximal long bones. With insulin, an increasingly severe shortening along the proximo-distal axis was consistently observed by Landauer (1953), yet Duraiswami (1950) found no such effect.

Barbieri and Bonetti (1953) conducted a series of experiments with multiple injections of insulin between the 4th and 15th days of incubation. They obtained the usual deformed, micromelic embryos, many of which had bent tibiotarsi, and classed the general pathology as a form of "condro-osteo-distrofia" (chondrodystrophy). In considering the underlying mechanisms for these changes in normal development, they suggested that alterations in chondrocyte glycogen and/or interference with mineral exchange might be the direct effects of insulin treatment. One additional explanation offered for the teratologic effects of insulin is that the deformities are the result of a generalized shock (i.e. hypoglycemia).

The first application of an in vitro approach to the problem of insulin teratology was made by Chen (1954). He removed 6-7 day hindlimb buds from incubating chicken eggs and grew them on a fowl plasma/embryo extract medium. To one group of limb buds he added insulin, to a concentration of 0.16 units/ml of medium, and then examined the growing explants from normal and insulin-supplemented media at intervals up to ten days. He found that the insulin-supplemented

group of limb buds showed enlargement of the epiphyses, while the central part of the shaft failed to lengthen. Also, secondary shafts, complete with periosteal sheaths, occasionally were formed. Histologically, the insulin-treated long bones did not show the normal organization of the growth plate (term suggested by Rang, 1969, to replace the more usual one of "epiphyseal plate", which in fact contributes little to growth of the epiphyses). The three usual zones of resting, flattened and hypertrophic cells were imperfectly differentiated, and the diaphyseal hypertrophic chondrocytes never underwent normal disintegration, nor were they ever fully hypertrophic. Furthermore, staining with toluidine blue revealed a decreased, yet uniform intensity of metachromasia in the cartilage matrix of the insulin-treated group of rudiments. It was also shown that these effects were not due to the presence of any hyperglycemic factor present in the insulin. Chen suggested that the abnormal bone growth was a result of "a specific interference with the development of the diaphysis and with the differentiation of the zones of hypertrophic and flattened cells".

It was shown by Duraiswami (1955) that various substances (soluseptasine, thallium nitrate, lead nitrate, cortone acetate, and 3-acetylpyridine) each produce their own characteristic deformities in chick embryos, and if injected into the yolk in conjunction with insulin, both the malformations typical of insulin treatment and the given substance would appear in the deformed embryo.

De Bastiani and Lunardo (1956a) also conducted experiments

with chick embryos exposed to insulin early in development, and ascertained that the effects of insulin were attributable to the hormone itself, and not to other factors such as the presence of hyperglycemic factor (see also Chen, 1954). In their insulin-treated embryos, they described bending of the tibiotarsus in its lower (distal) portion, together with increased subperiosteal bone formation in the concavities of these bends. Epiphyseal cartilage was reported to have become separated from the growth plate cartilage, and the normal cartilage zonation was irregular and indistinct. Periodic acid-Schiff histochemistry revealed a highly variable glycogen content of ossifiable cartilage in the long bones of insulin-treated embryos, and this led them to conclude that variations in glycogen content are unrelated to the pathology, contrary to the hypothesis of Barbieri and Bonetti (1953). Additional studies showed no significant variations in mucopolysaccharide content of cartilage from micromelic bones, thus disagreeing with the findings of Duraiswami (1950). In addition, there were no alterations in the inorganic components of the cartilage.

These authors also challenge Duraiswami's (1950) diagnosis of reduced tibiotarsal ossification and pathological fractures, since they found none of the histological signs indicative of a fracture site (e.g.-hemorrhage). In this study, De Bastiani and Lunardo do not propose any mechanism for the teratologic effects of insulin.

In a second study, De Bastiani and Lunardo (1956b) discovered that almost identical histological abnormalities could be induced in chick embryos by steroid hormone (methylandrosterone) injection.

From this finding, they conclude that the direct effect of insulin in producing skeletal abnormalities might be an acceleration of protein synthetic activities, rather than any effect on carbohydrate metabolism.

Hay (1958) repeated the earlier in vitro experiments of Chen and, in addition, studied the effects of growth hormone and growth hormone plus insulin on explanted chick femora and tibiotarsi. Growth hormone alone increased wet and dry weights of the bones without affecting length, and did not appear to produce any histological changes. Insulin alone initially increased the growth rate of the rudiments, then slowed growth. Bending of the bones often occurred, and there was an increased deposition of glycogen in hypertrophic chondrocytes as compared with controls. In addition, insulin appeared to stimulate hypertrophy of the chondrocytes, in contrast with Chen's (1954) results. The combination of growth hormone plus insulin yielded a picture similar to that of insulin treatment alone.

In an effort to clarify the micromelia-hypoglycemia relationship, Zwilling (1959) also turned to in vitro analyses of femoral and tibiotarsal rudiments. Whether the rudiments received the insulin in ovo before excision, or whether they were exposed to insulin after excision, the same structural alterations were seen: shortened diaphysis, swollen epiphyses, irregular orientation of the epiphyseal small-celled cartilage, reduction or absence of the zone of proliferative chondrocytes, and delayed hypertrophy of the chondrocytes. In addition, ossification was reported to be retarded in a few instances. Results similar to those of Landauer (1948) and Zwilling (1949) were seen, in

that nicotinamide could relieve these disturbances if added to the culture medium. Since there is evidently no embryonic blood circulation under culture conditions, it was concluded that the micromelic response of hindlimb bones is a direct effect of insulin, and insulin hypoglycemia is largely a parallel event. Also, Zwilling (1959) disagreed with Duraiswami's (1950, 1952) diagnosis of osteogenesis imperfecta, which he says was based on "a rather cursory treatment of this subject".

Parhon et al (1956), in a paper comprising part of a series of studies on the effects of hormones on embryonic development, described in detail the histology of normal and micromelic (achondroplastic, according to the terminology of the authors) chick tibiotarsi from days 8 to 14 of incubation. Their experimental methodology differed markedly from that of all previous authors, since their insulin was given in multiple doses, and was administered by dropping onto the chorio-allantoic membrane, rather than by injection into the yolk. The principal histological changes which they observed were a precocity and acceleration of calcification, curvature of the distal portion of the tibiotarsus, a tendency for the periosteum to invade and separate epiphysis from diaphysis, and a "transformation" of the epiphyseal cartilage. Insofar as the biochemical mechanisms behind the observed malformations are concerned, they suggested a disturbance of carbohydrate metabolism, since bone development is "étroitement liée à la présence du glycogène", and the insulin hypoglycemia will have reduced availability of free glucose required for chondrocyte glycogen stores, as well as diminishing the amount of circulating blood phosphate.

Anderson et al (1959) conducted histochemical, biochemical and autoradiographic/liquid scintillation studies in an effort to determine what alterations there might be in the carbohydrate components of cartilage from insulin-treated embryos. They found no significant differences with respect to metachromasia (thionin and toluidine blue staining), glycogen (PAS and Best carmine methods), alkaline phosphatase, phosphorylase or calcium between normal and insulin-treated bones. Biochemical analyses for glycogen revealed no alteration in the ratio of glycogen to total cartilage weight. With regard to calcification, the only difference between the two groups of bones was the occlusion of the central portion of the tibiotarsal shaft with interlacing trabeculae, in insulin-treated bones. Within the insulin-treated group, there was disuniformity of staining with aldehyde fuchsin and alkaline phosphatase. Autoradiographic and liquid scintillation studies revealed no apparent difference in uptake and incorporation of  $S^{35}$ . Cell-to-matrix ratios were calculated for hypertrophic areas, and there was found to be less matrix per cell in the deformed tibiotarsi. It should be emphasized that all these observations were made exclusively from surviving 18 day embryos. The authors' contention is that " . . . the injection of insulin does not alter the basic metabolic processes for utilization of carbohydrate, but rather deprives the cartilaginous tissue of those derivatives from which the matrix may be fabricated".

The most comprehensive histological analyses of insulin-treated long bones in chicks are those of Erhard (1959). Since his observations are extremely detailed, they will be more fully considered

13

in the Results and Discussion sections. Suffice it to say that he accurately described the development of necrosis of the epiphyseal cartilage, and proposed a mechanism of impaired diffusion of nutrients within the avascular cartilage. With regard to the histochemistry of the aberrantly differentiating cartilage, he notes reduced glycogen (cf. Hay, 1958) and reduced chondroitin sulphate. More recently, Rang (1969) has stated that insulin increases the biosynthesis of chondroitin sulphate in cartilage. Altman and Dittmer (1968) also note that insulin stimulates mucopolysaccharide synthesis, as well as increasing the incorporation of sulphate into chondroitin sulphate.

In 1963, two reports were presented by Sevastikoglou on insulin micromelia in chick embryos. In the first of these (1963a), he found a statistically significant reduction both in length and weight of micromelic tibiotarsi over the period of 7th to 16th day of incubation. Both normal and micromelic tibiotarsi followed a linearly rising curve for growth in length (the latter depressed and divergent), while weight curves rose parabolically, the curve for micromelic bones again being depressed and divergent. Histologically, 9th day micromelic tibiotarsi showed retarded periosteal ossification and a less pronounced, but uniform metachromatic staining. By days 15 and 17 of incubation, the epiphyseal cartilage cones showed irregular organization, with the normal zone of flattened chondrocytes (proliferative zone) narrowed or almost absent (cf. Zwilling, 1959). At this time, there were more hypertrophic chondrocytes in the experimental group (cf. Chen, 1954; Zwilling, 1959). He also reported a reduction in diaphyseal periosteal



bone, with thinner, more irregular trabeculae which show a "special arrangement" at the sites of tibiotarsal angulation. Metachromatic staining was reportedly less pronounced in deformed limbs. Unfortunately, the author presents no photomicrographs of any of these results.

His second report (Sevastikoglou, 1963b) centered on biochemical analyses of acid and alkaline phosphatases, and hydroxyproline content of whole tibiotarsi. Alkaline phosphatase follows a progressive rise from days 6 to 16 of incubation then abruptly drops, with both control and insulin-treated tissues following this course, although the levels in the latter group tend to become more erratic from days 14 to 18. Acid phosphatase pursues an irregular course with development, and again the insulin group is more deviant. Hydroxyproline content rises fairly regularly with growth, but levels for the insulin-treated bones were generally lower. Thus, biochemical differences do exist, but he states that it is "impossible to analyze the results . . . statistically".

Tests by Landauer and Clark (1963, 1964) of the effects of various uncouplers of oxidative phosphorylation (chlorpromazine, sodium salicylate, 2,4-dinitrophenol, p-hydroxymercuribenzoate, and carbonyl cyanide m-chlorophenylhydrazine) on teratogenic manifestations of insulin led them to believe that insulin in some way interferes with specific step(s) in the oxidative phosphorylative pathway.

The teratogenic properties of insulin are by no means restricted to chickens. Other studies have demonstrated pathologies of development in mice (Lichtenstein et al, 1951; Smithberg and Runner, 1963) as well as in rabbits (Chomette, 1955; Brinsmade et al, 1956) and

ducks (Landauer, 1951). Furthermore, the suggestion has been made that insulin may even be implicated in human birth defects (Wickes, 1954).

In summary, it is clear from the results of all these authors that we are dealing with a specific teratogenic effect of insulin, and the exact particulars of morphologic change will vary with such factors as egg stock, timing and dosage of treatment, and individual susceptibility. The emphasis in this previous research has been on the statistical aspects of the problem (frequencies of deformity, mortality, etc.), the interactions of insulin with other compounds and their effect on the teratogenic activity of insulin, or has concerned itself with somewhat limited histological comparisons over a restricted period of incubation. Discrepancies exist in the descriptions of the histological and histochemical alterations involved, so that there are considerable divergences of opinion among authors in their interpretation of the experimental data. Moreover, the precise nature of the biochemical alterations of metabolism during pathological differentiation are not yet fully resolved.

Thus, the aims of the present study are threefold:

1. To provide comparative descriptions of hindlimb development, with particular emphasis on the tibiotarsus, in both normal and insulin-treated chick embryos, from the standpoint of anatomy and histology.
2. To apply various histochemical tests and assays for those substances which are considered important in the histogenesis of skeletal tissues, in an effort to detect any deviations from the norm in composition of bone and cartilage in the insulin-treated tibiotarsi.

3. To carry out these investigations over the entire period of incubation between exposure to insulin and hatching, in order to study the progressive development of the insulin syndrome.

## MATERIALS AND METHODS

### Introduction

Chicken eggs of White Leghorn stock, obtained from the Poultry Science Department, MacDonald College, St. Anne de Bellevue, Quebec, were used throughout this study. The use of chick embryos as experimental subjects avoids the problem of maternal influence during prenatal development, particularly the selective transfer of materials across a placenta. For example, studies by Keller and Krohmer (1968) on the isolated human placenta have shown that insulin will traverse the placenta from fetal to maternal systems, but the placenta appears to be impermeable to insulin passage in the opposite direction. On the other hand, contradictory results have been reported for humans (Gitlin *et al*, 1965) and for rhesus monkeys (Josimovich and Knobil, 1961).

All eggs were incubated in a forced-air incubator (Brower Manufacturing Company, Quincy, Illinois, U.S.A.), thermostatically kept at 101°F and at a hygrometer reading of 86-88°F. Eggs were viewed by transillumination on the 3rd day of incubation to ascertain fertility, and were rolled once daily throughout the period of incubation.

### Injection Protocol

The injection procedures employed in this study are essentially those of Landauer (1945). Trial injections of the dye neutral red were made into the yolk, using various needle lengths and gauges, with subsequent hard-boiling to localize the dye distribution within the egg. On the basis of these trials, a stainless steel 25 gauge hypodermic needle, 3/4 inch long (Becton, Dickinson and Company, Rutherford, New Jersey, U.S.A.),

fitted to a 1 ml tuberculin syringe manufactured by the same company, was selected for use.

Determination of the dosages, type of insulin, and timing of injection also required some preliminary experimentation. As Fisher (1955) has pointed out, all commercial preparations of insulin contain some contaminants, notably protamine and zinc. NPH or Isophane Insulin (Connaught Medical Research Laboratories, Toronto, Ontario) was chosen for use because of its low zinc content, and only moderate content of other compounds; its exact composition is given in Table 1. In a study of a similar commercial insulin preparation, Landauer (1945) found that the teratogenic properties of the insulin solution reside with the insulin molecule itself, and not with any of the various preservatives or buffers added by the manufacturer. Similarly, Parhon et al (1956) found that treatment of 144 chicken eggs with phenol, cresol, acidified cresol or distilled water did not produce any malformations in the embryos.

For judgement of dosage and timing of injection, 315 fertile eggs were given a single injection of either 2 or 4 International Units of NPH Insulin, administered at 120 or 144 hours of incubation. An equal volume (0.05 ml) of sterile 0.9% NaCl was injected into the eggs at 120, 132 or 144 hours of incubation to serve as controls. The results of these trials are given in Tables 2 - 5. On the basis of these trials, it was decided to use 4 units of insulin, given as a single injection at 132 hours of incubation, for all further studies.

Eggs were randomly divided into control (saline-injected) and treated (insulin-injected) groups. The eggs were viewed by transillumination and a fine probe was used to puncture the egg shell at a point along the equator directly opposite to the location of the embryo, thereby

avoiding direct injury to the embryo itself or any of the major blood vessels. The insulin was then injected through this puncture hole deep into the center of the yolk mass, the hole sealed with cellulose tape and returned to the incubator. Control eggs received an identical volume of sterile 0.9% NaCl, to ensure that any developmental disturbance was not the outcome of injection trauma or introduction of an exogenous volume of fluid.

Some 294 eggs were treated with insulin in this manner, and 81 eggs were injected with saline; the results are presented in Tables 6 - 11. All embryos examined histologically and histochemically were derived from this series.

The tibiotarsus was selected for intensive study, since Haardick (1941) has demonstrated that the tibiotarsus shows the highest growth rate of all hindlimb bones in the chicken, and therefore would be expected to show most clearly the effects of disrupted growth and development.

#### Anatomical Preparations

Whole mounts of normal and insulin-treated embryos were prepared daily from days 8 through 20 of incubation, after the method given by Dawson (1926). Details of the actual procedure used are given in Appendix A. In a few instances the differential staining method of Burdi and Flecker (1968), employing alizarin red S and toluidine blue, was used. With this latter method, uncalcified cartilage is stained blue, while calcified cartilage and bone are coloured red.

### Histological and Histochemical Preparations

For histological and histochemical studies, embryos were removed from their eggs on days 8, 9, 10, 11, 12, 13, 15, 17 and 20 of incubation. Wherever possible, the tibiotarsi were quickly dissected free of the embryos and placed in the appropriate fixative for further studies. For particularly large tibiotarsi, the bones were longitudinally split in half before fixation. All microscopic sections were serially cut in the longitudinal plane of the limb with steel knives on a Jung rotary microtome, and flattened on a water bath or slide warmer. Decalcification procedures were avoided, being necessary only in a few instances. In these unavoidable cases, the tissues were treated either with 5% nitric acid in 70% ethanol, or an equal parts mixture of 2% formic acid and 20% sodium citrate.

For routine histology, tissues were fixed in Bouin's fluid (15 parts saturated aqueous picric acid: 5 parts commercial formalin: 1 part glacial acetic acid) for at least 24 hrs, embedded in Tissuemat (Fisher Scientific Company), and stained by the standard hematoxylin and eosin sequence, using Ehrlich's hematoxylin and 0.25% alcoholic eosin Y (C.I. No. 45380).

Differentiation of bone matrix from cartilage matrix was achieved by the aldehyde fuchsin - phloxine - fast green FCF method of Scott (1952), as modified by Gibson (1966). With this staining combination, aldehyde fuchsin stains cartilage matrix and elastic fibers intensely purple, the fast green FCF stains bone matrix and collagen fibers intensely green, while phloxine stains muscle fibers and acts as a nuclear stain. The exact procedure and staining times are given in Appendix B.

As to the nature of the material stained by aldehyde fuchsin,

Walker (1961) compared a number of mucopolysaccharide stains (aldehyde fuchsin, toluidine blue, alcian blue, orcinol-new fuchsin) and found that aldehyde fuchsin staining corresponded closely with areas of  $S^{35}$  incorporation, as shown autoradiographically. As Spicer et al (1967) have noted, "Aldehyde fuchsin shows a broad spectrum of affinity for sulfated mucosubstances, coloring both those with strong metachromatic properties but negligible alcianophilia, and those with strong affinity for alcian blue and weak azurophilia".

For microscopic demonstration of calcification, the von Kossa (1901) technique was employed. Essentially, the method involves substitution of silver for the calcium in tissue calcium phosphate, then a photic reduction of silver phosphate to silver. Various authors recommend different counterstains, and it was found that the counterstains of safranin O, as suggested by Lillie (1965), or neutral red, as advised by Pearse (1961), were unsatisfactory since they stained uncalcified cartilage matrix a deep orange colour which could be confused with the brown or brown-black silver deposits. The counterstain of nuclear fast red (Thompson, 1966) proved satisfactory, staining nuclei a vivid red and uncalcified matrix a pale pink. Complete details of the method used are given in Appendix C.

Metachromasia was studied, using toluidine blue, a cationic thiazine dye. Without extensively considering the theories of metachromasia, it is generally held that sulphated compounds are the chromotrope responsible for the metachromasia of cartilage matrix, and with this dye will display the red or purple coloration of gamma and beta metachromasia respectively. Bélanger and Hartnett (1960) associate toluidine blue



metachromasia with chondroitin sulphate and possibly heparin. In any event, an intense, alcohol-resistant metachromatic response with toluidine blue is considered diagnostic for sulphated acid mucopolysaccharides (Barka and Anderson, 1963). The method is presented in Appendix D.

Further consideration of acid mucopolysaccharides (or, "glycosaminoglucuronoglycans", a biochemically more suitable term suggested by Jeanloz, 1960) was accomplished using two copper phthalocyanine dyes, alcian blue and alcian yellow. The method developed by Steedman (1950) was initially employed, and then the combined alcian blue-alcian yellow procedure of Ravetto (1964) was used.

According to Quintarelli et al (1964), either alcian dye at pH=2.0 stains both carboxylic and sulphate groups; at pH=0.5, however, they would react only with sulphate groups, as carboxyls would remain completely associated at this low pH. By using each of the two dyes at different pH levels, one can then spectrally distinguish those areas of cartilage rich in sulphated compounds (sulphomucins) from those containing minimal or no sulphate groups (carboxymucins). Both methods for glycosaminoglucuronoglycans are presented in Appendix E.

Glycogen was histochemically localized by two different methods. The first of these is the periodic acid-Schiff reaction, developed by McManus (1946) and Hotchkiss (1948). The basic operation of this method involves initial periodic acid oxidation of the tissue, thereby cleaving adjacent 1:2-glycol groups and converting them into dialdehydes. These reactive dialdehydes can then combine with the Schiff reagent (leucofuchsin) to give a substituted dye which is red in colour. The chief advantage in use of periodic acid as oxidizing agent, rather

than others such as hydrogen peroxide or potassium permanganate is that it does not continue oxidation of the dialdehydes to carboxyls (Spicer et al, 1967).

Because of the large number of compounds containing susceptible 1:2-glycol groupings (including glycoproteins and mucopolysaccharides), the specific identification of glycogen must include a diastase-digested control. By comparison of an undigested section with a companion section incubated in diastase, the staining due to glycogen content may be assessed. Details of the method used are given in Appendix F.

The second method for glycogen demonstration is the carmine method of Best (1906). Although this particular technique is highly empirical, and its precise mode of action is not fully understood, its specificity for glycogen has been recognized by most histochemists. It is recorded by Thompson (1966) that oleic acid, mucins and fibrin are also stained, but the reaction is far less intense than that displayed by glycogen. As with the PAS technique discussed above, a diastase-digested control is necessary to ensure full specificity. According to Lhotka and Anderson (1968), if a tissue possesses very much or very little glycogen, the negative image in the PAS control section may be obscured or absent, whereas with the Best carmine method one is dealing with a positive glycogen image which is easier to judge. These authors advocate usage of both techniques when examining glycogen histochemically.

Most authors recommend that sections be coated with a thin film of celloidin prior to the Best carmine staining sequence, as the strongly alkaline solutions involved tend to loosen sections from the slides.

This was done, but it was found that the celloidin film tended to be stained rather heavily with the carmine, a feature noted by Drury and Wallington (1967). Omission of the protective film altogether was found to be satisfactory, section "fall-off" being minimal. The complete particulars of the procedure are given in Appendix G.

Because of its importance in ossification (Robison, 1923; Pritchard, 1952), the alkaline phosphatase (AlkPase) activity of normal and insulin-treated tibiotarsi was investigated, using the Gomori (1952) calcium-cobalt method. The technique involves the splitting of phosphate from added glycerophosphate by tissue AlkPase; these free phosphate ions may then combine with calcium ions in the substrate and insoluble calcium phosphate is precipitated. This calcium phosphate, visible in the electron microscope, but not in the light microscope, is reacted with cobalt sulphate to yield cobalt phosphate which is finally converted to a visible, black precipitate of cobalt sulphide by treatment with ammonium sulphide. Also, since a false positive reaction will be given by calcium previously present in the tissue, as noted by Drury and Wallington (1967), tissues must first be exposed to a citrate buffer to remove these preformed calcium salts. Finally, to ensure specificity of localization, companion sections are incubated in the substrate minus the glycerophosphate. The entire method is outlined in Appendix H.

It should be noted that for some of the older, more mineralized tibiotarsi, various decalcification procedures were attempted before embedding, in order to facilitate sectioning of tissues destined for AlkPase staining. The "Decalcification with Enzyme Preservation" method given by Pearse (1961) and based on the citric acid-sodium hydroxide-hydrochloric

acid mixture of Lorch (1946), with subsequent enzyme reactivation by a veronal acetate buffer satisfactorily softened the bones, but AlkPase was lost. Similarly, the method given by Lillie (1965), using an ammonium citrate-citric acid buffer with enzyme reactivation by sodium barbital with glycine, was unsuccessful. The problem was overcome by avoiding decalcification procedures altogether, since prolonged periods of immersion in decalcifying fluids probably results in enzyme loss through diffusion. Instead, difficult to section tissues were double-embedded in 3% celloidin in ether-alcohol and low melting point paraffin, keeping the paraffin infiltration times brief to minimize heat inactivation of AlkPase. Sections were serially cut at 8 micra as usual, and where difficulty in sectioning still persisted, the cellulose tape method of Palmgren (1954) proved useful.

#### Photography

Photographs of the alizarin-stained whole mounts were taken by transmitted light on 35 mm Kodak Panatomic-X film, while photographs of the doubly-stained whole mounts were taken in daylight on Kodak Ektachrome-X film. All microscopic preparations were recorded on the same two types of film, using a Zeiss Photomicroscope and either bright field illumination or phase contrast. All illustrations were taken and processed by the author.

#### Tibiotarsal Lengths

Comparative rates of growth in length were calculated for control and insulin-treated tibiotarsi. Measurements were made directly

from microscopic sections, using a calibrated ocular micrometer. A total of 90 bones ~~was~~ measured, taking five tibiotarsi from different embryos for each of nine days, in both control and insulin-treated groups of embryos. If the tibiotarsus exhibited one or more bends, the straight portions were individually measured and the results summed. These data are given in Table 12. The results were graphically plotted as least-squares lines fitted to the means of the measured lengths, according to the linear regression method of Stanley (1963), and are seen in fig. 2. In addition, the chi-squared test for statistical significance was applied to the regression lines for both sets of data in order to verify "goodness-of-fit".

#### Hypertrophic Cell Size and Matrix/Cell Studies

To determine if there were any changes in matrix production by cartilage cells as a result of insulin treatment, the amount of extracellular matrix per hypertrophic chondrocyte was calculated as follows: microscopic sections were viewed at a magnification of 40X through a calibrated ocular net reticule (American Optical Company, Buffalo, New York), and hypertrophic cell counts were made in an area varying from 40,000 to 75,000 square micra. These counts were then reduced to their equivalent values for a standardized field area of 10,000 square micra. Counts were made on four different tibiotarsi for each of nine days, in both groups of embryos. The diameters of the chondrocytes were measured with a calibrated ocular micrometer at 100X, using a sample size of ten cells per section. Assuming the hypertrophic cells to be circular, single cell areas could be calculated according to the formula for a circle, namely  $\text{Area} = \pi r^2$ ; these

values, multiplied by the number of cells in the standard field, reveals the percentage of the total area which is occupied by cells. The difference between these latter values and 10,000 square micra gives the total matrix area. Finally, the total matrix area divided by the number of cells in the standardized field yields the average amount of matrix per hypertrophic chondrocyte. The mean values for hypertrophic chondrocyte cell diameters and amount of matrix/cell for control tibiotarsi and insulin-treated tibiotarsi are given in Tables 13 and 14, respectively, while mean values in both groups are statistically compared in Table 15, using the method of standard error of the difference between means (Stanley, 1963). No attempt was made to carry out similar analyses for the other cartilage cell types.

## RESULTS AND DISCUSSION

### I - OBSERVATIONS AND ANALYSIS

#### Dosage and Timing of Injection Studies

A total of 315 fertile eggs was injected with either two or four International Units of NPH Insulin at 120 or 144 hours of incubation, while a total of 75 fertile eggs were injected with an equal volume (0.05 ml) of sterile 0.9% sodium chloride. The results of these various injections, in terms of mortality and deformity frequencies is presented in Tables 2-5. It can be seen that with two units of insulin the frequency of deformed embryos is lower (5-10%) than with four units of insulin (15-37%), while at the same time the mortality rises with the higher dosage (51.9-70.0% with four units, as compared with 50.0% with two units). This, together with the observation that those embryos exposed to four units of insulin usually showed more severe skeletal malformations, resulted in the choice of four units as the dosage to be employed for further studies. With regard to the timing of injection, eggs treated at 144 hours showed a higher maximum (37%) for deformity frequency than those injected with insulin at 120 hours (22%). However, the latter group displayed a greater involvement of the tibiotarsus in the limb deformities, while the later injection tended to promote disturbances centered primarily in the femur. Accordingly, an intermediate time of 132 hours was selected for all further treatments.

These results are generally in agreement with the findings of Duraiswami (1950), whose diagram illustrating the type of deformity in relation to the time of injection is reproduced as fig. 1 .

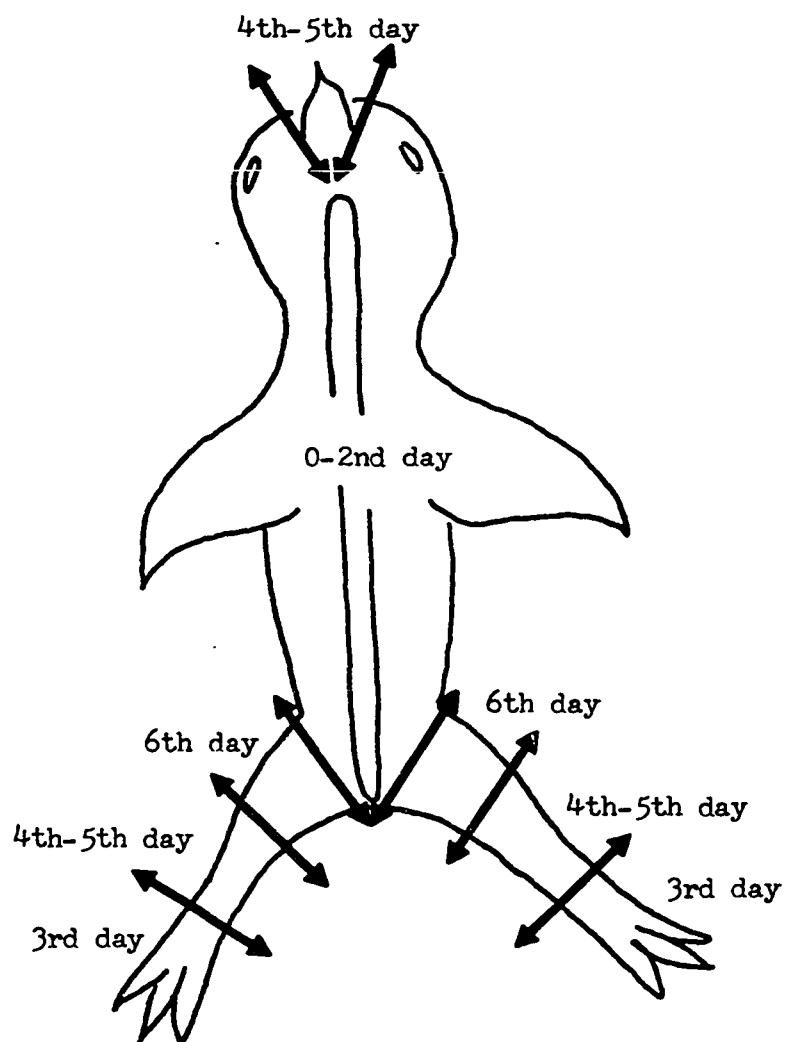


Figure 1 - Diagram illustrating the relationship between time of insulin injection and those parts of the skeleton principally affected (after Duraiswami, 1950).

0-2nd day: vertebral column

3rd-4th day: tarsometatarsus, metatarsus, phalanges

4th-5th day: tibiotarsus, fibula, beak

6th day: femur



Of the 75 fertile eggs treated with saline at 120, 132 or 144 hours of incubation, none were deformed after injection. The frequency range of mortalities after saline treatment was 10.0-19.2%, and this frequency must be borne in mind when considering what appear to be excessive mortalities after insulin treatment.

#### Results of Injection at Preferred Dose and Time

The results of treatment of 375 fertile eggs with four units of insulin or 0.05 ml of 0.9% NaCl at 132 hours of incubation are given in Tables 6-10, and are summarized in Table 11. It is evident that insulin insult kills many embryos (average mortality frequency of 69.7%), yet of the surviving embryos (N=89), some 69.7% are clearly micromelic. In the case of embryos whose micromelic status could not be readily determined, the individuals were counted as normal, so that the figure of 69.7% is really a minimal value. This latter per cent is very close to the value of 72% reported by Erhard (1959), and is obviously significant, so that one may assume a causal relationship between exposure to insulin and disproportionate dwarfing of the hindlimbs. At the same time, saline injections led to a mean mortality of 27.2% (N=81), without a single instance of definite micromelia, although a few embryos were very slightly smaller in overall size than untreated embryos.

Clearly then, the observed micromelia after insulin treatment is not a nonspecific response to trauma of injection, introduction of foreign fluid into the yolk, or any other physical factors.

### Non-Skeletal Deformities Among Insulin-Treated Embryos

While no particular attempt was made to extensively examine the effects of insulin on soft tissues, five features were sometimes encountered:

1. There was often a generalized edema, especially marked in the abdominal area, and may be seen to particular advantage in fig. 22. This would appear to be a nonspecific response to the teratogen, as it occurs with a number of other drugs and chemicals.
2. Occasionally, ectopia viscerum (eversion of the viscera) was seen, as has been described in untreated chick embryos (Hutt and Greenwood, 1929), and in embryos treated with other teratogens such as cortone acetate (Duraiswami, 1955).
3. In a few instances, the heart appeared enlarged and located somewhat more caudally than normal. This was always associated with an edematous abdomen.
4. During the course of dissection of the tibiotarsi, blood clotting seemed more rapid than normal.
5. Relative muscle hypertrophy and/or hyperplasia was often associated with hindlimb micromelia, and tended to be acute at the epiphyses of the tibiotarsus so that the diaphysis of a bent tibiotarsus appeared to be covered only by the skin of the embryo. This is readily seen in many of the whole mount and low magnification photographs (e.g. fig. 45). Its<sup>U</sup> relationship to curvatures of the tibiotarsus will be discussed later.

### Non-Micromelic Skeletal Anomalies

Of the total of 765 fertile eggs employed in this study, two embryos were found to have developed hyperencephaly or complete absence of the roof of the skull, while one embryo was found with an exencephaly or meningocele in which a portion of the brain extrudes through the cranium, but is still confined by the meninges. These embryos were all alive when discovered.

Since only one of these (insulin-treated, hyperencephalic, Table 5, fig. 4) was associated with micromelia, while the second (insulin-treated, hyperencephalic, Table 6, not illustrated) had normal limbs, and the third (exencephalic, Table 6, fig. 3) was a product of saline injection, it is unlikely that these defects of intramembranous ossification bear any relationship to insulin treatment.

These two pathological conditions represent deformity frequencies of 0.26% (hyperencephaly) and 0.13% (exencephaly), values which fall in the range of spontaneously occurring mutations. Hutt and Greenwood (1929b) obtained somewhat higher incidences for these same anomalies in a considerably larger sample (N=11,797) of untreated chicken eggs.

Other than the two defects referred to above, there did not seem to be any interference with the formation of membrane bone; in fact, the skull was usually of the same size in insulin-treated embryos as in controls of the same age, despite a generally stunted torso.

Calcification of vertebrae and ribs appeared to be delayed by one or two days in a few instances (figs. 16, 18). This will be further discussed.

### Gross Anatomy and Calcification

A series of whole mount photographs covering each day of incubation from day 8 through 20 (day before hatching) is given in figs. 5-30. In addition, there is one photograph (fig. 31) of an insulin-treated chick that successfully hatched. Specific details for each stage may be found in the accompanying figure legends.

It is seen from first glance that most of the insulin-treated embryos are of smaller stature than control (saline-injected) embryos of the same chronological age, although this is not always true (e.g. fig. 8). However, the head nearly always retains its normal dimensions, thus contributing to the dwarf- or gnome-like appearance on the gross level.

In addition to this generalized stunting of growth, there are more specific disorders of the shape of certain of the skeletal elements, and of the general pattern of skeletal mineralization. Prime among these is a consistent disproportionate shortening of the appendicular skeleton, a pathological condition described as micromelia. This micromelia is always bilateral, and more pronounced in the hindlimbs than in the wings. All of the photographs of insulin-treated specimens display this micromelia.

Within the hindlimbs of insulin-treated individuals, the tibiotarsi are not only shortened and thickened, but commonly exhibit one or more bends or angulations along their lengths. Usually, this curvature occurs at the junction of the diaphysis with the distal epiphysis (figs. 16, 18, 20), but it may occur in the mid-diaphysis of less severely deformed embryos (figs. 22, 26), or, in more extreme cases, at the

junctions of both epiphyses with the diaphysis (figs. 12, 24). Bends in other hindlimb bones may also occur (e.g. - femoral bend in figs. 24, 28), although less frequently, since the location of the maximally deformed hindlimb bone is a function of the time of insulin injection into the embryonic system (fig. 1). It is of interest that these bends, when they occur, are such that the entire hindlimb is rotated inward, and never away from the body.

Despite the reduction in length of the hindlimb bones, the associated skeletal muscle bundles (e.g. - gastrocnemius, peroneus longus) appear to undergo normal enlargement, so that the stunted bones are surrounded by disproportionately large masses of muscular tissue, creating the impression of elephantiasis.

At this macroscopic level, there appears to be a delay in the onset of calcification of tarsals, vertebrae and vertebral ribs among the insulin-treated embryos. Vertebral ossification is reported to commence on day 12 or 13 of incubation in normal embryos, beginning with the fourteen cervical vertebrae (Romanoff, 1960). In the present material, the first signs of cervical vertebral mineralization are seen as early as day 11 in control embryos (fig. 11). However, among insulin-treated embryos, there is usually a delay of one to two days in the start of any vertebral ossification (figs. 14, 16), although there is at least one instance (fig. 18) of a delay of more than three days in the commencement of vertebral mineralization. A similar lag period may occur in the case of the tarsal elements (see above figs.).

The normal adult chicken possesses seven vertebral (dorsal) ribs articulating with the thoracic vertebrae, and five sternal (ventral)

ribs articulating with the last five vertebral ribs and the midventral sternum. The vertebral ribs are known to ossify before the sternal portions, beginning on the 10th or 12th day of incubation (Romanoff, 1960). With the present alizarin red S method, there is a faint staining of three vertebral ribs by the 9th day of incubation in control embryos (fig. 7). This increases in number to five ribs by day 10 (fig. 9). One more vertebral rib undergoes calcification each day for the next two days of incubation, so that the full complement of seven vertebral ribs is calcified by the 12th day of incubation. Since the ribs are endochondral bones, and calcification of cartilage in the fowl does not commence before the 15th day of incubation (Fell and Robison, 1934), the alizarin red S deposits thus represent periosteal bone formation.

The ossification sequence of insulin-treated ribs is more erratic. It may seem normal (figs. 10, 16) or delayed (figs. 12, 14), but in certain instances may be both delayed and bilaterally asymmetrical (fig. 18).

Fig. 31 shows an insulin-treated chick that successfully hatched, yet was unable to stand normally as a result of hindlimb torsion and tibiotarsal bending. Unlike achondroplastic or chondrodystrophic embryos, insulin-treated chick embryos are therefore capable of hatching.

At no time did formation of feathers appear retarded, contrary to the findings of Barvieri and Bonetti (1953).

Anatomically then, the insulin-treated embryos form a group of individuals distinct from normal embryos at all stages of incubation, in terms of general morphology, shape of certain skeletal elements, and temporal pattern of mineralization of the skeleton.

Figure 3

Control embryo, 15 days incubation. Note spontaneous proencephalic exencephaly (arrow) and abruptly shortened upper beak. Hindlimb length appears normal. Formalin preserved.

Figure 4

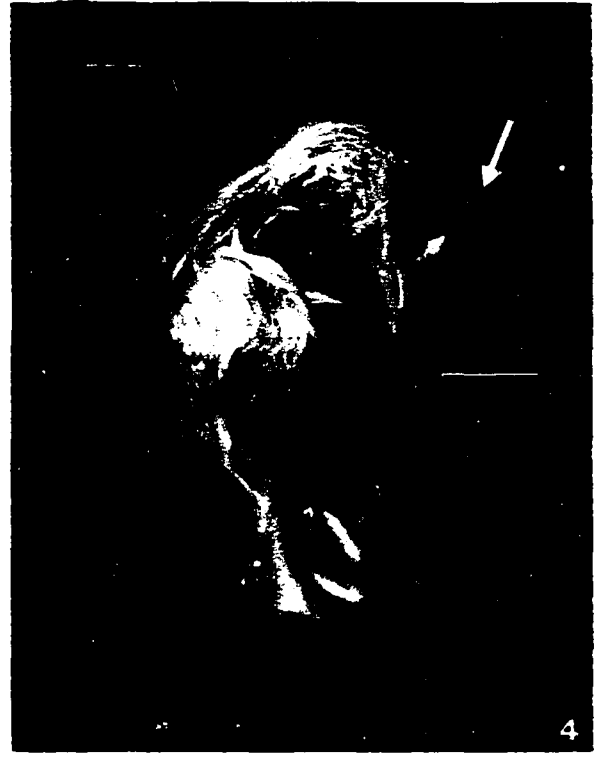
Insulin-treated embryo, 19 days incubation. In addition to shortening and inward rotation of the hindlimbs, there is a pronounced hyperencephaly (arrow). Despite the completely exposed brain, this embryo was alive when removed from the egg. Formalin preserved.

Figure 5

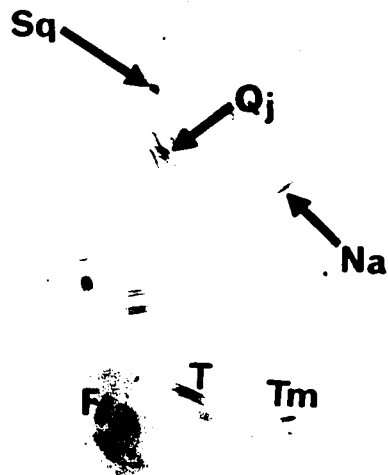
Control embryo, 8 days incubation. Femur (F), tibiotarsus (T), and tarsometatarsus (Tm) show the beginnings of diaphyseal calcification, most intense in the mid-diaphyses. In the facial region, squamosal (Sq), quadratojugal (Qj) and nasal (Na) bones have begun to show mineralized deposits. Whole mount, alizarin red S method.

Figure 6

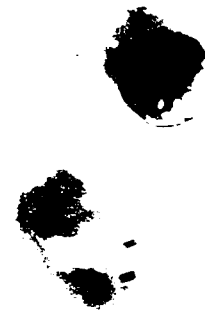
Insulin-treated embryo, 8 days incubation. As compared to the control embryo in fig. 5, there is only slight calcification of the tarsometatarsus. Note severe shortening of all hindlimb bones and general dwarfism. Whole mount, alizarin red S method.



Scale : 1cm



5



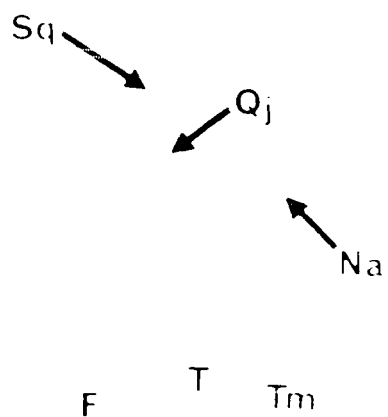
6

Scale: cm





Scale : cm



5

6

Scale : cm

#### Figure 7

Control embryo, 9 days incubation. Hindlimb bones are longer, and show greater calcification than in the previous day. As the fibula lies lateral to the tibiotarsus, it is not seen in this lateral view. Early ossification of three vertebral ribs may be seen (arrow). Whole mount, alizarin red S method.

#### Figure 8

Insulin-treated embryo, 9 days incubation. Although the crown to rump length is about the same as the control embryo (fig. 7), the hindlimb is notably shorter, directed posteriorly, and its rotation brings the fibula (f) into view. The intensity of stain in the hindlimb bones appears somewhat greater than in the control embryo of the same age. Note also the upper beak curvature ("parrot-beak"). Whole mount, alizarin red S method.

#### Figure 9

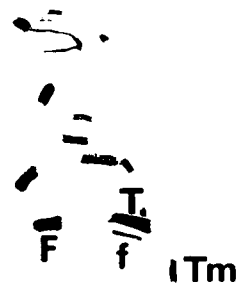
Control embryo, 10 days incubation. Calcification of five vertebral ribs is now apparent. Hindlimb calcification continues to increase. Whole mount, alizarin red S method.

#### Figure 10

Insulin-treated embryo, 10 days incubation. Disproportionate shortening and thickening of femur and tibiotarsus. The three elements of the tarsometatarsus are seen in end view (arrow). As in the control embryo, five calcified vertebral ribs are present. Whole mount, alizarin red S method.



7




8



9



10

Scale :  cm

#### Figure 11

Control embryo, 11 days incubation. First suggestive traces of calcification of tarsal elements (arrows) and cervical vertebrae. The number of calcified vertebral ribs has risen to six. Unlike earlier embryos, the stain intensity appears uniform throughout the diaphysis of each calcified long bone. Whole mount, alizarin red S method.

#### Figure 12

Insulin-treated embryo, 11 days incubation. Note curvature of the thickened tibiotarsus, and absence of calcification in the tarsals. Whole mount, alizarin red S method.

#### Figure 13

Control embryo, 12 days incubation. Hindlimb bones continue to lengthen, with complete diaphyseal calcification of the proximal elements, while calcification of the tarsals is now definitive. There are seven calcified vertebral ribs. Whole mount, alizarin red S method.

#### Figure 14

Insulin-treated embryo, 12 days incubation. The tibiotarsus is again markedly stunted and curved. The three elements comprising the tarsometatarsus are more widely separated than normal. Only metatarsus I of the foot shows calcification. Whole mount, alizarin red S method.



11



12



13



14

Scale: | cm |

Figure 15

Control embryo, 13 days incubation. Calcified portions of tarsals and vertebrae now sharply delimited. Whole mount, alizarin red S method.

Figure 16

Insulin-treated embryo, 13 days incubation. Tibiotarsus again exhibits a bend in its distal third, while the fibula remains straight, thus projecting outward at an angle. Tarsal calcification is minimal, as are the calcified portions of the vertebrae. The entire hindlimb projects laterally, then medially, rather than directly forward. Whole mount, alizarin red S method.

Figure 17

Control embryo, 14 days incubation. Much the same as the preceeding day (fig. 15). Whole mount, alizarin red S method.

Figure 18

Insulin-treated embryo, 14 days incubation. The relationship of tibiotarsus to fibula, mentioned for fig. 16, is again seen. The lateral projection of the entire hindlimb is extremely marked. There are only five calcified ribs on the right side, and six on the left. This embryo shows no calcification of the tarsal elements or vertebrae. Whole mount, alizarin red S method.



15



16



17



18


Scale :  cm

Figure 19

Control embryo, 15 days incubation. Little difference from the preceeding day, other than a general increase in size. Whole mount, alizarin red S method.

Figure 20

Insulin-treated embryo, 15 days incubation. Other than a curved upper beak, the skull is as well calcified and of the same size as the control embryo in fig. 19. The appendicular skeleton, as in the preceeding illustrations, is disproportionately reduced and deformed. The vertebrae appear closer together. Calcification of the tarsal elements has finally occurred. Whole mount, alizarin red S method.

Figure 21

Control embryo, 16 days incubation. Tarsal calcification is better defined. Whole mount, alizarin red S method.

Figure 22

Insulin-treated embryo, 16 days incubation. This embryo has the same approximate crown to rump length as the comparable control, yet the tibiotarsus is once again much shorter, as well as being bent in the mid-diaphysis. Note that the wings are of almost normal dimensions. This embryo also displays the edematous abdomen which is characteristic of many of the insulin-treated embryos. Whole mount, alizarin red S method.





19



20

Scale: | cm |



21



22

Scale: | cm |

Figure 23

Control embryo, 17 days incubation. Whole mount, alizarin red S method.

Figure 24

Insulin-treated embryo, 17 days incubation. The tibiotarsus is badly deformed, with bends at both ends, resulting in an "S"-shaped appearance instead of the normal straight profile. The femur is also bent, although the tarsometatarsus is straight. Whole mount, alizarin red S method.

Figure 25

Control embryo, 18 days incubation. The downward curvature of the plantar surface of the foot is now apparent. Whole mount, alizarin red S method.

Figure 26

Insulin-treated embryo, 18 days incubation. Particularly prominent is the lordotic appearance of the cervical vertebrae. Formation and calcification of the caudal vertebrae approximates the normal condition, but the extremities remain micromelic. Whole mount, alizarin red S method.



23



24



25



26


Scale:  cm

Figure 27

Control embryo, 19 days incubation. Whole mount, alizarin red S method.

Figure 28

Insulin-treated embryo, 19 days incubation. In this particular specimen, the bend in the tibiotarsus is somewhat flattened, as is the bend in the femur. Further, both of these bends occur in the mid-diaphysis, rather than at the more common site of the junction of the diaphysis with the distal epiphysis. The plantar surfaces of the feet again are rotated to face the abdomen. Note that even though the bones of the hindlimb are smaller than normal, the associated muscle masses are of normal thickness. Whole mount, alizarin red S method.

Figure 29

Control embryo, 20 days incubation. This photograph represents the general morphology and extent of calcification that is present at hatching. Whole mount, alizarin red S method.

Figure 30

Insulin-treated embryo, 20 days incubation. The deformities of the skeleton are as previously described, again noting the relatively large muscle masses of the hindlimb. Whole mount, alizarin red S method.



27



28



29



30

Scale: |cm|



Figure 31

Insulin-treated chick, 3 days post-hatching, ventral view. Calcified tissues are stained red, while uncalcified cartilage is blue. Note the abrupt bends in the tibia-tarsi (arrows), and clawed appearance of the left foot only. Large muscle masses are associated with the femora and proximal tibia-tarsi. The sternum (st) is completely unossified. Feather development seems normal. Whole mount, Burdi and Flecker (1968) technique.

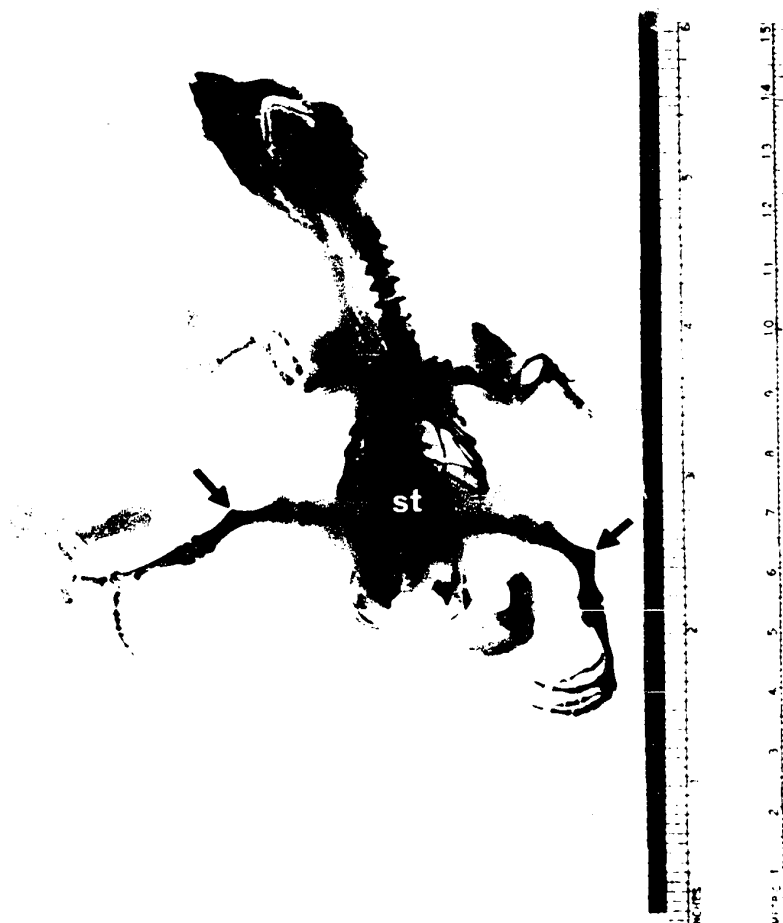


Figure 31

Insulin-treated chick, 3 days post-hatching, ventral view. Calcified tissues are stained red, while uncalcified cartilage is blue. Note the abrupt bends in the tibiotarsi (arrows), and clawed appearance of the left foot only. Large muscle masses are associated with the femora and proximal tibiotarsi. The sternum (st) is completely unossified. Feather development seems normal. Whole mount, Burdi and Flecker (1968) technique.

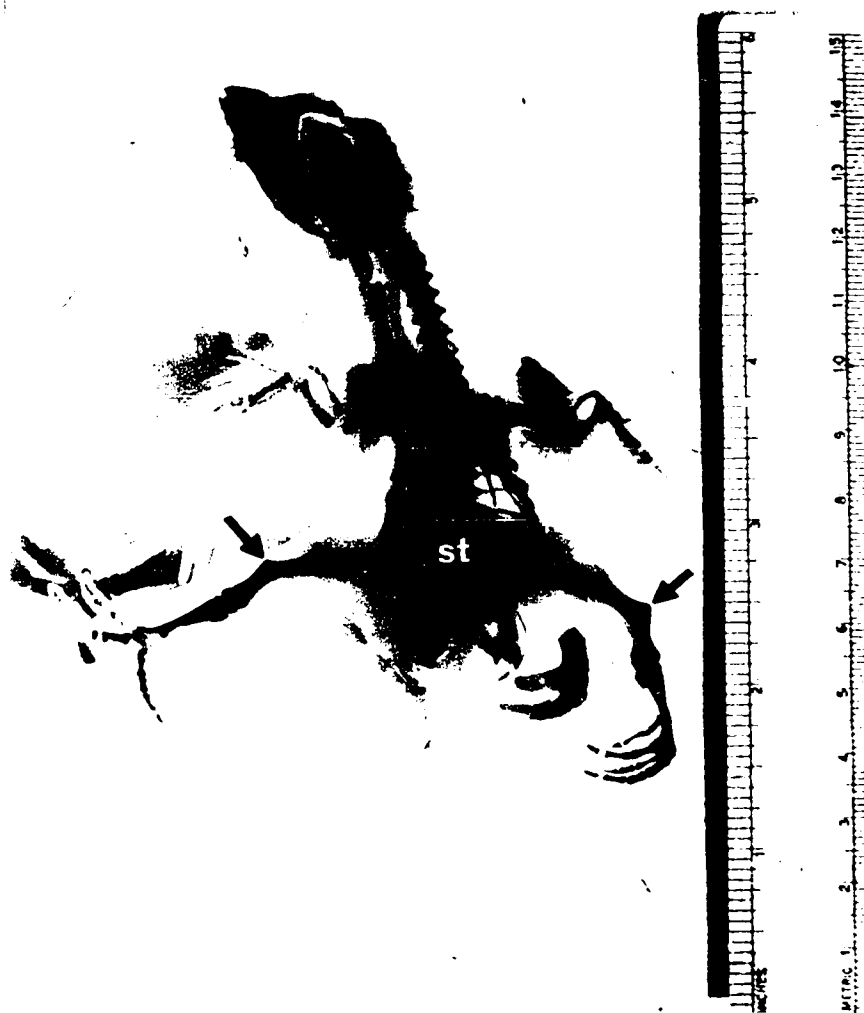


Figure 31

Insulin-treated chick, 3 days post-hatching, ventral view. Calcified tissues are stained red, while uncalcified cartilage is blue. Note the abrupt bends in the tibiotarsi (arrows), and clawed appearance of the left foot only. Large muscle masses are associated with the femora and proximal tibiotarsi. The sternum (st) is completely unossified. Feather development seems normal. Whole mount, Burdi and Flecker (1968) technique.





Figure 31

Insulin-treated chick, 3 days post-hatching, ventral view. Calcified tissues are stained red, while uncalcified cartilage is blue. Note the abrupt bends in the tibia-tarsi (arrows), and clawed appearance of the left foot only. Large muscle masses are associated with the femora and proximal tibia-tarsi. The sternum (st) is completely unossified. Feather development seems normal. Whole mount, Burdi and Flecker (1968) technique.

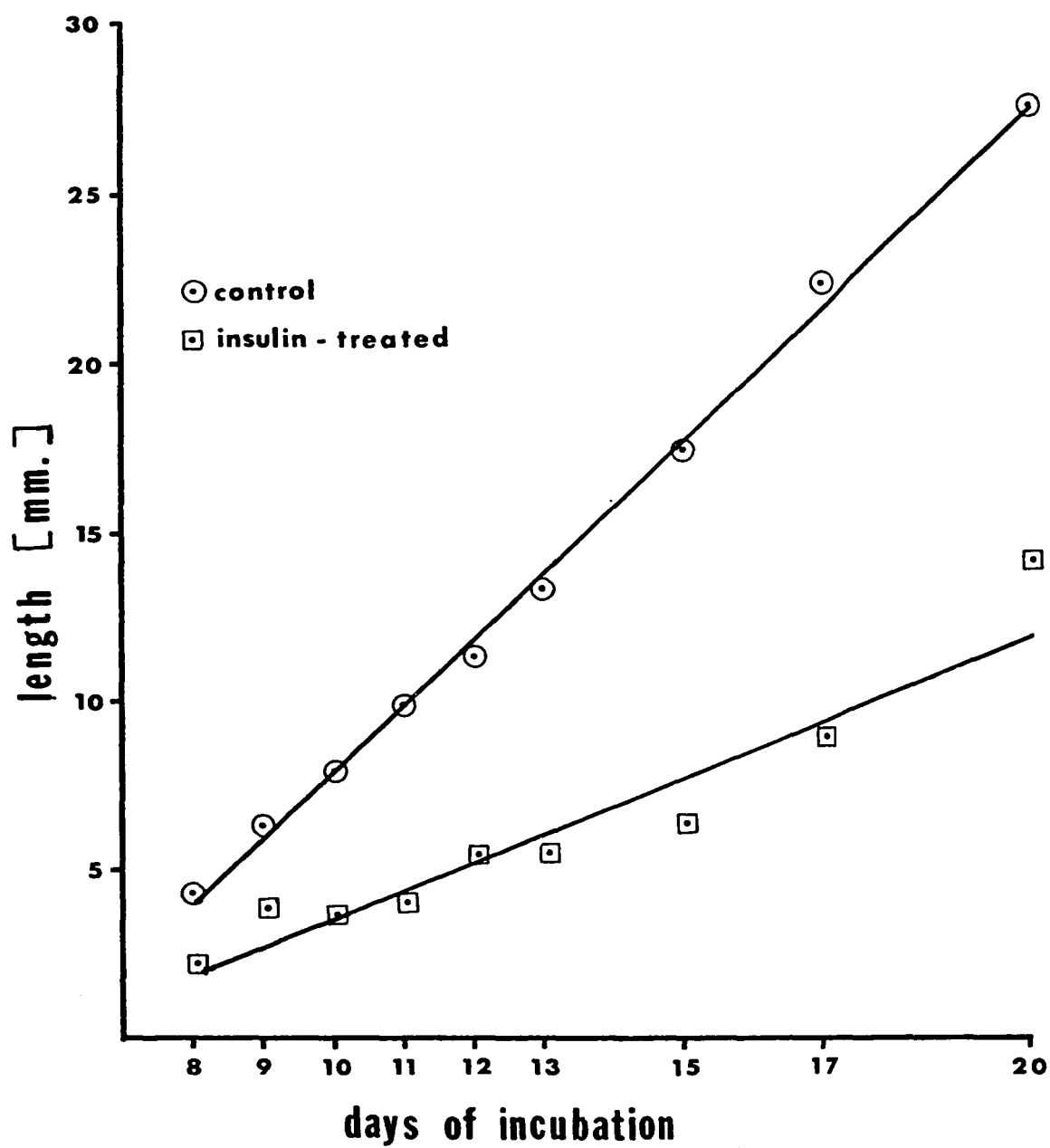
### Tibiotarsus Lengths

Analyses of the results of studies carried out on the growth in length of control and insulin-treated tibiotarsi (Table 12 and fig. 2) reveal striking differences both in absolute length and in rates of growth. The control tibiotarsi exhibit an almost perfect linear increase in length with incubation, while the plotted values for insulin-treated bones pursue a more erratic course, although a statistically valid linear plot may be drawn ( $\chi^2=0.123$ , degrees of freedom=8,  $P>0.95$ ). What is of prime importance is that not only is the line for the insulin-treated tibiotarsi depressed below that of the control bones (fig. 2), but rises more slowly (i.e. has a slower growth rate).

Close scrutiny of Table 12 reveals that for any given day of incubation, the longest insulin-treated tibiotarsus measured is always shorter than the shortest control tibiotarsus. Thus, there is absolutely no overlap between the two groups. Roughly speaking, control bones are always about twice as long as insulin-treated bones of the same chronological age.

In absolute terms, the length values for control tibiotarsi obtained here are comparable to those compiled by Romanoff (1960), while the values for insulin-treated tibiotarsi roughly parallel those of Sevastikoglou (1963a) and Erhard (1959).

If one examines fig. 2 and considers only the values for insulin-treated tibiotarsi at days 15 to 20, one could plot a curve more nearly parallel to the control curve. This observation suggests recovery from the growth retardant effects of insulin, as the growth rate would then more closely match that of control bones, rather than be of

FIGURE 2**GROWTH OF TIBIOTARSI**

lower slope. This may bear some relationship to Zwillling's (1948) report that injection of insulin into the yolk at 120 hours of incubation leads to a marked hypoglycemia which lasts until about the 14th day of incubation, after which there is recovery to normal blood sugar levels.

#### Cell Diameters, Areas and Amount of Matrix/Cell

The results of measurements of hypertrophic cell diameters, areas and amount of matrix per hypertrophic chondrocyte are given in Tables 13 and 14, and mean values for control and insulin-treated cells are compared in Table 15. From this data, the following conclusions may be drawn:

1. In the insulin-treated tibiotarsi, the hypertrophic chondrocytes are slightly smaller (mean diameter of 16.5 micra) than their control counterparts (mean diameter of 17.3 micra).
2. There are more cells in a given field area for insulin-treated cells than cells from control sources (mean values of 22.9 and 18.0 cells per 10,000 square micra, respectively).
3. There is 39.7% more matrix per individual hypertrophic chondrocyte in the control group than in the insulin-treated group (mean values of 338 and 242 square micra of matrix/cell, respectively).

These differences in cell size, number and amount of matrix/cell are all statistically significant, according to the standard error of the difference ( $SE_{diff}$ ) between mean values, since the calculated values for  $diff/SE_{diff}$  all exceed three (Stanley, 1963).

Control cell diameters appeared to show some fluctuation

from day-to-day (Table 13), while insulin-treated cell diameters seemed to increase with incubation (Table 14), perhaps signifying a recovery from the effects of insulin and a return to full hypertrophy.

The above findings thus confirm those of Anderson et al (1959), whose measurements were based exclusively on hypertrophic cartilage from embryos after 18 days incubation. These same authors found no differences in cell densities or cell diameters in the other regions of the cartilage. Excluding the large erosion areas of the insulin-treated tibiotarsi, this is probably also true for the material in this present study, although no measurement studies were made.

## Histology and Cartilage Matrix Histochemistry

Photomicrographs illustrating the results obtained with aldehyde fuchsin, toluidine blue, alcian blue, and alcian blue-alcian yellow are presented in figs. 32-91. Comprehensive figure legends accompany these illustrations, and it is suggested that these be examined in sequence for an overall comparison of tibiotarsal histogenesis in control and insulin-treated embryos. This section will focus attention on certain selected aspects of development under the following sub-headings:

- a. Growth Plate and Epiphyseal Cartilage
- b. Cartilage Resorption and Marrow Cavity Formation
- c. Joint Formation
- d. Tibiotarsal Angulations

### a. Growth Plate and Epiphyseal Cartilage

#### Control tibiotarsi

At day 8 of incubation it is possible to recognize the two cell types comprising the growth plate: the flattened proliferative zone cartilage (fig. 32), although the cells are still somewhat elliptical, and secondly, the incompletely enlarged hypertrophic cells (fig. 33). The epiphyseal cartilage consists of small spherical cells, in places not yet fully distinct from the surrounding mesenchyme (fig. 32).

The staining properties of these three cartilage zones is uniform with the four staining techniques under discussion, at least for the subsequent several days of development. During these early stages

it is often difficult to decide where small-celled epiphyseal cartilage ends and proliferative zone cells begin. By the 12th day of incubation the three zones are readily distinguishable on the basis of morphology alone (fig. 56), and further demarcation of epiphyseal cartilage from growth plate cartilage (on the basis of toluidine blue staining of matrix ground substance) is completed by day 13 (fig. 61).

Still later in incubation, strong staining differences between cartilage of the epiphysis and of the growth plate become apparent (figs. 80, 81, 87). Towards the end of the incubation period, cells of the growth plate become arranged in parallel rows, and this may be seen in figs. 87, 88.

Epiphyseal cartilage at first shows uniform staining of matrix with all techniques employed. By day 15, however, matrix staining of this region of the cartilage becomes irregular with alcian blue (fig. 74-A). Controlled pH staining with alcian blue-alcian yellow reveals some areas of matrix to be richer in sulphate groups than others (fig. 74-B). During this time, proliferative and hypertrophic cartilage matrix stains uniformly bluish-green.

#### Insulin-treated tibiotarsi

Just  $2\frac{1}{2}$  days after exposure to insulin, major differences exist in the structure and organization of tibiotarsal cartilage in insulin-treated embryos (figs. 34, 35). The beginnings of necrosis are present in the central portion of the cartilage mass: intact matrix and cells at the edges give way to pyknotic cells embedded in a thinned matrix. Further, the epiphyseal cartilage is even less well defined than in 8-day control

50

bones (fig. 34).

This pattern of cartilage necrosis occurs in both epiphyses, although the degeneration appears to be more severe in the proximal epiphysis (e.g. fig. 45).

There would seem to be two forms which the necrosis may assume, although they may represent alternate features of the same pathology. In the first of these two forms, three zones may be distinctly recognized at the edge of the necrotic regions:

- i. Laterally, normal chondrocytes of epiphyseal, proliferative or hypertrophic cartilages, depending on the level under consideration. This corresponds to the "Randzone" described by Erhard (1959).

- ii. Centrally, a zone of decreased matrix, where the staining properties of the matrix may differ from the rest of the cartilage (fig. 68), and the orientation of the cells is frequently at right angles to the normal lateral cartilage. ("Zwischenzone", Erhard, 1959).

- iii. Medially, the actual necrosis region where the matrix is considerably less dense than normal, and is fibrillar or vacuolar. Cells here may appear relatively normal (figs. 77, 78) or, more frequently, are lysed or reduced to nuclei or dense spherules suggestive of end products of a lysosomal-mediated autophagy. ("Erweichungszone", Erhard, 1959).

Examples of this tripartite zonation associated with the necrotic events in the cartilage may be seen in figs. 41, 48, 68.

In the second pattern of necrosis, there is no central or intermediate zone of reduced matrix; rather, the cells simply "come apart" and disintegrate from the normal condition directly to the necrotic. This is seen in figs. 35, 46, 55.



The material in the center of the necrotic area evidently has its origins in normal cartilage; the staining properties of this material is identical to normal cartilage matrix with respect to mucopolysaccharides, and it is always possible to demonstrate the sequence from normal chondrocytes at the edges of the cartilage mass to the debris in the middle (figs. 35, 41, 48, 55, 59, 68). In this respect, figs. 77 and 78 are particularly illuminating, as they show chondrocytes which retain the lacunae and capsules characteristic of cartilage even under conditions of disintegration.

It must be noted that the overall shape of this cartilage necrosis always conforms to the shape of the epiphysis and/or diaphysis in which it is situated (figs. 34, 38, 40, 45, 46, 53, 54, 58, 65). This provides a valuable clue to the etiology of the necrosis, as will be seen later.

It has been mentioned that normal cartilage zonation is present in the intact cartilage at the edges of the central necrosis; these zones, however, are compressed (figs. 58, 83, 90) or may be difficult to distinguish from one another (fig. 67). Further, up until the time of hatching, growth plate cartilage never shows the normal organization of parallel columns of cells (figs. 89, 90).

These defects of cartilage integrity are present in other hindlimb bones, although not as consistently. As mentioned earlier, this would be a function of the time of injection of the insulin (fig. 1). Occasional profiles of abnormal cartilage of femur and tarsometatarsus may be seen for example in figs. 38, 45.

## b. Cartilage Resorption and Marrow Cavity Formation

### Control tibiotarsi

At the first stage examined (day 8 of incubation), the entire diaphysis consists of a solid cylinder of cartilage, surrounded by a thin sleeve of subperiosteal bone (fig. 32). By the following day, vascular buds have broken through the periosteum from the surrounding mesenchyme and commence erosion or resorption of the hypertrophic cartilage in the mid-diaphysis (figs. 36, 37). Initially, there appears to be no change in the chemical structure of the cartilage matrix which is being broken down by these vascular processes (figs. 36, 37, 42), as shown by staining with alcian blue or toluidine blue. However, staining with aldehyde fuchsin at the 11th day of incubation (fig. 51) reveals decreased dye binding at sites of cartilage resorption.

These subperiosteal vascular buds enter the cartilage in increasing numbers, fusing to form a central structure which is the basis of the future definitive marrow cavity (fig. 50). Finger-like processes extend from this central marrow space towards the epiphyses, forming marrow channels containing blood cells, osteoclasts and osteoblasts (figs. 43, 82). Through the continued resorption of cartilage, the central marrow cavity increases in length with incubation (figs. 57, 65, 73). By the 20th day of incubation, numerous marrow channels extend to the level of the proliferative zone of the growth plate (figs. 85, 88). As Fell (1925) has pointed out, the eroded cartilage is not replaced by bony trabeculae, as is the case with mammalian long bones.

### Insulin-treated tibiotarsi

Erosion of diaphyseal cartilage by subperiosteal vascular buds initially follows a similar time course to control tibiotarsi (figs. 39, 45) but formation of the central or definitive marrow cavity is delayed. While the control bones possess a central marrow cavity at day 11 of incubation (fig. 50), insulin-treated bones still have a considerable amount of cartilaginous tissue in the mid-diaphysis at this time (figs. 53, 54). Further, this central cartilage persists for several days further (fig. 65).

Towards the end of the incubation period, however, advance of the marrow channels towards the epiphyses exceeds the rate of control specimens (figs. 60, 83). This occurs once the marrow reaches the level of the necrotic areas in the cartilage: encountering little resistance to advance because of the decreased amount of cells and matrix, the marrow quickly reaches the level of the epiphyseal cartilage. Erhard (1959) has reported marrow channels reaching the proximal epiphyseal cartilage by the 12th day of incubation, but this was not the case in the present material, since a definitive central marrow cavity had not yet formed.

### c. Joint Formation

Two defects in normal joint formation have been noted among insulin-treated tibiotarsi. The first of these involves the persistence of a thick strand of fibrous material across the joint space to the femur, forming a syndesmosis (figs. 53, 83, 88). The presence of this material would evidently restrict normal joint movement, thus contributing to the

rigid outstretched appearance of hindlimbs in many embryos (see whole mount photographs). Erhard (1959) considers this to be the chief reason for leg stiffness.

The second type of joint pathology involves extension of the cartilage necrosis across adjacent epiphyses (tibiotarsus and femur or tibiotarsus and tarsometatarsus) to form the so-called "Hohlraum" (Erhard, 1959) or "mucoid degeneration" (Duraismami, 1952). This condition may be seen in figs. 38, 45. This "Hohlraum" or hollow may be relatively structureless, but a special condition may exist, as exemplified in fig. 67. Here, there is quite a large space joining the adjacent epiphyses, and it is filled with a highly globular and vacuolated material that takes up cartilage matrix stains, and may contain cells of unknown type and origin (figs. 70, 71).

The above pattern is thus quite different from the normal condition of complete separation of tibiotarsus and femur by the 10th day of incubation (fig. 42. Also, Fell and Canti, 1934).

Interestingly, joint differentiation in vitro is halted after long periods of cultivation, so that the bone rudiments become fused (Fell and Canti, 1934; Fell and Landauer, 1935).

#### d. Tibiotarsal Angulations

As was frequently pointed out (whole mount studies), it is quite common to find one or more bends in the insulin-treated tibiotarsi. Most frequently, this was seen to occur towards the distal epiphysis, although it could occur near both epiphyses or in the middle of the diaphysis.

As a result of the presence of this angulation, bone spicules are laid down asymmetrically, forming a greater mass on the concave side of the bend than on the convex side (figs. 39, 47, 54, 65). Since the spaces in the subperiosteal spicules are the source of the vascular elements that resorb the cartilage, vascular buds were found at abnormally high levels in the growth plate so that, for example, cells of the lower proliferative zone were exposed to the scouring action of vascular buds before hypertrophic cartilage (fig. 47).

Bending of the tibiotarsus after insulin treatment is believed to be a secondary morphogenetic effect of growth dislocations (Landauer, 1953; Erhard, 1959), while the micromelia is not, since Zwilling and DeBell (1950) have shown that nicotinamide alleviates the micromelic effects of insulin without significantly altering the generalized dwarfism.

The observed bending likely stems from a weakening of the structural integrity of the epiphyses as a result of necrotic developments. Thus, as the normal surrounding musculature develops and exerts pull on the tibiotarsus, the latter bends in response to the pull, since its partially hollow epiphyses lack the necessary amount of rigid cartilage matrix. Why the bend is always directed inwards towards the body is less clear; there is the possibility of unequal pull by surrounding muscles and tendons, as suggested by Erhard (1959), but this would require experimental validation. Perhaps the confinement of the egg shell prevents an outward bending of the tibiotarsus and other hindlimb long bones.

Figure 32

Control tibiotarsus, 8 days incubation. Small-celled epiphyseal cartilage (EC) and flattened cells of the proliferative zone (PZ) are present. Matrix staining becomes weaker towards the future articulating surfaces of this proximal epiphysis. Aldehyde fuchsin method. 138X.

Figure 33

Control tibiotarsus, 8 days incubation. Subperiosteal bone (green, arrows) flanks the uniformly stained hypertrophic cartilage of the diaphysis. Aldehyde fuchsin method. 36X.

Figure 34

Insulin-treated tibiotarsus, 8 days incubation, proximal epiphyseal and diaphyseal cartilage. The central region of the cartilage mass shows a breakdown of structure: strands of matrix, still displaying alcianophilia, are found in the most central region where the cells are necrotic (star). An area equivalent to that denoted by the box is shown at higher magnification in fig. 35. Alcian blue method. 144X.

Figure 35

Insulin-treated tibiotarsus, 8 days incubation. Early stage in the genesis of the necrotic events in the cartilage. There is a gradual transition from normal early hypertrophic cartilage (HC) beneath the perichondrium (PE) to a degenerate, elongated cell type, and finally to cellular debris in a tangle of matrix strands which maintain their normal aldehyde fuchsin staining. Phase contrast, aldehyde fuchsin method. 360X.

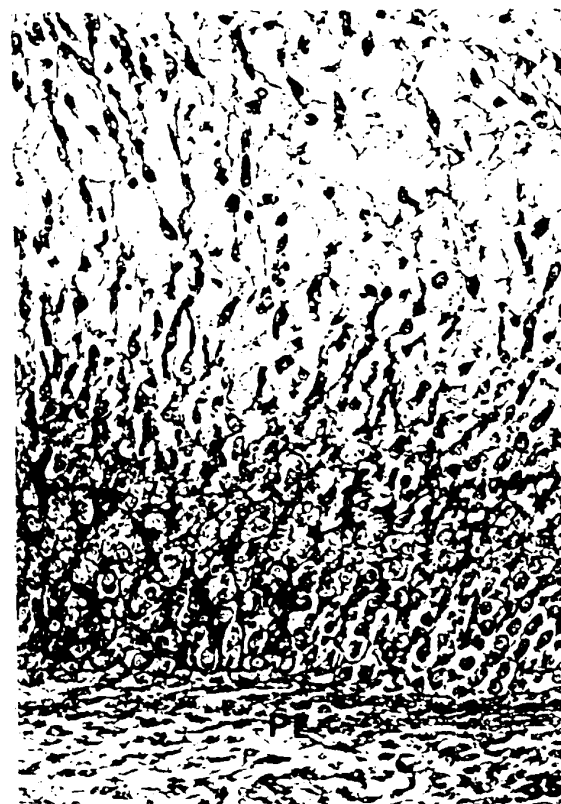
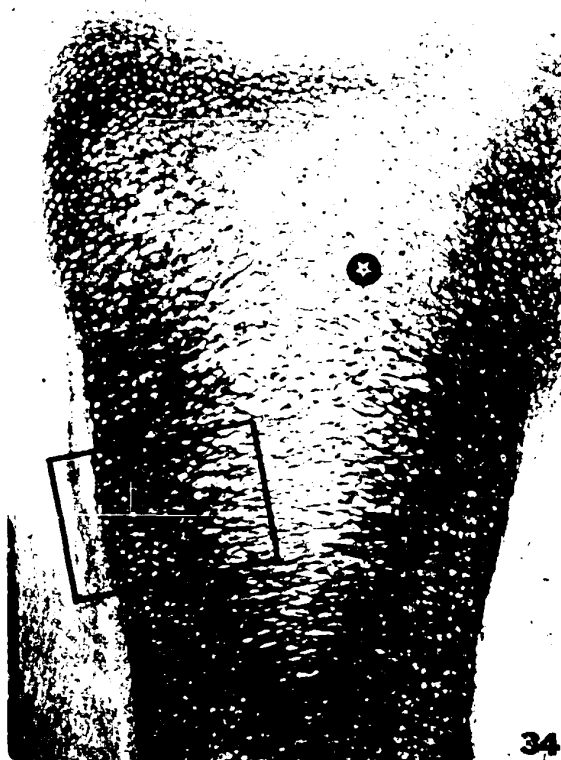


Figure 36

Control tibiotarsus, 9 days incubation, proximal half. Matrix stains uniformly with alcian blue, except for the articular cartilage. Two subperiosteal vascular buds have begun erosion of the mid-diaphyseal hypertrophic cartilage (arrows). Alcian blue method. 36X.

Figure 37

Control tibiotarsus, 9 days incubation, mid-diaphysis. Shows early erosion (surface view) of diaphyseal cartilage by subperiosteal vascular buds. The hypertrophic cartilage matrix retains its metachromasia at the erosion fronts, while subperiosteal bone spicules are orthochromatically stained. Toluidine blue method. 144X.

Figure 38

Insulin-treated tibiotarsus, 9 days incubation. Observe necrosis of the proximal epiphysis, and continuity of this necrosis across the joint space into the distal femoral epiphysis. Hypertrophic cartilage (HC) is homogeneously stained. Aldehyde fuchsin method. 36X.

Figure 39

Insulin-treated tibiotarsus, 9 days incubation. A solid bar of uniformly stained cartilage is present through the diaphysis. Ovoid shaped necrotic areas are present in both epiphyses, and there is an abrupt right-angled bend at the junction of the diaphysis with the distal epiphysis (arrow). Toluidine blue method. 36X.





#### Figure 40

Insulin-treated tibiotarsus, 9 days incubation. Proximal cartilage with necrosis pattern similar to fig. 34. Central region of necrosis appears highly vacuolated, yet the matrix retains the normal alcianophilia, although less intensely stained than the normal cartilage matrix at the edges. An area equivalent to that denoted by the box is seen in fig. 41. Alcian blue method. 144X.

#### Figure 41

Insulin-treated tibiotarsus, 9 days incubation. As in fig. 35 there is a gradual transition of cell morphology from the perichondrium (PE) to the central part of the necrotic area. Between the normal early hypertrophic chondrocytes (HC) and the fully degenerate cell types with thinned matrix is the zone of reduced matrix (zrm). The most central region has the normal aqua coloration of cartilage matrix. Alcian blue-alcian yellow method. 360X.

#### Figure 42

Control tibiotarsus (proximal half), 10 days incubation. Marrow excavation proceeds (arrow), but cartilage is still continuous through the mid-diaphysis. Cartilage matrix is uniformly metachromatic, and more intensely stained just under the periosteum. Cartilage canals (cc) are forming in the epiphyseal cartilage. Toluidine blue method. 36X.

#### Figure 43

Control tibiotarsus, 10 days incubation. Hypertrophic cartilage shows no loss of staining at sites of marrow resorption. Aldehyde fuchsin method. 144X.

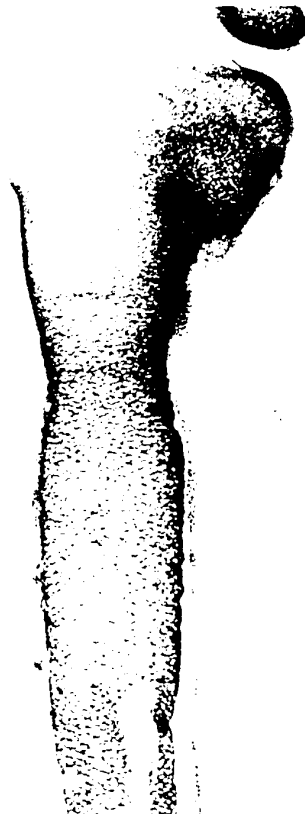
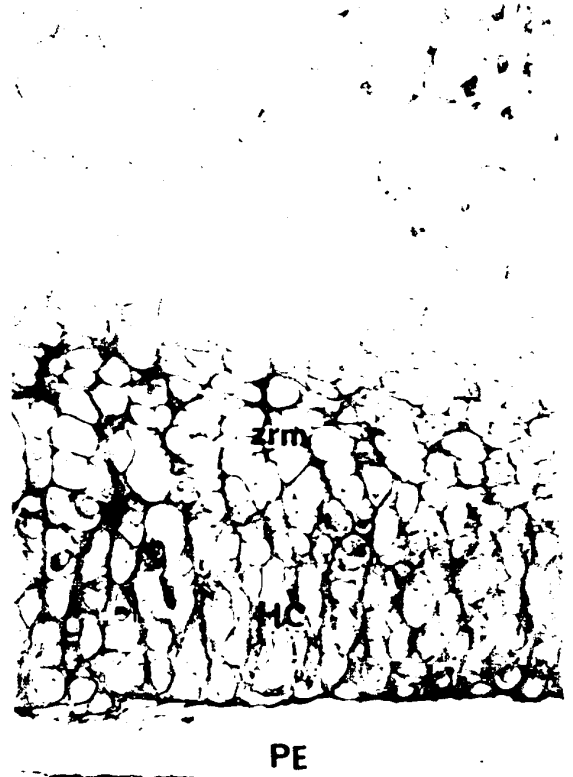
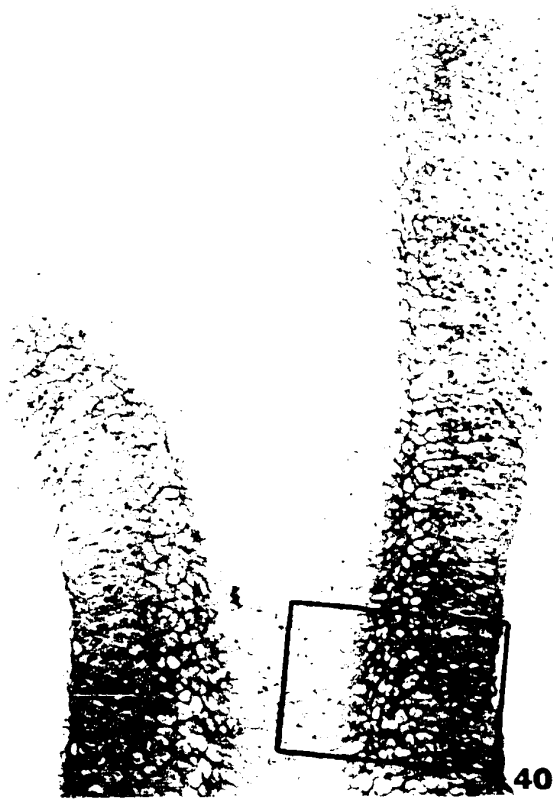


Figure 44

Control tibiotarsus, 10 days incubation. Uniformly stained matrix of mid-diaphyseal hypertrophic chondrocytes, and more lightly stained subperiosteal spicules. Alcian blue method. 144X.

Figure 45

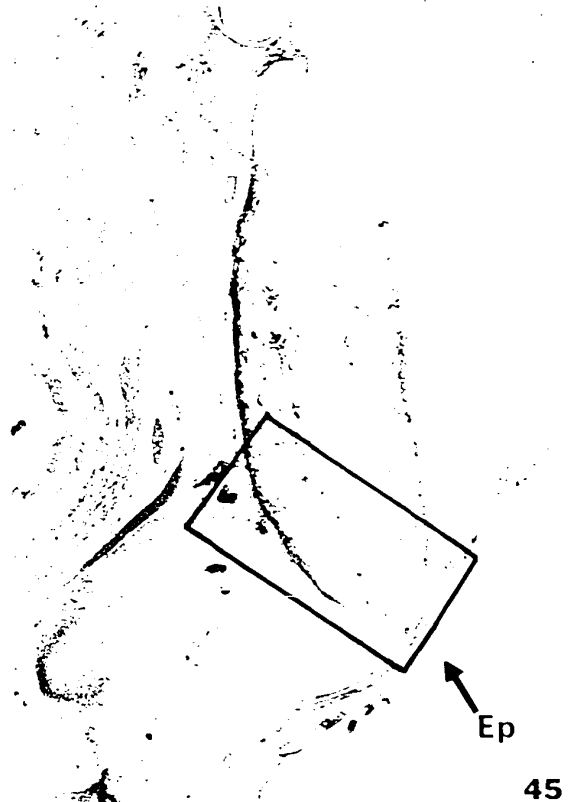
Insulin-treated tibiotarsus, 10 days incubation. Observe bend near the distal epiphysis, bringing the periosteum close to the epidermis (Ep). Both epiphyses are necrotic, and show erosion continuity across both joint spaces to the femur and tarsometatarsus. An area equivalent to that indicated by the box is seen in fig. 47. Aldehyde fuchsin method. 36X.

Figure 46

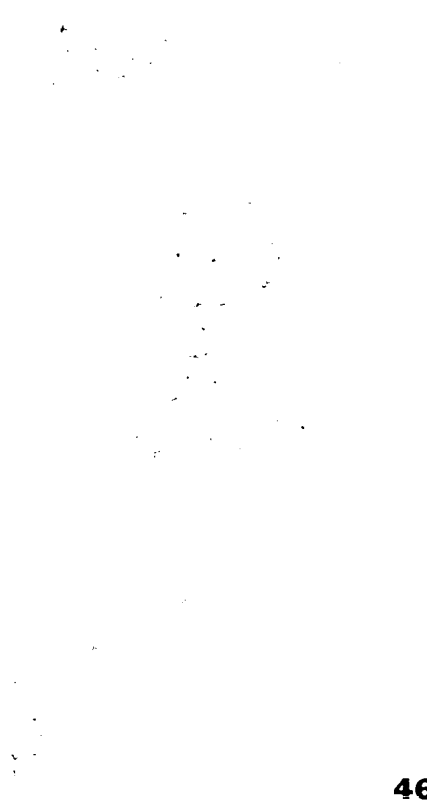
Insulin-treated tibiotarsus, 10 days incubation. Necrosis in proximal epiphysis. Reduced amount of matrix associated with all cells of the epiphysis. Central necrosis area reveals greenish (aqua) strands of matrix plus cellular debris. Alcian blue-alcian yellow method. 144X.

Figure 47

Insulin-treated tibiotarsus, 10 days incubation. Bone spicules fill the concavity at the junction of the diaphysis with the distal epiphysis. In addition, a vascular sprout or bud (vs) has entered at this point to erode the cartilage of the late proliferative zone. Bone spicules are barely stained with alcian blue. Alcian blue method. 144X.



45



46



47

Figure 48

Insulin-treated tibiotarsus, 10 days incubation. Edge of necrosis in the proximal cartilage, at the level of proliferative (PZ) and hypertrophic (HC) zones. As before (fig. 41), note the intermediate type of cells between the normal chondrocytes and the necrotic area. The central region consists of matrix strands and dense spherules. Aldehyde fuchsin method. 360X.

Figure 49

Control tibiotarsus, 11 days incubation, proximal cartilage cone. Uniform alcianophilia of cartilage, except at articulating surfaces (ac=articular cartilage). Note well defined joint between the femur and the tibiotarsus. Alcian blue method. 36X.

Figure 50

Control tibiotarsus, 11 days incubation, mid-diaphysis. A definitive central marrow space (MS) is now present, flanked by subperiosteal bone spicules. Aldehyde fuchsin method. 36X.

Figure 51

Control tibiotarsus, 11 days incubation. Loss of cartilage matrix staining at site of marrow resorption. Bone spicules coloured green. Aldehyde fuchsin method. 144X.

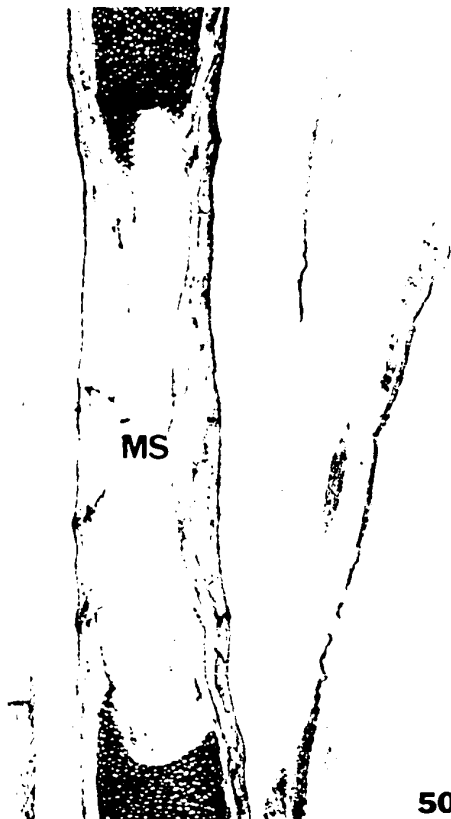
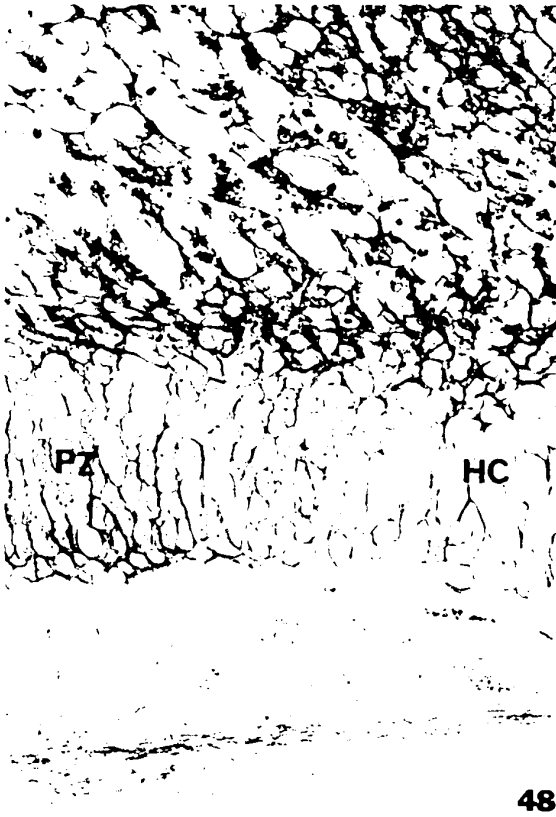


Figure 52

Control tibiotarsus, 11 days incubation. Diaphyseal hypertrophic cartilage is coloured greenish-yellow in the center and somewhat more bluish towards the edges. Alcian blue-alcian yellow method. 144X.

Figure 53

Insulin-treated tibiotarsus, 11 days incubation. Necrosis in both epiphyses. Area comparable to box is seen at higher magnification in fig. 55. Observe conformity of shape of necrotic areas to epiphyseal contours. Note also that cartilage is still present in the mid-diaphysis, unlike controls of the same age (cf. fig. 50). Aldehyde fuchsin method. 36X.

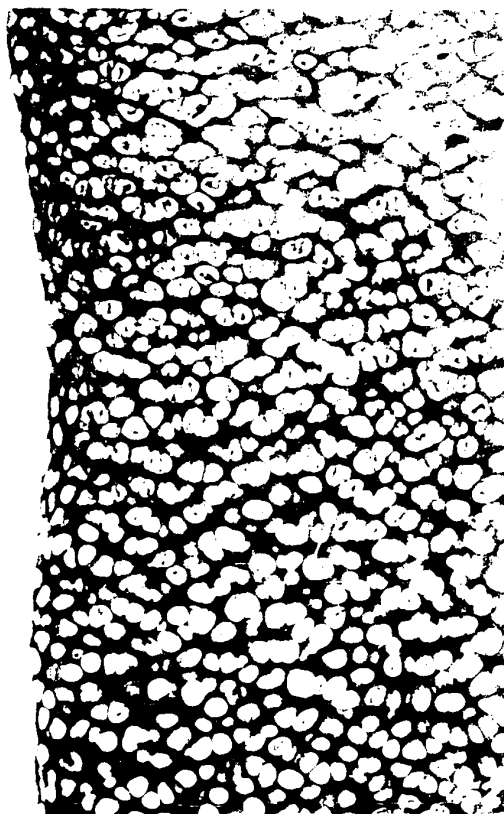
Figure 54

Insulin-treated embryo, 11 days incubation. Necrosis in both proximal tibiotarsus (Tib) and proximal fibula (f). A subperiosteal vascular bud (arrow) is penetrating the necrotic area of the tibiotarsus. Joint formation appears normal in this instance. Cartilage is metachromatic (purple) while bone and muscle are orthochromatic (blue). Toluidine blue method. 36X.

Figure 55

Insulin-treated tibiotarsus, 11 days incubation. Edge of necrosis in proximal cartilage. Here there is no intermediate zone of reduced matrix, but rather a sudden disintegration of cells and matrix. Alcian blue method. 360X.





53



54

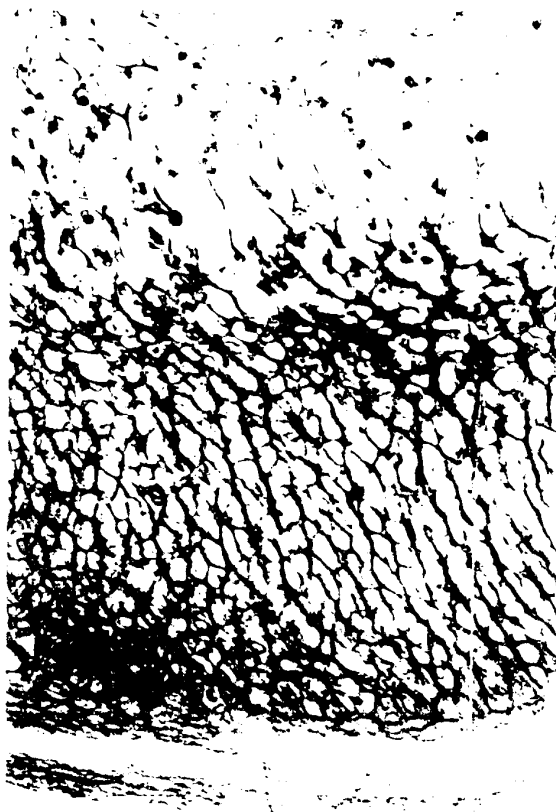


Figure 56

Control tibiotarsus, 12 days incubation, proximal cartilage cone. Three zones are now clearly recognized: small spherical cells of the epiphyseal cartilage (EC), flattened cells of the proliferative zone (PZ), and hypertrophic cartilage (HC). These cartilage zones are all equally metachromatic. Toluidine blue method. 36X.

Figure 57

Control tibiotarsus, 12 days incubation. The central marrow space (MS) continues to lengthen through the cytolytic action of marrow cells (cf. fig. 50, 11 days incubation). The tips of proximal and distal cartilage cones may be seen. Toluidine blue method. 36X.

Figure 58

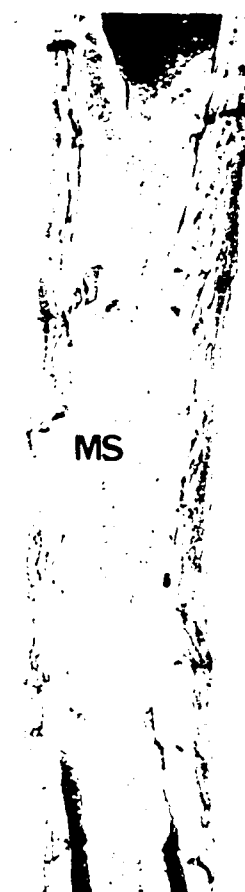
Insulin-treated tibiotarsus, 12 days incubation. Necrosis of proximal cartilage, with alcianophilic matrix strands. As before (cf. figs. 35, 41, 48, 55), there is cell degeneration in a pattern conforming to the epiphyseal contours. Marrow channel (mc) entering the necrotic area, and fibrous material extending across the joint space to the femur (arrow). Alcian blue method. 36X.

Figure 59

Insulin-treated tibiotarsus, 12 days incubation. Edge of necrosis at the level of proliferative (PZ) and hypertrophic cartilages (HC). Note shift in cell axes around central necrosis. The central matrix strands are metachromatic. Toluidine blue method. 144X.



56



57



58

#### Figure 60

Insulin-treated tibiotarsus, 12 days incubation. Region adjacent to that shown in fig. 59. Marrow has entered the central necrotic area. There is no loss of metachromasia in either the normal hypertrophic cartilage (HC) or in the necrotic region (star). Toluidine blue method. 144X.

#### Figure 61

Control tibiotarsus, 13 days incubation, proximal cartilage cone. There is a change in the staining properties over the previous day (fig. 56): epiphyseal cartilage (EC) now stains more intensely than growth plate cartilage (PZ and HC). Toluidine blue method. 36X.

#### Figure 62

Control tibiotarsus, 13 days incubation. Mid-sagittal section showing marrow erosion of hypertrophic cartilage. Cartilage matrix retains the normal greenish-yellow hue. Alcian blue-alcian yellow method. 144X.

#### Figure 63

Control tibiotarsus, 13 days incubation. Grazing section of hypertrophic cartilage, showing a predominantly yellow matrix, suggesting the absence of sulphate at the surface of the diaphyseal cartilage. Alcian blue-alcian yellow method. 144X.

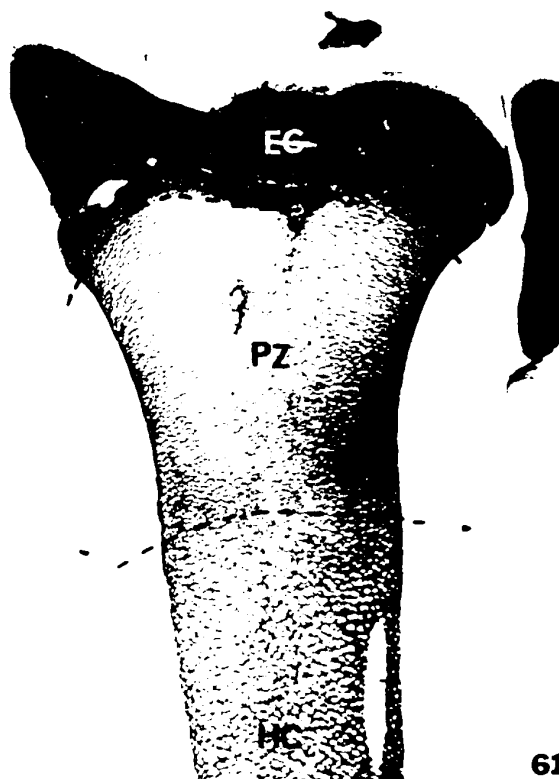


Figure 64

Control tibiotarsus, 13 days incubation. The central marrow space (MS) is well differentiated, containing a variety of cell types. Aldehyde fuchsin method. 36X.

Figure 65

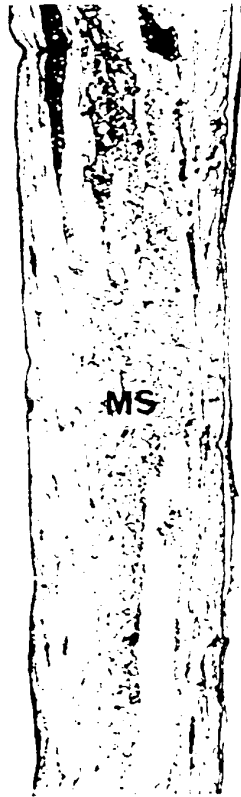
Insulin-treated tibiotarsus, 13 days incubation. Necrosis of both epiphyses, conforming to the epiphyseal contours. Hypertrophic cartilage still present through the diaphysis, so that formation of the central marrow space is delayed by more than two days (cf. fig. 50). Bone spicules are coloured pale blue, and there is a bend near the distal epiphysis. Alcian blue method. 36X.

Figure 66

Insulin-treated tibiotarsus, 13 days incubation. Serial section to fig. 65, of an area equivalent to the box in fig. 65. Note loss of green alcianophilia where marrow cells are eroding the hypertrophic cartilage. With this method of staining at controlled pH, bone spicules do not stain with either alcian dye. Alcian blue-alcian yellow method. 144X.

Figure 67

Insulin-treated tibiotarsus, 13 days incubation. Development of joint frothiness between the proximal tibiotarsus and the distal femur. Note yellow colour of the zone of reduced matrix (zrm), adjacent to the necrotic area (star). See fig. 70 for boxed area. ipt=infrapatellar tissue. Alcian blue-alcian yellow method. 36X.



64

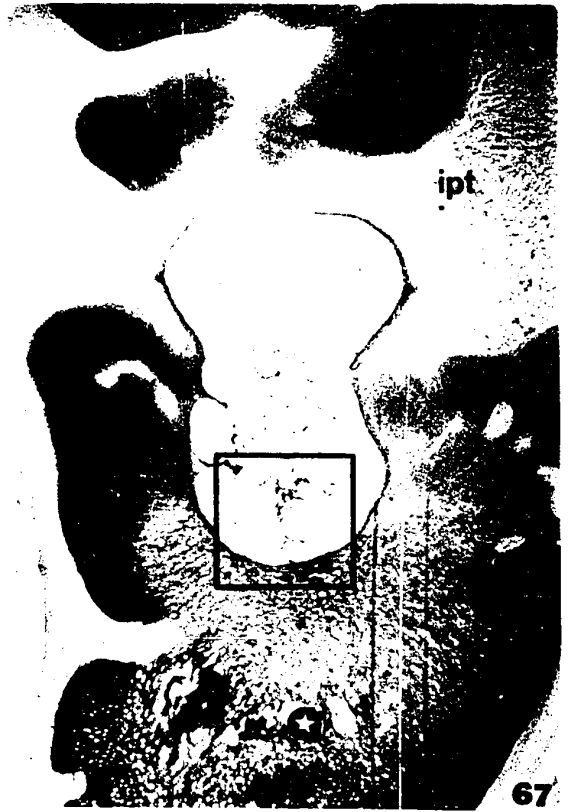


Figure 68

Insulin-treated tibiotalarsus, 13 days incubation. Edge of the proximal epiphyseal necrosis. Note especially the bright yellow colour of the extracellular material in zone of reduced matrix (zrm). Alcian blue-alcian yellow method. 144X.

Figure 69

Insulin-treated tibiotalarsus, 13 days incubation. Central portion of the proximal epiphyseal necrosis, showing the frothy or globular appearance of the matrix, which nevertheless stains green. Alcian blue-alcian yellow method. 360X.

Figure 70

Insulin-treated tibiotalarsus, 13 days incubation. Higher magnification of boxed area in fig. 67. Note amorphous, vacuolated appearance of the material in the joint space. The purple coloration of this material implies its origin from normal cartilage matrix. Extremely elongated cells line the space (arrows). Aldehyde fuchsin method. 144X.

Figure 71

Insulin-treated tibiotalarsus, 13 days incubation. Serial section to fig. 70, showing flattened cells lining the frothiness in the joint space. Inclusions of nuclear fast red-stained cells of unknown type (not erythrocytes) are present in the globular matrix of the joint space. Alcian blue-alcian yellow method. 360X.





PE

68



69



#### Figure 72

Control tibiotarsus, 15 days incubation. Excavation of proximal hypertrophic cartilage by central marrow (MS) elements. Cartilage matrix uniformly purple. Aldehyde fuchsin method. 36X.

#### Figure 73

Control tibiotarsus, 15 days incubation, central diaphysis. Note the thickened collar of subperiosteal bone (cf. figs. 57, 64). Alcian blue method. 36X.

#### Figure 74

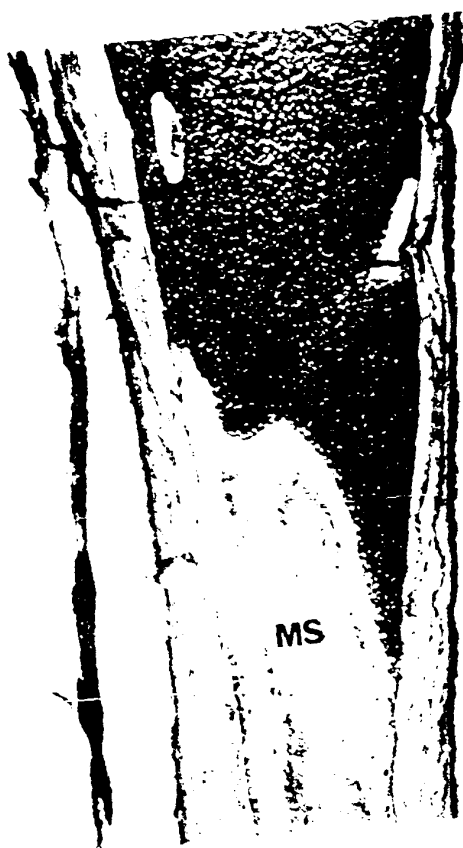
Control tibiotarsus, 15 days incubation. Epiphyseal cartilage (EC) with cartilage canals (cc) and perichondrium (PE).

A - Matrix does not stain uniformly, some areas being more intensely stained than others. Alcian blue method. 100X.

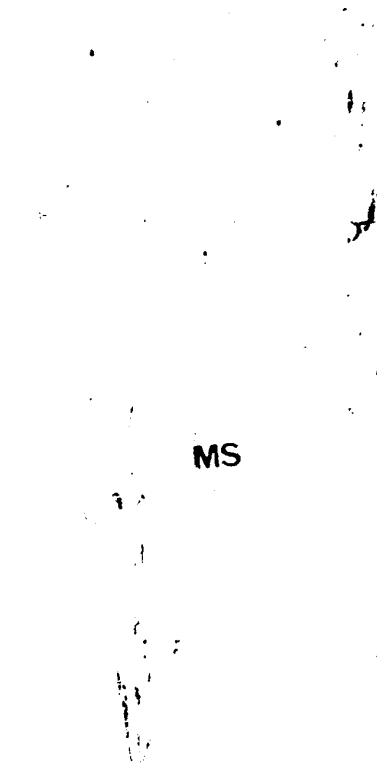
B - Densely stained areas of "A" are here coloured green (primarily the lacunar capsules), while most of the cartilage matrix is yellow. Alcian blue-alcian yellow method. 100X.

#### Figure 75

Insulin-treated tibiotarsus, 15 days incubation. Proximal cartilage cone with central necrosis (star). Some irregularity of matrix staining, especially within the epiphyseal cartilage (EC). Note also the perforating canal (pc) extending between the diaphyseal growth plate and the epiphyseal cartilage. Boxed area shown at higher magnification in fig. 77. Aldehyde fuchsin method. 36X.

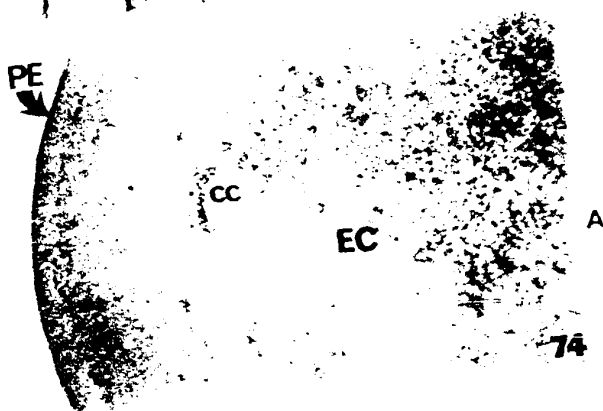


72



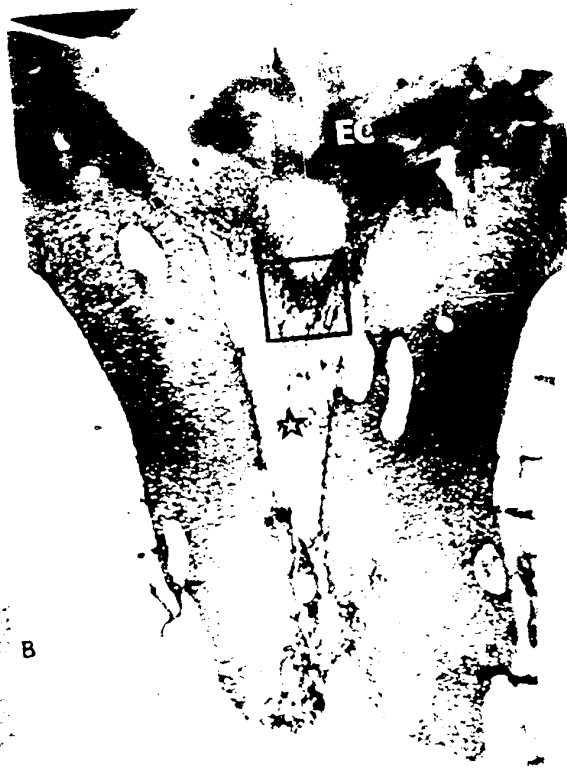
MS

73



A

74



B

74

75

#### Figure 76

Insulin-treated tibiotarsus, 15 days incubation. Resorption of proximal cartilage by marrow (m). Normal hypertrophic pattern for the chondrocytes is altered by the presence of necrosis (star). All cartilage, including the necrotic region, is metachromatic (reddish-purple); subperiosteal spicules (lower right) are orthochromatic (blue). Toluidine blue method. 144X.

#### Figure 77

Insulin-treated tibiotarsus, 15 days incubation. Necrotic region from fig. 75. Note that the chondrocytes retain their darkly-stained lacunar capsules, even when "released" from intact cartilage (arrows). The thin dark strands in the necrosis may represent unmasked collagen bundles. Aldehyde fuchsin method. 360X.

#### Figure 78

Insulin-treated tibiotarsus, 15 days incubation. Chondrocytes from the proximal necrosis of a different embryo than that in fig. 77. Note that the cells show a lacunar halo, and are embedded in a thinned metachromatic fibrillar matrix. Both the absence of darkly-stained capsules and the unmasking of fibers are indicative of reduced matrix ground substance. Toluidine blue method. 576X.

#### Figure 79

Insulin-treated tibiotarsus, 15 days incubation. Increased basophilia around a cartilage canal (cc) in the epiphyseal small-celled cartilage. Toluidine blue method. 360X.

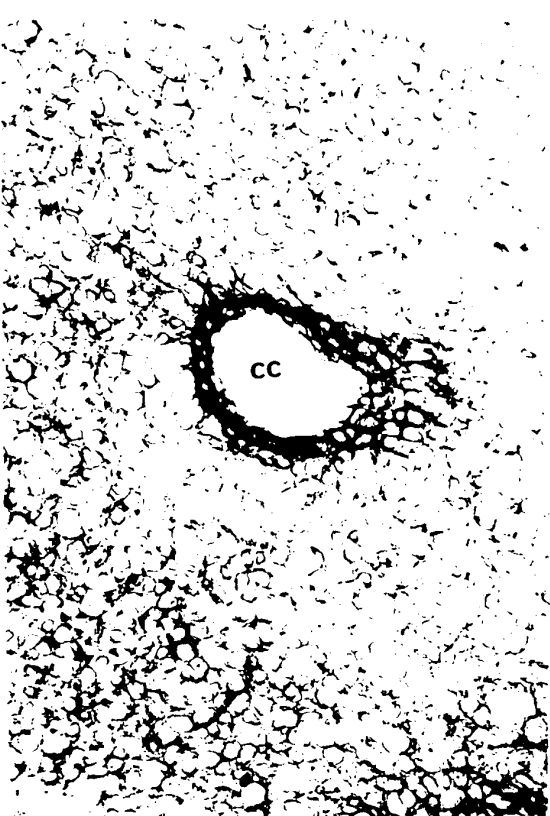
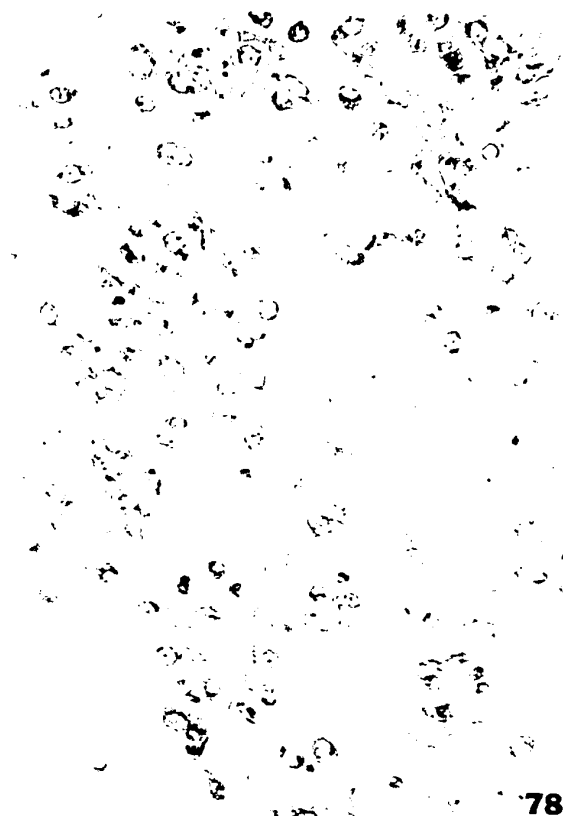


Figure 80

Control tibiotarsus, 17 days incubation. Epiphyseal cartilage (EC) with numerous cartilage canals, and proliferative zone (PZ) of the proximal growth plate. Note weaker staining of epiphyseal cartilage. Aldehyde fuchsin method. 36X.

Figure 81

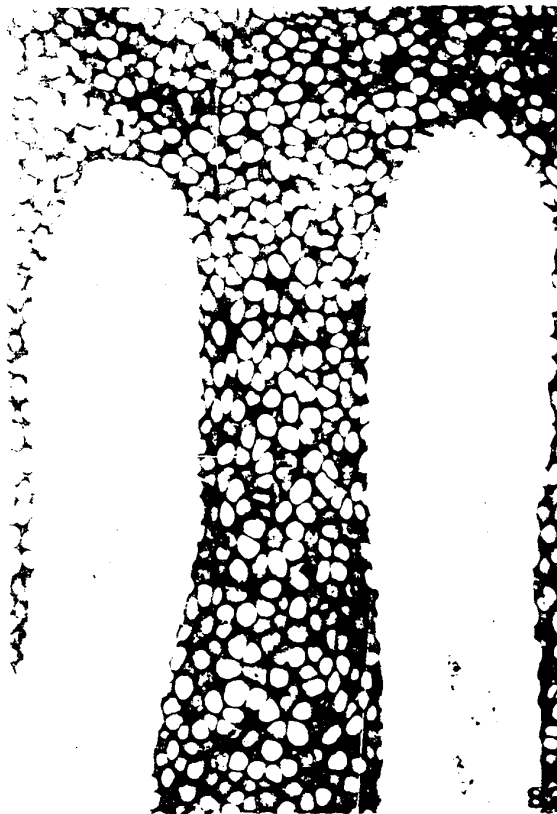
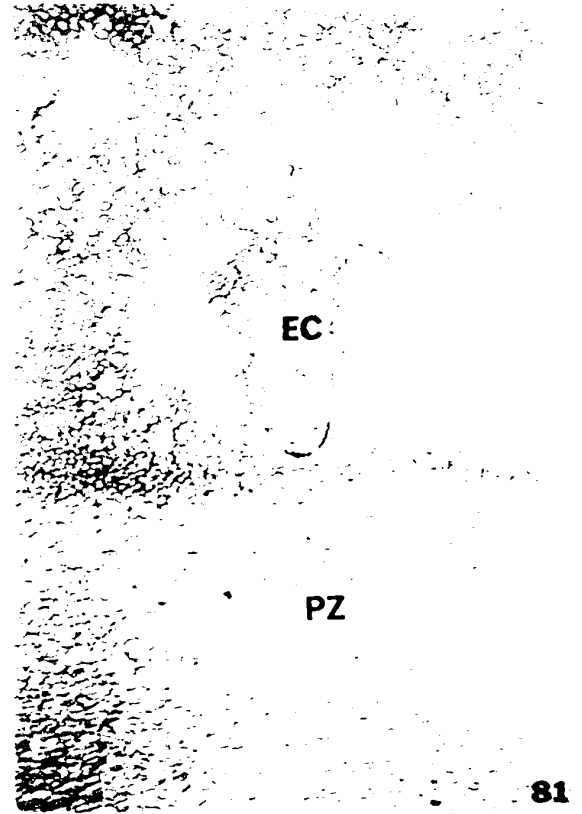
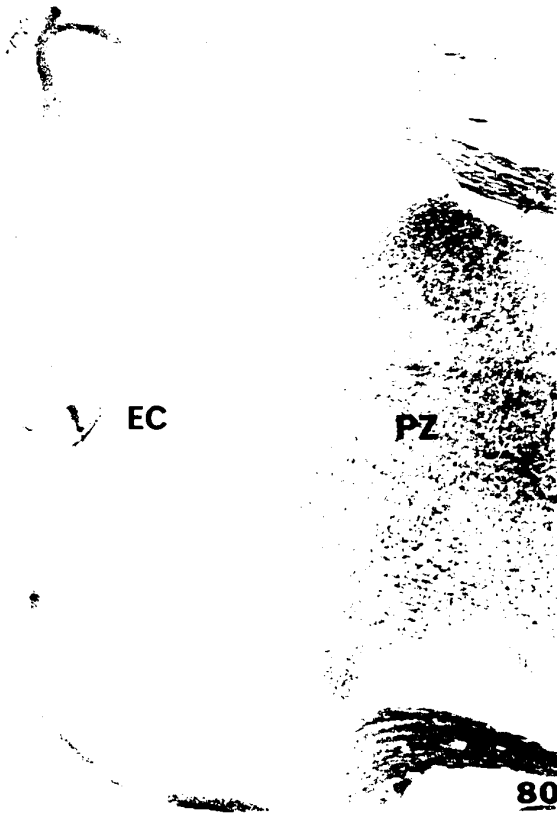
Control tibiotarsus, 17 days incubation. Junction of epiphyseal cartilage (EC) with proliferative cartilage (PZ). Latter matrix stains uniformly bluish, while the former has irregular patches of yellow matrix, suggesting loss of or incomplete sulphation. Alcian blue-alcian yellow matrix. 144X.

Figure 82

Control tibiotarsus, 17 days incubation. Two long marrow channels are seen penetrating the growth plate hypertrophic cartilage, with no loss of alcianophilia of matrix. Alcian blue method. 144X.

Figure 83

Insulin-treated tibiotarsus, 17 days incubation, proximal cartilage cone. Note decreased thicknesses of all zones of the cartilage, as compared with the comparable control at the same magnification in fig. 80. Marrow has completely filled the former central necrosis, so that it is now at the level of the epiphyseal cartilage (arrows). Aldehyde fuchsin method. 36X.



#### Figure 84

Insulin-treated tibiotarsus, 17 days incubation. Bend towards the distal end of the bone, with altered orientation of bone spicules. Note local accumulation of white adipose tissue (A) in the concavity of the angulation (myodystrophy). Aldehyde fuchsin method. 36X.

#### Figure 85

Control tibiotarsus, 20 days incubation. Stain intensity of the various cartilage zones is reversed over that seen in fig. 80, possibly an effect of  $\text{HNO}_3$  decalcification procedures. Note the many marrow channels extending to the level of the junction of hypertrophic cartilage (HC) with proliferative zone cartilage (PZ). Numerous cartilage canals in the epiphyseal cartilage (EC). Aldehyde fuchsin method. 36X.

#### Figure 86

Insulin-treated tibiotarsus, 17 days incubation. Epiphyseal cartilage.

- A - Irregular matrix alcianophilia, as in fig. 74. Alcian blue method. 100X.
- B - Some areas of the matrix show the usual green colour associated with chondroitin sulphate, while other regions display the unsulphated yellow colour (see Appendix E). Alcian blue-alcian yellow method. 100X.

#### Figure 87

Control tibiotarsus, 20 days incubation. Junction of epiphyseal cartilage (EC) with proliferative zone (PZ). Note orderly arrangement of chondrocytes towards the bottom of the photo. Nitric acid decalcification. Aldehyde fuchsin method. 144X.



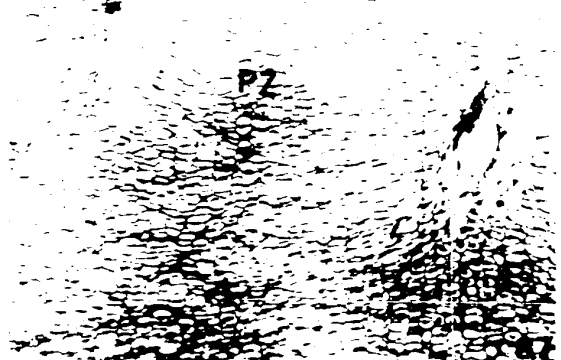
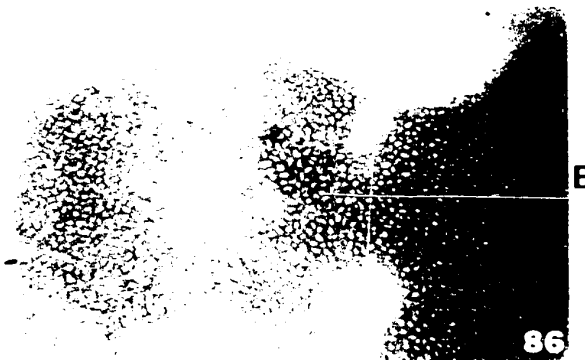
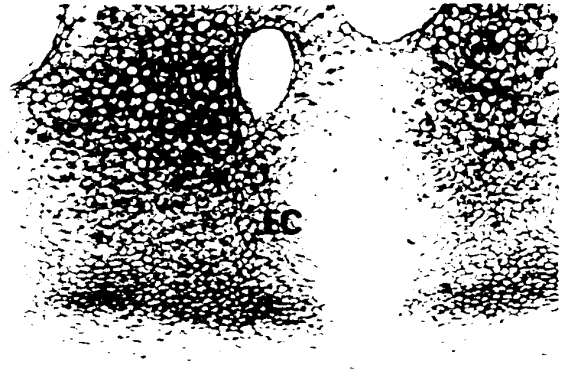
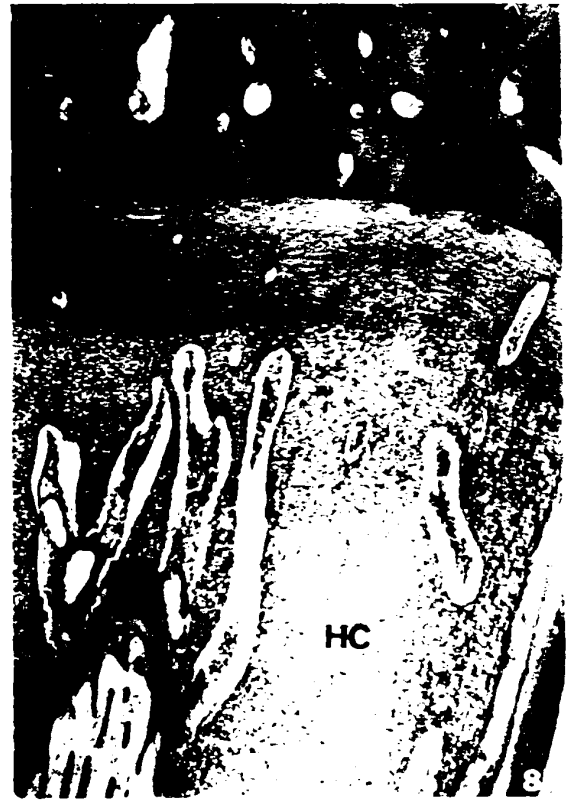


Figure 88

Control tibiotarsus, 20 days incubation. Lower proliferative zone (PZ) and hypertrophic cartilage (HC). Note particularly the rows of chondrocytes, parallel to one another and to the long axis of the tibiotarsus. Nitric acid decalcification. Toluidine blue method. 144X.

Figure 89

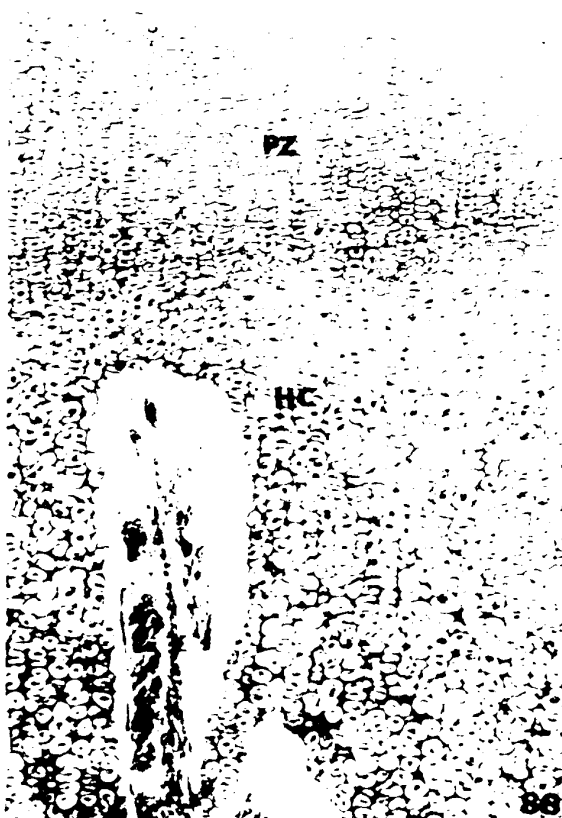
Insulin-treated tibiotarsus, 20 days incubation. Hypertrophic cartilage of growth plate, showing complete lack of row formation. Compare with fig. 88. Nitric acid decalcification. Toluidine blue method. 144X.

Figure 90

Insulin-treated tibiotarsus, 20 days incubation. As in an earlier stage (fig. 83), marrow has broken through to the former necrotic zone and now extends to the level of the thin layer of epiphyseal cartilage (EC). Normal growth plate zonation (PZ and HC) is confined to the edges. Nitric acid decalcification. Alcian blue method. 36X.

Figure 91

Insulin-treated tibiotarsus, 20 days incubation. Bizarre arrangement of subperiosteal bone spicules in the mid-diaphysis, enclosing a portion of the marrow. Arrows indicate the long axis of the tibiotarsus. Nitric acid decalcification. Aldehyde fuchsin method. 36X.



## Glycogen

The presence of glycogen in cartilage was described by Harris (1932), although earlier investigators were aware of its presence, and mentioned it briefly as early as 1859 (Rouget). Its evolution and distribution in endochondral ossification has been described by Gendre (1938), Pritchard (1952), and Schajowicz and Cabrini (1958), just to name a few.

Basically, glycogen levels in cartilage cell cytoplasm increase with chondrification and reach a maximum in hypertrophic cells. In fact, permanent hyaline cartilage retains intense glycogen storage levels indefinitely (Pritchard, 1952). With calcification of cartilage matrix (in mammals) and cellular degeneration, the glycogen content of hypertrophic cartilage is reported to drop sharply (Follis and Berthrong, 1949; Pritchard, 1952). However, Schajowicz and Cabrini (1958) report that under conditions of slow growth, hypertrophic chondrocytes retain their high glycogen levels right up to the cartilage erosion front.

As indicated in the Materials and Methods section, the glycogen content of cells in the present study was assessed by means of the periodic acid-Schiff (PAS) and Best carmine histochemical methods. As previously mentioned, the PAS technique will also stain other substances in addition to glycogen, such as glycoproteins and some mucopolysaccharides. Thus, extracellular (matrix) staining in bone and cartilage, as reported in this section, does not represent glycogen. This is readily shown by diastase digestion (see Appendix F). Representative photomicrographs of the results obtained with the above two methods are given in figs. 92-114.

In the growth plate of control tibiotarsi, small amounts of glycogen are present in the cytoplasm of proliferative zone chondrocytes (figs. 93, 110, 113-A). With further differentiation, glycogen levels rise, so that maximal amounts of PAS-stainable material are present in early hypertrophic cells (figs. 93, 110, 113-B). As the hypertrophic cells mature, the glycogen content is seen to drop to a level no longer detectable with the PAS method (figs. 94, 96, 98, 105, 113-C). The more medial regions of the hypertrophic mass are the first to lose their glycogen (fig. 110).

Small-celled epiphyseal cartilage from control tibiotarsi at first shows little or no intracellular glycogen (fig. 92). The glycogen level increases during the 12th day of incubation (fig. 100), and becomes quite apparent by the 13th day of incubation (fig. 103). At this stage, epiphyseal cartilage matrix (not glycogen) stains with the same intensity as the adjacent proliferative cartilage matrix of the growth plate (fig. 103). At later incubation stages, however, epiphyseal cartilage matrix stains more intensely (fig. 110). Similar changes in the chemical composition of cartilage matrix have already been noted with other staining techniques (e.g. fig. 61), but at an earlier stage of development.

The glycogen pattern for insulin-treated tibiotarsi is somewhat more irregular than control tibiotarsi. The rise and fall of glycogen in the growth plate may parallel that of control cartilage, at least in intact areas (figs. 101, 109, 114) or, less frequently, there may be practically no glycogen in any of the growth plate chondrocytes (fig. 97). Early hypertrophic cells are usually rich in glycogen (figs. 99, 102-A, 114-B) and lose this glycogen when they approach the marrow erosion front (figs. 95, 101, 106, 109, 114-C) or when the matrix around

them becomes calcified (fig. 111).

No glycogen is associated with the cellular debris of the necrotic areas (figs. 97, 99, 101), and the remnants of matrix in this region stain very faintly or not at all with the Schiff reagent. At the edges of the necrosis, the cells may lose their glycogen progressively, paralleling the stages of degeneration (figs. 101, 102-A), or there may be an increase in glycogen immediately prior to disintegration (fig. 107).

The glycogen levels in epiphyseal chondrocytes may be lower than controls (fig. 104) or slightly higher (fig. 114-A).

A striking difference was found in the epiphyseal cartilage of insulin-treated tibiotarsi. Normally, this region consists exclusively of small, spherical cells throughout the incubation period. In the insulin-treated epiphyseal cartilage after 20 days of incubation, regions of hypertrophying chondrocytes were found, showing a progressive accumulation of glycogen with cell enlargement, and then a loss of glycogen concomitant with full hypertrophy (fig. 112). This strongly suggests that a precocious secondary center of ossification has formed and, as will be seen later (fig. 164), the alkaline phosphatase activity in this presumed secondary center follows the course associated with normal ossification.

Throughout the time interval examined, bone matrix from both groups of tibiotarsi always reacts strongly with Schiff reagent. This staining does not represent glycogen, as can be shown by comparison of diastase-digested and undigested sections (figs. 102, 109). It can be clearly seen that the loss of PAS staining in the digested sections

is confined primarily to the cytoplasm of bone and cartilage cells. The bone matrix staining is presumably due to mucoprotein, glycoprotein and non-acidic mucopolysaccharides.

Best carmine staining yielded essentially similar results to PAS staining, except that hypertrophic chondrocyte glycogen seemed to be better demonstrated (fig. 108). However, as tissue fixation differed for each of these two techniques for glycogen, and as considerable difficulty was met in obtaining consistent results with the Best carmine method, quantitative comparisons between the two methods are perhaps not justified.

In summary, no uniform increases or decreases in chondrocyte glycogen were found, contrary to the findings of some previous authors.

Figure 92

Control tibiotarsus, 9 days incubation. Proximal epiphyseal cartilage, with virtually no cytoplasmic PAS staining and a very faint matrix reaction. PAS method. 360X.

Figure 93

Control tibiotarsus, 9 days incubation. Moderate cytoplasmic reaction in early proliferative zone (PZ) chondrocytes, stronger staining in late PZ cells, and intensely stained early hypertrophic chondrocytes (HC). Moderate matrix staining. PAS method. 144X.

Figure 94

Control tibiotarsus, 9 days incubation, mid-diaphysis. The majority of the hypertrophic chondrocytes are PAS-negative, although a few exhibit bright red spherules. Bone matrix is deep red (this staining does not represent glycogen). PAS method. 144X.

Figure 95

Insulin-treated tibiotarsus, 9 days incubation, mid-diaphysis. Virtually no glycogen in any of the hypertrophic chondrocytes. PAS method. 144X.



PZ

HC

93

92

95

Figure 96

Control tibiotalarsus, 10 days incubation, mid-diaphysis. Absence of glycogen in late hypertrophic cells of region which is undergoing marrow excavation. Bone spicules are bright red. PAS method. 144X.

Figure 97

Insulin-treated tibiotalarsus, 10 days incubation. Absence of PAS-stainable material in the necrotic region (star), in the chondrocytes surrounding the necrosis, and in hypertrophic cartilage (HC). PAS method. 144X.

Figure 98

Control tibiotalarsus, 11 days incubation. Marrow excavation of distal cartilage cone, showing absence of glycogen in hypertrophic cells. PAS method. 144X.

Figure 99

Insulin-treated tibiotalarsus, 11 days incubation. Note presence of glycogen in early hypertrophic chondrocytes (HC). No cytoplasmic PAS staining of central necrosis (star) at proximal end of the tibiotalarsus, nor in the zone of reduced matrix (zrm), seen here in surface view. PAS method. 144X.



96

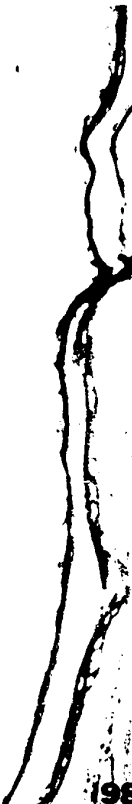


HC

97



98



HC

99



Figure 100

Control tibiotarsus, 12 days incubation. Proximal articular and epiphyseal cartilage. Slight PAS reaction in cells of epiphyseal cartilage. PAS method. 144X.

Figure 101

Insulin-treated tibiotarsus, 12 days incubation, proximal half. Chondrocyte glycogen appear normal in the intact growth plate at the edges of the central necrosis: cytoplasmic glycogen first appears in early proliferative cartilage (1), increases towards the hypertrophic cartilage (2), then decreases towards the marrow resorption front (3). No glycogen in central necrosis. PAS method. 36X.

Figure 102

Insulin-treated tibiotarsus, 12 days incubation. Edge of necrosis in proximal growth plate, at the level of early hypertrophic cartilage.

- A - Note intense glycogen storage in normal hypertrophic cells subjacent to the periosteum. Loss of glycogen in degenerating and necrotic cells. PAS method. 250X.
- B - Equivalent area to "A". Note identical colouration of cartilage matrix and bone, but absence of the intense red cytoplasmic staining seen in "A". PAS method, diastase digestion. 250X.

Figure 103

Control tibiotarsus, 13 days incubation. Epiphyseal (EC) and proliferative (PZ) chondrocytes are both positive for glycogen, and cartilage matrix is uniformly pink in both regions. PAS method. 250X.

Figure 104

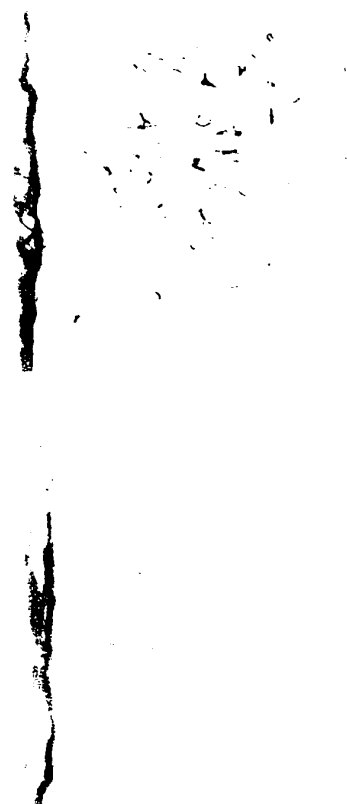
Insulin-treated tibiotarsus, 13 days incubation. Area equivalent to fig. 103. Note decreased epiphyseal cartilage (EC) glycogen. PAS method. 250X.



100



101



102

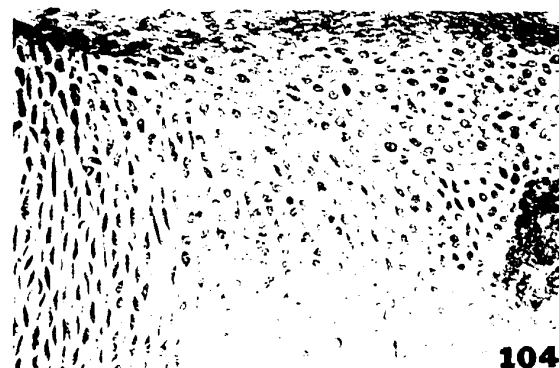
A



103

B

102



104

Figure 105

Control tibiotarsus, 13 days incubation. Diaphyseal hypertrophic cartilage, capped with subperiosteal bone (SB). Chondrocytes lack glycogen, while cartilage matrix is PAS-positive. Bone matrix is strongly PAS-positive. PAS method. 360X.

Figure 106

Insulin-treated tibiotarsus, 13 days incubation. Distal tibiotarsal angulation. Hypertrophic cartilage is PAS-negative, while bone matrix stains deep red. PAS method. 144X.

Figure 107

Insulin-treated tibiotarsus, 13 days incubation. Edge of necrosis at level of proliferative zone cartilage of the growth plate. Note the increased amount of PAS-stainable material in the cytoplasm of the cells at the edge of the necrosis, then an abrupt disappearance of glycogen in the necrotic region proper. PAS method. 360X.

Figure 108

Insulin-treated tibiotarsus, 15 days incubation. Glycogen in hypertrophic chondrocytes at site of marrow resorption. Observe loss of basophilia where marrow is in contact with the cartilage. Best carmine method. 144X.



Figure 109

Insulin-treated tibiotarsus, 17 days incubation, proximal cartilage cone.

- A - Entry of marrow into former necrotic zone (cf. fig. 83). Glycogen present in late proliferative and early hypertrophic zones (arrows). PAS method. 25X.
- B - Removal of diastase-labile material (glycogen) from areas indicated in "A". Colouration of bone and cartilage matrices is unaffected by enzyme treatment. PAS method, diastase digestion. 25X.

Figure 110

Control tibiotarsus, 17 days incubation. Distal epiphysis and growth plate cartilage. Note increased matrix staining with PAS in the epiphyseal cartilage. Cytoplasmic glycogen appears in the proliferative zone, rises to a maximum in the mid-hypertrophic region, then tapers off as the marrow resorption front is approached. PAS method. 36X.

Figure 111

Insulin-treated tibiotarsus, 20 days incubation. Calcified cartilage island in the central marrow cavity. Deeply stained matrix, and absence of cellular glycogen. PAS method. 360X.  $\text{HNO}_3$  decalcification.

Figure 112

Insulin-treated tibiotarsus, 20 days incubation. Nodule of hypertrophic cartilage in the distal epiphysis. The presence of cytoplasmic glycogen in the early hypertrophic cells at the bottom of the photo, and the reduction of cytoplasmic staining as the cells enlarge further suggests that this is a secondary center of ossification (cf. fig. 164). PAS method. 360X.  $\text{HNO}_3$  decalcification.





A



B



Figure 113

Control tibiotarsus, 20 days incubation, illustrating PAS staining at different levels in the cartilage.  $\text{HNO}_3$  decalcification. PAS method. 250X.

- A - Epiphyseal and early proliferative cartilages. Matrix of former more intensely stained. Little cellular glycogen.
- B - Late proliferative and early hypertrophic zones of growth plate. Intensity of matrix staining similar to epiphyseal cartilage. Cells are rich in glycogen. Note row formation (cf. figs. 87, 88).
- C - Late hypertrophic cartilage and marrow front. Although greatly reduced in intensity from above levels, small amounts of glycogen appear in these cells.

Figure 114

Insulin-treated tibiotarsus, 20 days incubation, illustrating PAS staining at different cartilage levels.  $\text{HNO}_3$  decalcification. PAS method. 250X.

- A - Epiphyseal and early proliferative zone cartilages. Somewhat more glycogen in epiphyseal chondrocytes than fig. 113-A.
- B - Late proliferative and early hypertrophic zones. PAS staining similar to fig. 113-B, although the matrix reaction is less intense. Proliferative cells are incompletely flattened, and row formation is absent.
- C - Late hypertrophic cartilage and marrow. No PAS staining of cytoplasm, and equal staining of matrix as in fig. 113-C.

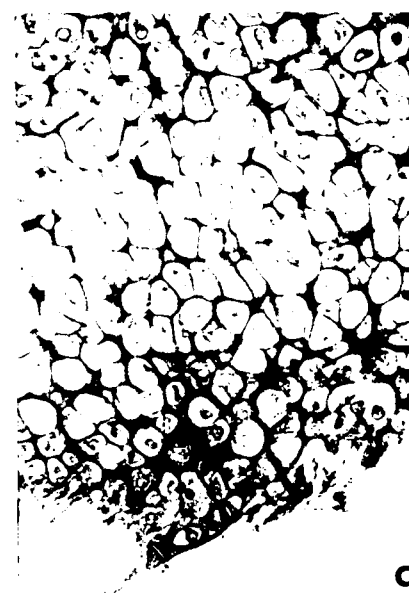
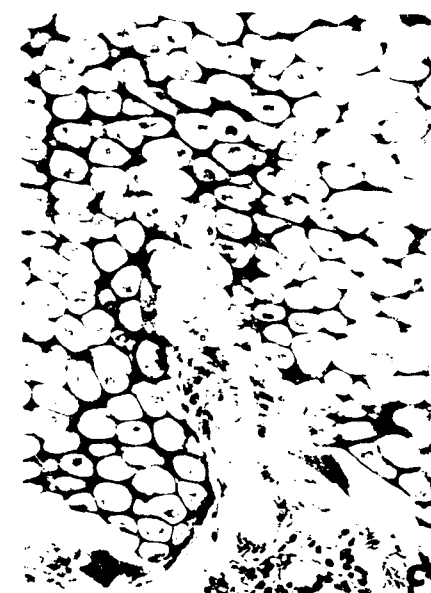
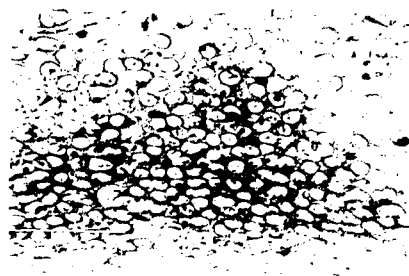
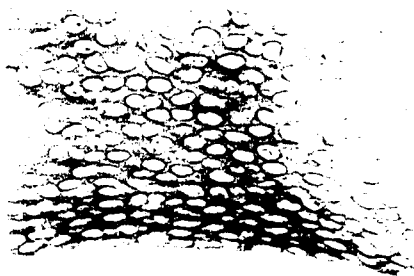


Figure 113

Figure 114

## Microscopic Calcification and Ossification

Representative micrographs illustrating the sequential events of calcification and ossification in control and insulin-treated tibiotarsi are given in two series:

A: Figures 115-132 are survey sections of entire tibiotarsi to show the general development of the mineralization process on a day to day basis.

B: Figures 133-148 are higher magnification photomicrographs demonstrating certain features of particular interest.

Particular details may be found in the accompanying figure legends.

At the earliest stage examined (8 days of incubation), subperiosteal ossification is well underway in control tibiotarsi (fig. 115), forming a calcified collar or sheath of bone around the middle  $1/3$  of the diaphysis. A short segment of osteoid (uncalcified bone) continues from the ends of this collar but does not reach the epiphyses. By contrast, 8 day insulin-treated tibiotarsi have a less intense subperiosteal von Kossa reaction (fig. 116), although this mineralization also occupies approximately  $1/3$  of the total length of the diaphysis.

By the 9th day in control embryos, the bony collar has lengthened further towards the epiphyses, so that some  $2/3$  of the diaphyseal cartilage is surrounded by osseous tissue between it and the periosteum (fig. 117). The pattern for insulin-treated tibiotarsi is roughly similar (fig. 118).

The first indication of differences in calcification patterns between the two groups of tibiotarsi is seen on day 10 of incubation.

Both control and treated specimens continue to expand their subperiosteal ossification activities (figs. 119, 120) but the latter tibiotarsi also show calcification of cartilage matrix (figs. 120, 134) while the former do not. This slight, irregular calcification is associated with necrotic cells of the growth plate, and does not occur among control bones of the same age.

The curvature of the tibiotarsus in insulin-treated embryos leads to changes in the deposition pattern of the mineralized spicules (fig. 120). Instead of the normal, symmetrical deposition of spicules on each side of the diaphyseal cartilage (as seen in longitudinal section), spicules proliferate on the concave sides of the bends, while the convex surfaces are covered only by a thin layer of osseous tissue.

As mid-diaphyseal hypertrophic cartilage continues to be excavated by marrow channels in control tibiotarsi, the thickness of the subperiosteal collar increases, assuming more of an hourglass shape (fig. 121). The bone spicules are organized parallel, or at a slight angle, to the long axis of the tibiotarsus. The insulin-treated tibiotarsi have their spicules oriented in a more irregular fashion, often at right angles to the long axis of the bone (fig. 122) and again there are calcified deposits in cartilage matrix. At higher magnification, it can be seen that normal cartilage matrix does not calcify prior to marrow excavation (fig. 135), while abnormal mineralization in association with penetration of the cartilage by subperiosteal vascular canals may occur in the insulin-treated tibiotarsi (fig. 136).

Subperiosteal ossification of the control tibiotarsi progresses as simple increase in length and thickness of the bony collars

previously described, with no evidence of calcification of any cartilage matrix prior to the 15th day of incubation. In the present material, fibular cartilage matrix was observed to calcify as early as day 12 (fig. 137). This is in accordance with the observation of Fell and Canti (1934) that chondrogenesis is more advanced in the fibula than in the tibiotarsus. At day 13 of incubation, insulin-treated tibiotarsi display foci of calcified cartilage matrix in regions of apparently healthy hypertrophic cartilage which is being resorbed by marrow elements (figs. 126, 139). Nor is this abnormal, precocious pattern confined to the tibiotarsus in the hindlimb, as it may also be found in the femur and tarsometatarsus.

The irregular organization of the fully mineralized bone spicules during days 12 and 13 of incubation may be seen in figs. 124 and 126, as compared to the linear orientation in comparable control tibiotarsi (figs. 123, 125). This difference becomes even more pronounced at later stages (figs. 127-132, survey sections; figs. 145, 146, higher magnification).

The 15th day of incubation marks the first occurrence of deposition of calcium salts in control cartilaginous tissue. The matrix between hypertrophic chondrocytes at the surface of the cartilage cones at each end of the diaphysis, subjacent to subperiosteal bone, becomes calcified to a depth of two to three layers of cells (fig. 142). The timing of this event in the present material is in agreement with the findings of Fell and Robison (1934) and Romanoff (1960), but disagrees with Matukas and Krikos (1968) who state that "calcification was first noted at 16 days in the lateral areas of the hypertrophic zone next to the bone".

In any event, the extent of this lateral cartilage matrix

continues to increase up to the 20th day of incubation (figs. 143, 144), but the bulk of the diaphyseal cartilage of control tibiotarsi is still uncalcified at hatching. Meanwhile, the pattern of calcification for insulin-treated tibiotarsi continues to be accelerated, showing calcification in areas not normally calcified until well after hatching (fig. 130), as well as a deeper lateral matrix reaction.

One final aspect of calcification must be considered. Normally, the epiphyses of chick long bones do not undergo ossification prior to hatching (Romanoff, 1960). In fact, the only secondary center of ossification recognized in avian long bones is the proximal tibiotarsal epiphysis (Haines, 1942). Further, normal cartilage matrix mineralization in endochondral bones is always associated with cellular hypertrophy, and if for some reason the chondrocytes fail to hypertrophy, calcification does not occur (Fell and Landauer, 1935).

Among the insulin-treated tibiotarsi of the present study, however, it was common to find patches of calcified cartilage matrix in small-celled epiphyseal cartilage of 20 day embryos that otherwise appeared normal (fig. 148), or in epiphyseal cartilage that showed signs of "softening" (fig. 147). Curiously, this calcified matrix surrounded small cartilage cells in the distal epiphyses, and not the epiphyseal hypertrophic cells discussed elsewhere (figs. 112, 164). These latter regions may correspond to the secondary centers reported by Landauer (1931) for Creeper fowl.

In summary, there is no evidence of failure of subperiosteal bone formation in the insulin-treated tibiotarsi, nor of prolongation of the osteoid condition beyond the normal small amount associated with early

subperiosteal activities. After an initial retardation of subperiosteal ossification, the rate of ossification becomes accelerated in a fashion similar to Creeper chick embryos, as described by Landauer (1931). These findings are therefore in complete disagreement with Duraiswami's (1950, 1952) diagnosis of osteogenesis imperfecta.

In the present material, mineralization of cartilage is precocious and at times associated with necrotic events of the metaphysis. The configuration of bone spicules in the diaphysis was frequently altered from the normal linear pattern.

Glucksmann (1942) has analyzed the bending of long bone rudiments in organ culture, and found that bends can be induced by mechanically obstructing a long bone at each epiphysis. In these cases, the long bone develops a bend and shows greater ossification on the concave side of the bend than on the convex side. As well, the bone spicules on the concave side are aligned at right angles to the long axis of the developing rudiment. This effect is morphologically identical to that found in the insulin-treated tibiotarsi of the present study, and the mechanical factors responsible for creating the conditions of unequal stress on the growing tibiotarsus have already been mentioned.



Figure 115

Control tibiotarsus, 8 days incubation. Observe the calcified bone spicules (black) between the periosteum (pe) and hypertrophic cartilage (hc) in the mid-diaphysis. Von Kossa method. 340X.

Figure 116

Insulin-treated tibiotarsus, 8 days incubation. The amount and intensity of mineralized material between the periosteum and hypertrophic cartilage is reduced, as compared to fig. 115, forming only a thin dark grey line. Note also the smaller size of the mid-diaphyseal hypertrophic chondrocytes. Von Kossa method. 340X.

Figure 117

Control tibiotarsus, 9 days incubation. This survey section shows subperiosteal ossification now occupying approximately 2/3 of the total length of the diaphysis. The dark spots in the distal (left side) epiphysis are cartilage canals, while the dark lines at each end of the diaphysis are artifactual folds in the tissue. Von Kossa method. 14X.

Figure 118

Insulin-treated tibiotarsus, 9 days incubation, survey section. The tibiotarsus is continuous with the femur (F) and tarsometatarsus (Tm) across the joint spaces. Dashed lines indicate the limits of the tibiotarsus. The large calcified mass (arrow) is a grazing section of subperiosteal bone. Von Kossa method. 14X.

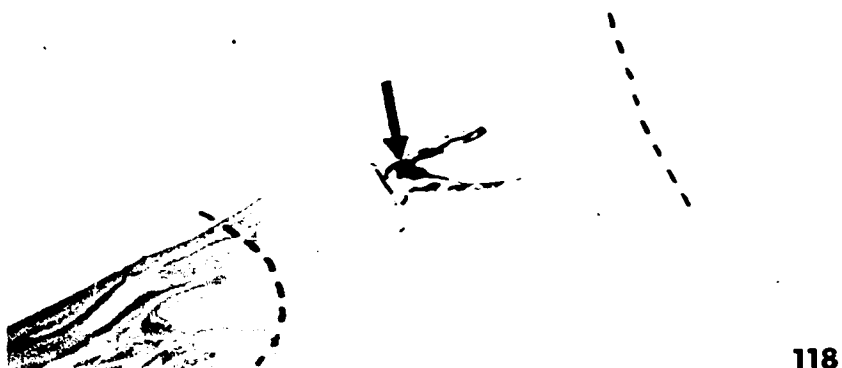


Figure 119

Control tibiotarsus, 10 days incubation, survey section. A few more bone spicules are seen than in the preceeding day. A bar of cartilage still extends across the mid-diaphysis, although not indicated in this particular section. Von Kossa method. 14X.

Figure 120

Insulin-treated tibiotarsus, 10 days incubation, mid-sagittal survey section. The extent of subperiosteal ossification appears somewhat greater, particularly in the concavities of the bends at each end, than in the control bone of the same age. Some calcification of distal cartilage matrix (arrow), seen again at higher magnification in fig. 134. Von Kossa method. 14X.

Figure 121

Control tibiotarsus, 11 days incubation, survey section. The number of calcified bone spicules has increased over the preceeding day, so that a thicker subperiosteal bone collar surrounds the remaining cartilage model. There is as yet no calcified cartilage (cf. fig. 135). Von Kossa method. 14X.

Figure 122

Insulin-treated tibiotarsus, 11 days incubation, survey section. In addition to the usual subperiosteal ossification, a region of calcified cartilage matrix is present in the proximal diaphyseal cartilage (arrow). This same area is seen at higher magnification in fig. 136. Von Kossa method. 14X.



119



120



121



122

Figure 123

Control tibiotarsus, 12 days incubation, mid-sagittal survey section. A definitive central marrow cavity has formed in the mid-diaphysis, flanked by subperiosteal bone. No calcified cartilage matrix. Von Kossa method. 14X.

Figure 124

Insulin-treated tibiotarsus, 12 days incubation, survey section grazing diaphysis. Note anastomosing bone spicules over the mid-diaphysis. Subperiosteal ossification has not spread quite as far towards the epiphyses as in fig. 123. Von Kossa method. 14X.

Figure 125

Control tibiotarsus, 13 days incubation, survey section grazing diaphysis. Diaphyseal ossification continues to proceed towards the epiphyses, and the tips of the cartilage cones are covered with calcified bone matrix (arrow). Cartilage remains unmineralized. Von Kossa method. 14X.

Figure 126

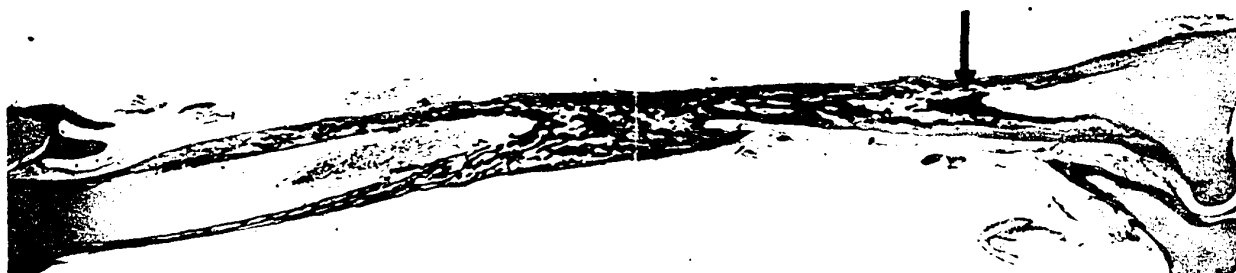
Insulin-treated tibiotarsus, 13 days incubation, survey section grazing diaphysis. Again there are patches of calcified cartilage matrix (arrows). A more mid-sagittal section would reveal that the proximal and distal cartilage cones seen here are in fact a continuous mass extending through the diaphysis. Von Kossa method. 14X.



123



124



125



126

Figure 127

Control tibiotarsus, 15 days incubation, survey section, not quite mid-sagittal. Marrow resorption of the cartilage cones is well advanced, as is the ingrowth of subperiosteal spicules. The center of the diaphysis is not occluded with spicules, as the photo suggests, but is simply an effect of the plane of section. The mineralized spicules are oriented for the most part in a direction parallel to the long axis of the tibiotarsus. Von Kossa method. 11.5X.

Figure 128

Insulin-treated tibiotarsus, 15 days incubation, mid-sagittal section. Note the altered direction of many of the spicules, especially in the concavities of the bends, and the patch of calcified cartilage matrix (arrow), seen at higher magnification in fig. 140. Von Kossa method. 14X.

Figure 129

Control tibiotarsus, 17 days incubation. A solid sheath of interlacing bone spicules fills the diaphysis, interrupted only by the central marrow cavity (not in plane of section). Cartilage matrix calcification is apparent at the lateral borders of the cartilage cones (arrow). Von Kossa method. 9X.

Figure 130

Insulin-treated tibiotarsus, 17 days incubation, grazing diaphysis. Many of the mineralized spicules are oriented at right angles to the long axis of the tibiotarsus. Calcified cartilage is present (arrows). Von Kossa method. 9X.



127



128



129



130

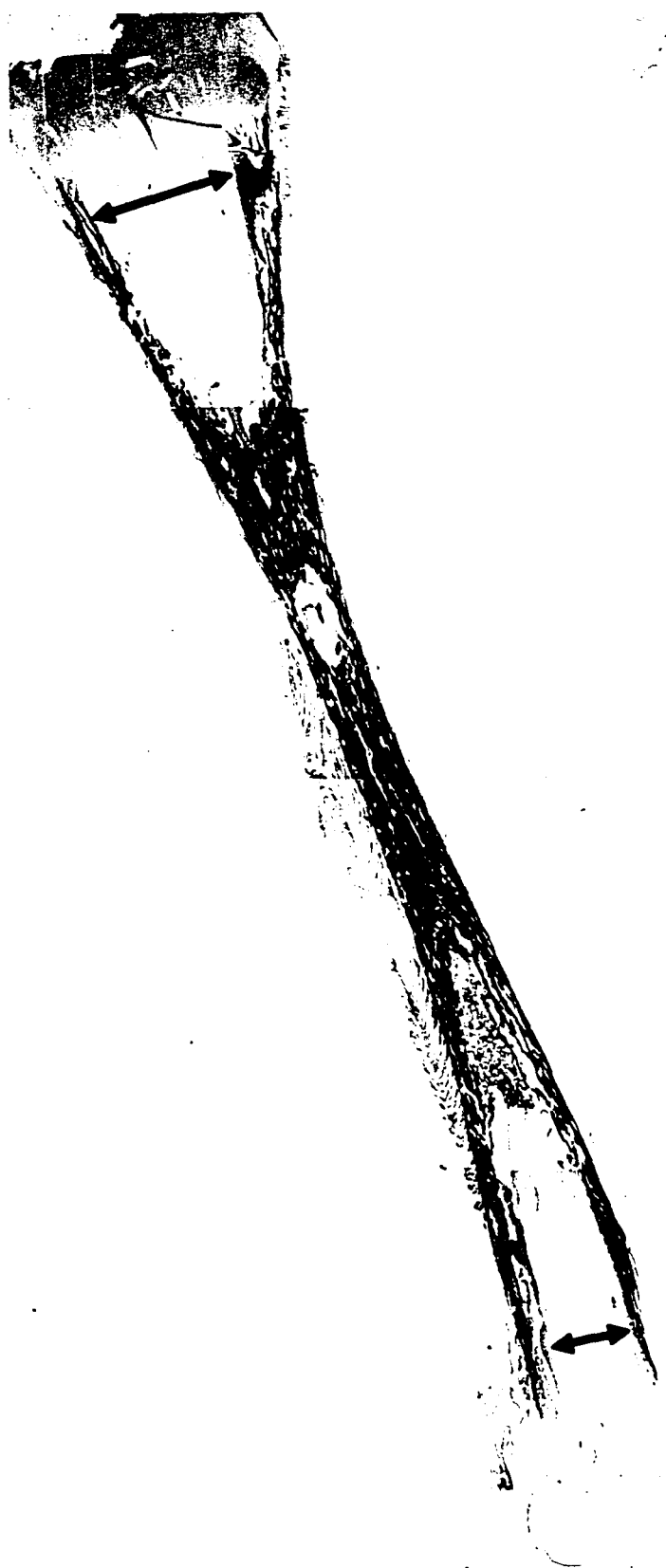


Figure 131

Control tibiotarsus, 20 days incubation. Complete longitudinal section, grazing the diaphysis. The extent of lateral cartilage matrix calcification (arrows) has increased over the previous day; this is seen at higher magnification in fig. 144. No calcification is seen in the small-celled cartilage of the epiphyses (the numerous darkly-stained structures seen in the distal epiphysis are cartilage canals). Von Kossa method. 6.8X.

Figure 132

Insulin-treated tibiotarsus, 20 days incubation. This severely stunted specimen (same magnification as fig. 131) shows lateral calcification of cartilage matrix to a greater extent than the comparable control (arrows). Although not seen in this particular section, calcification has occurred at this stage in the small-celled cartilage of the epiphyses (see figs. 147, 148). Von Kossa method. 6.8X.

**131****132**

proximal



distal

Figure 133

Control tibiotarsus, 10 days incubation. Note the periosteum (pe) in the diaphysis, with its underlying dark line of calcified bone. The large dark area on the left is not calcified cartilage, but subperiosteal bone, seen in superficial grazing section. Von Kossa method. 146X.

Figure 134

Insulin-treated tibiotarsus, 10 days incubation. This section, from the angulation region of the distal tibiotarsus, shows sparse irregular cartilage matrix calcification (arrows) between the necrotic zone (star) and normal hypertrophic cartilage (HC). Note also the increased subperiosteal ossification on the concave side of the bend. Von Kossa method. 146X.

Figure 135

Control tibiotarsus, 11 days incubation. This section shows a marrow channel (mc) penetrating the hypertrophic cartilage near the middle of the diaphysis. Note that cartilage remains unmineralized. Von Kossa method. 146X.

Figure 136

Insulin-treated tibiotarsus, 11 days incubation. Note intense, irregular calcification of cartilage matrix where a subperiosteal vascular bud is in contact with the proximal end of the diaphyseal cartilage. Von Kossa method. 146X.

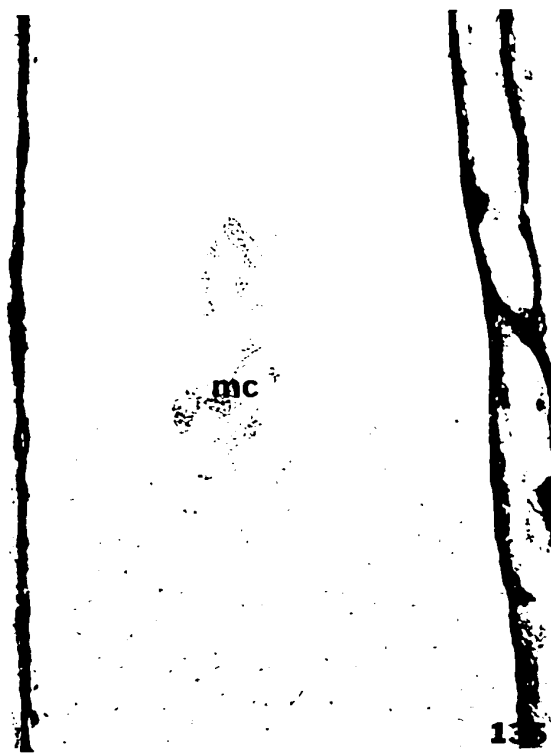
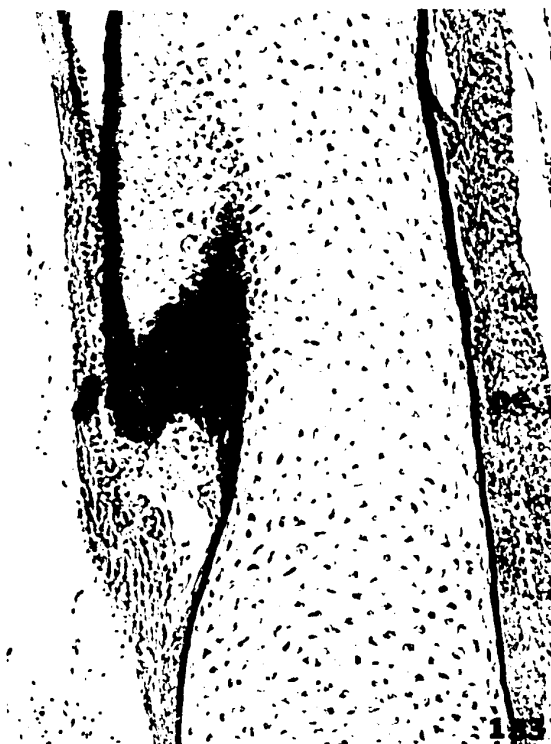


Figure 137

Control fibula, 12 days incubation. This illustrates the earlier calcification of fibular cartilage matrix than tibiotarsal cartilage matrix, the latter not showing calcified deposits until three days later. Note the uniformity of mineral deposition around the chondrocytes. Von Kossa method. 132X.

Figure 138

Insulin-treated tarsometatarsus, 13 days incubation. Note the heavy irregular calcification of cartilage matrix at the tip of the distal cartilage cone. Observe also that this calcification occurs in the medial region of the cartilage mass, while in control bones it occurs more laterally. Von Kossa method. 146X.

Figure 139

Insulin-treated tibiotarsus, 13 days incubation. Once again, note the intense irregular cartilage calcification characteristic of hind-limb bones from embryos exposed to insulin. Von Kossa method. 146X.

Figure 140

Insulin-treated tibiotarsus, 15 days incubation. Cartilage calcification is reduced, as compared to the two previous illustrations, and approaches the normal pattern (fig. 142). This is a higher magnification of a portion of fig. 128. Von Kossa method. 146X.



137

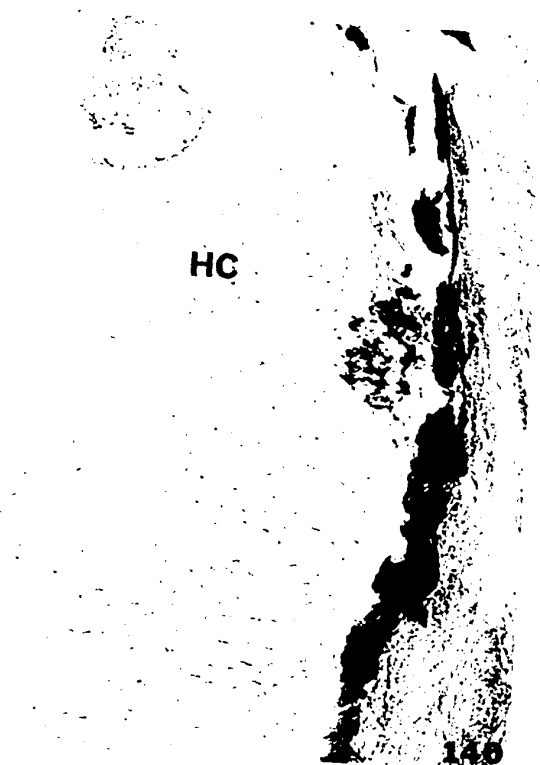


138



pe

139



HC

140

Figure 141

Control tibiotarsus, 13 days incubation. Calcification remains confined to the subperiosteal bone spicules forming a collar about the cartilage cone which is being eroded medially by a long marrow channel (mc). Von Kossa method. 36X.

Figure 142

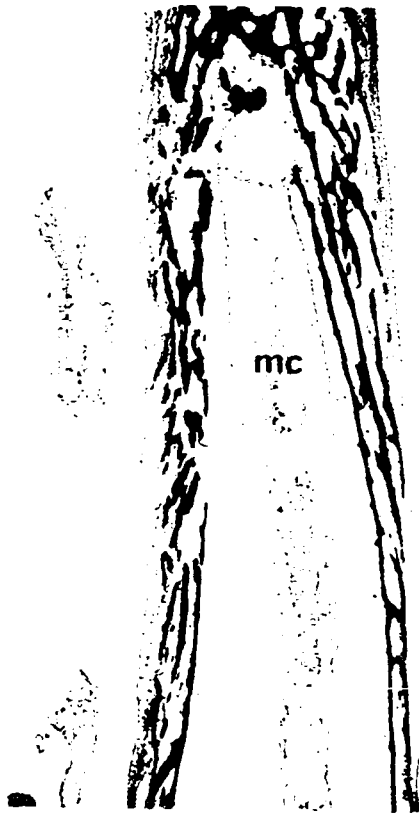
Control tibiotarsus, 15 days incubation. This shows the first appearance of calcified deposits in cartilage during normal development, and is confined to the more superficial layers of the cartilage cones; see fig. 127, a near mid-sagittal section in which the cartilage does not show calcification. Von Kossa method. 36X.

Figure 143

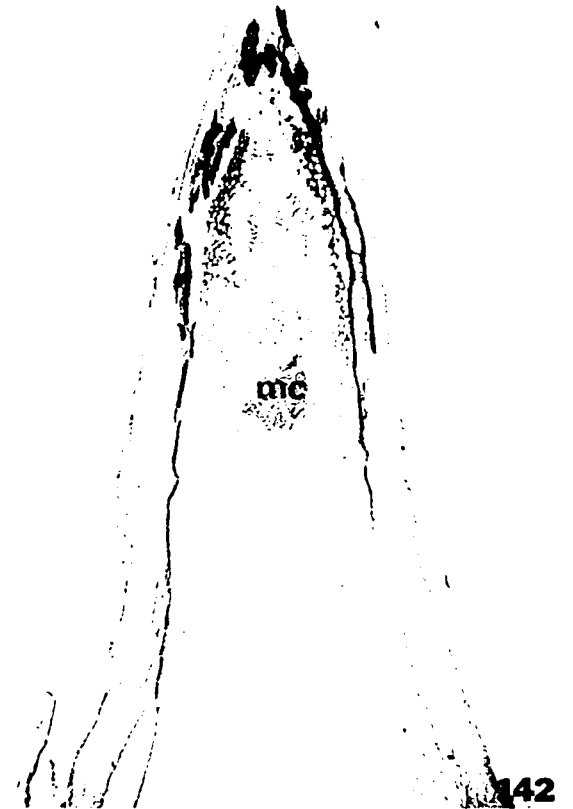
Control tibiotarsus, 17 days incubation. By this stage, the extent of calcified cartilage has increased towards the epiphyses, and forms regular circles or arcs about the hypertrophic chondrocytes. Von Kossa method. 36X.

Figure 144

Control tibiotarsus, 20 days incubation. The cartilage calcification has not only increased in length along the periphery of the cartilage cones, but also in depth into the cartilage mass. Von Kossa method. 46X.



141



142



143



144



Figure 145

Control tibiotarsus, 17 days incubation. This micrograph of the fully calcified diaphyseal bone spicules shows their orientation in a direction parallel to the long axis (arrows) of the tibiotarsus. Von Kossa method. 146X.

Figure 146

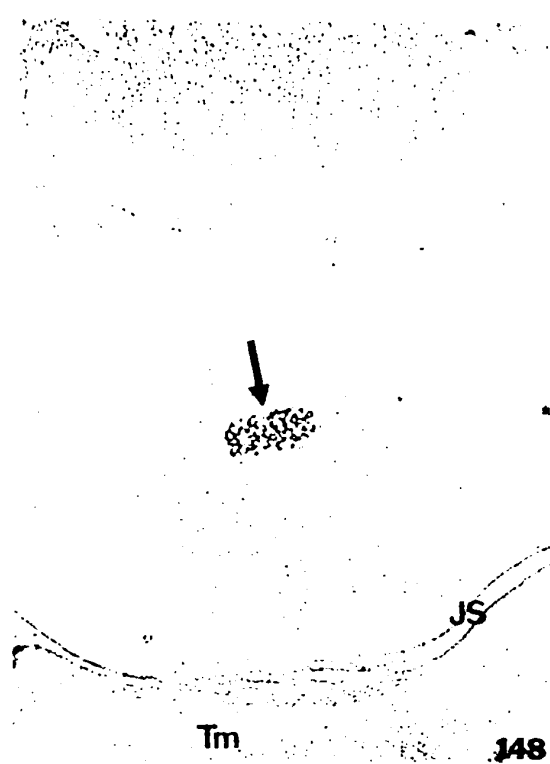
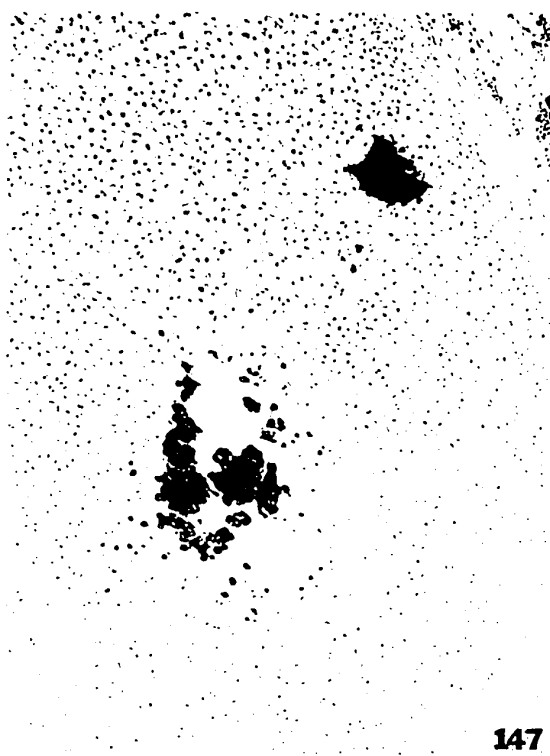
Insulin-treated tibiotarsus, 17 days incubation. By contrast with the preceeding figure, note the altered orientation of the diaphyseal spicules from a bent tibiotarsus. Arrows again indicate the long axis of the tibiotarsus. No osteoid is seen. Von Kossa method. 146X.

Figure 147

Insulin-treated tibiotarsus, 20 days incubation. Seen here are two patches of calcified cartilage in the small-celled cartilage of the distal epiphysis, the larger concretion being associated with an area of local degeneration. Von Kossa method. 146X.

Figure 148

Insulin-treated tibiotarsus, 20 days incubation. This low power micrograph shows yet another of these foci of calcification (arrow) in the small-celled epiphyseal cartilage (different embryo from that seen in fig. 147). Note also the continuity of tissue across the joint space (JS) to the tarsometatarsus (Tm). Von Kossa method. 46X.



### Alkaline Phosphatase

The presence of alkaline phosphatase (AlkPase) in developing skeletal tissues has been known for some time (Robison, 1923), although its precise role in the calcification mechanism has since been a center of strong controversy. An excellent review of the various theories is provided by Henrichsen (1958b).

As mentioned, the literature contains two previous studies of AlkPase in insulin-treated embryonic chick long bones. In the first of these (Anderson et al, 1959) there were reported to be no major differences in AlkPase localizations between normal hindlimb bones and bones from embryos exposed to insulin, although there was "somewhat greater variability" of staining within the latter group. The second relevant paper (Sevastikoglou, 1963b) dealt with biochemical assays of enzyme activity in whole tibiotarsi, with no attempt to differentiate between cartilage AlkPase and bone AlkPase.

In the present study, much of the general pattern of normal AlkPase distribution has been established by the 8th day of incubation (fig. 149). The inner or osteoblastic layer of the periosteum in the mid-diaphysis is heavily stained with cobalt sulphide in the Gomori technique, as are the osteoblasts lining the newly formed subperiosteal bone spicules. In fact, the appearance of AlkPase indicates differentiation of the perichondrium into a periosteum. In addition, those hypertrophic chondrocytes immediately subjacent to the subperiosteal bone are AlkPase-positive to a depth of one or two cell layers, while the bulk of the diaphyseal hypertrophic cartilage remains non-reactive in the Gomori procedure. These localizations

are valid for both control and insulin-treated tibiotarsi at the 8th day of incubation.

Qualitative and quantitative differences in enzyme localization become apparent by the 9th day of incubation. In the control tibiotarsi, cartilage AlkPase remains confined to the more superficial chondrocytes of the diaphysis (fig. 150) and the periosteal reaction is uniform along the length of the diaphysis. In insulin-treated tibiotarsi, however, major differences exist: there is far more reactivity in the thickened periosteum at the concavities of the tibiotarsal bends (fig. 151, "A"), while cartilage AlkPase is present in the center of the diaphysis (fig. 151, "B"), and the lateral reaction of normal hypertrophic chondrocytes is here involved to a deeper extent (fig. 151, "C").

Among the control tibiotarsi, additional hypertrophic chondrocytes at the edges of the cartilage mass acquire AlkPase, so that the enzyme is found to a depth of eight or more cells by day 13 of incubation (figs. 157, 158). During this time, however, a radically different enzyme distribution pattern emerges for the insulin-treated tibiotarsi and other hindlimb bones. The extent of AlkPase in cells and matrix at the convexities of the angulations increases to depths well in excess of the normal pattern (figs. 152, 159). The reduced matrix zone of the necrotic region in the cartilage displays very strong cellular and matrix AlkPase (figs. 153-155, 160). Also, while control tibiotarsi do not possess AlkPase in those hypertrophic chondrocytes being eroded by marrow channels before day 15, insulin-treated long bone hypertrophic cells display a strong irregular reaction in both cells and matrix (figs. 155, 156, 159). In the light of studies by Henrichsen (1958a, b), these results

are perhaps not unexpected; this point will be further discussed.

Towards the end of the incubation period (days 17, 20), the growth plate of control tibiotarsi becomes strongly reactive for AlkPase. At first, enzyme activity is detectable in a few cells of the proliferative zone (particularly at the edges of the cartilage cones), while hypertrophic cells and matrix are slightly stronger in their reactivity (fig. 163). Then a very strong reaction is found in the nuclei and cytoplasm of late proliferative zone cells, and in both cells and matrix of all hypertrophic cells down to the level of cartilage resorption (fig. 161). This same pattern develops in growth plates of insulin-treated tibiotarsi, although here the intensity of the cobalt sulphide deposits seems much greater (fig. 162).

One final difference between the two groups of tibiotarsi was found, and this concerned the epiphyseal cartilage. As previously stated, 20th day control epiphyseal cartilage still consists exclusively of the small-celled type of chondrocyte, and the present results reveal no AlkPase staining anywhere between the growth plate and the cap of articular cartilage. However, among the insulin-treated tibiotarsi, nodules of hypertrophying cartilage were found in the small-celled epiphyseal cartilage and, further, these nodules possessed intense AlkPase in both cells and matrix (fig. 164), suggesting the precocious appearance of a secondary center of ossification. This suggestion is supported by the accumulation and subsequent loss of glycogen in these cells, as previously demonstrated (fig. 112). In view of the statements of Haines (1942), previously discussed, it is particularly intriguing that these secondary centers were found in both proximal and distal

epiphyses of the tibiotarsus.

In summary, the insulin-treated tibiotarsi possess the normal pattern of AlkPase evolution and distribution which is associated with endochondral ossification of a long bone. As with deposition of calcium salts in cartilage from insulin-treated tibiotarsi, AlkPase appears to occur precociously and to greater extents than control tibiotarsi. In addition, a second pattern is found: regions associated with the necrotic events in the cartilaginous tissue are AlkPase-positive and, as was demonstrated earlier, these same regions undergo calcification. This suggests that under these pathological conditions there is an extremely close association between acquisition of AlkPase activity in cells and matrix of cartilage, and mineralization of that cartilage. Attainment of AlkPase activity with hypertrophy of small-celled epiphyseal chondrocytes was found, indicating formation of a premature secondary center of ossification.

Considering that ectopic AlkPase was found in conjunction with necrotic cartilage, the present findings tend to support Henrichsen's (1958a, b) contention that the appearance of AlkPase in cartilage is a function of degenerative events of the cartilage, in the same way that cultured heart fibroblasts acquire AlkPase with degeneration and subsequently calcify (Henrichsen, 1956).

Figure 149

Control tibiotarsus, 8 days incubation. Black deposits indicating AlkPase activity are present in the inner osteoblastic layer of the periosteum ( $P_i$ ) but not in the outer layer ( $P_o$ ). AlkPase also present in osteoblasts covering the early subperiosteal bone spicules, and in the cytoplasm of hypertrophic chondrocytes immediately subjacent to the bony collar. Gomori method. 180X.

Figure 150

Control tibiotarsus, 9 days incubation. This grazing section reveals a similar distribution of AlkPase as in fig. 149, the only difference being that the hypertrophic chondrocytes at the edges of fig. 149 are now seen in surface view. Gomori method. 227X.

Figure 151

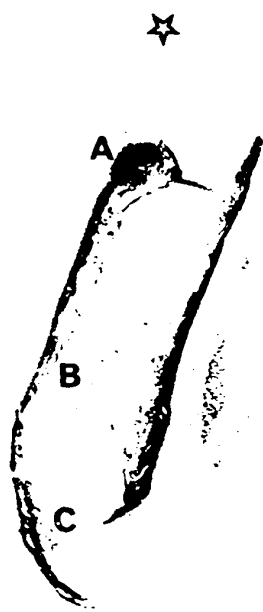
Insulin-treated tibiotarsus, 9 days incubation. Note the following unusual localizations of AlkPase: extremely high activity in the concavity of the bend near the proximal epiphysis (A), in the center of the mid-diaphyseal hypertrophic cartilage (B), and in the cartilage at the convexity of the distal angulation (C). There is no enzyme activity associated with the proximal epiphyseal necrosis (star). Gomori method. 36X.

Figure 152

Insulin-treated tibiotarsus, 10 days incubation. Positive AlkPase reaction in the cells and matrix at the convexity of the angulation near the distal epiphysis, and in the infolded periosteum at the concave surface. Gomori method. 144X.



150



151



152



Figure 153

Insulin-treated tibiotarsus, 11 days incubation. Very intense reaction in the periosteum and in the ring-shaped region of necrosis in the proximal diaphyseal cartilage (arrow). Gomori method. 45X.

Figure 154

Insulin-treated tibiotarsus, 11 days incubation. Higher magnification of a portion of the same bone as fig. 153, but not the same section. Note that both cells and matrix of the zone of reduced matrix (zrm) are intensely positive for AlkPase. Normal hypertrophic cartilage (HC) is positive beneath the periosteum only, as in control tibiotarsi. The central necrotic zone (star) is AlkPase-negative. Observe the subperiosteal vascular bud (vs) cutting across the necrotic zonation. Gomori method. 180X.

Figure 155

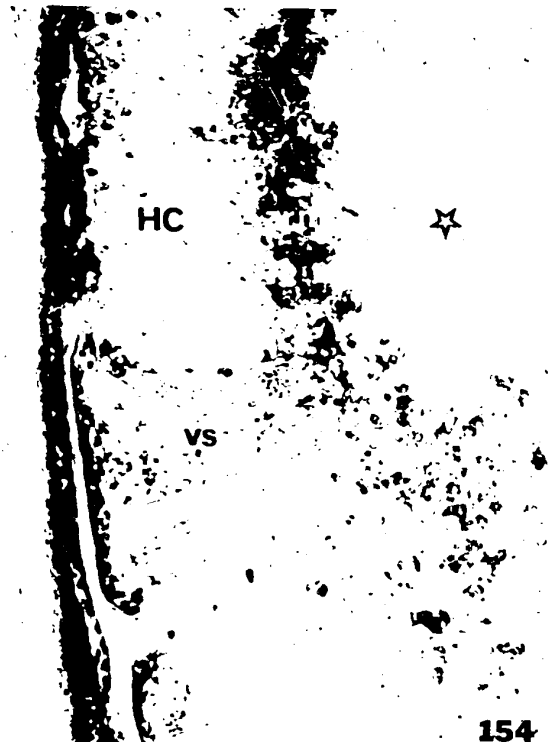
Insulin-treated proximal tibiotarsus (Tib) and fibula (f), 12 days incubation. Tibiotarsal marrow is penetrating the central necrotic cartilage (arrow), which is flanked on either side by the AlkPase-positive zone of reduced matrix. High fibular AlkPase. Gomori method. 36X.

Figure 156

- A - Insulin-treated tarsometatarsus, 12 days incubation. Note particularly the irregular matrix reaction for AlkPase (arrow) at the site of marrow resorption of cartilage. Gomori method. 96X.
- B - Control companion section to "A", to verify specificity of enzyme localization (see Appendix H). Note complete absence of cobalt sulphide deposits in the periosteum and cartilage. Gomori method. 96X.



153



154



155



156



156

Figure 157

Control tibiotarsus, 13 days incubation. Observe positive AlkPase reaction in the inner layer of the periosteum, in the osteoblasts lining the diaphyseal bone spicules (but not in the osteocytes), and in hypertrophic chondrocytes at the lateral borders of the proximal cartilage cone (arrows). Gomori method. 45X.

Figure 158

Control tibiotarsus, 13 days incubation. Higher magnification of a portion of the same section as fig. 157, but in a region closer to the proximal epiphysis. Note that the AlkPase reaction is present only in the more lateral hypertrophic chondrocytes, but to a much deeper extent than earlier stages (e.g. fig. 149), and that it is exclusively intracellular. Gomori method. 144X.

Figure 159

Insulin-treated tibiotarsus (distal) and fibula, 13 days incubation. Neither bone matrix nor the osteocytes embedded in the bone are AlkPase-positive. The periosteal of both tibiotarsus and fibula are strongly positive, as are many of the tibiotarsal hypertrophic chondrocytes at the edges (arrow). Gomori method. 40X.

Figure 160

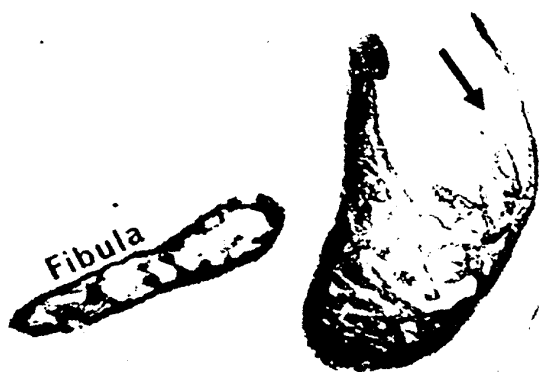
Insulin-treated tibiotarsus, 15 days incubation. This section shows a bar of hypertrophic cartilage (HC) covered with AlkPase-positive chondrocytes of the zone of reduced matrix (zrm), and overlain with subperiosteal spicules on the other side. A marrow channel (mc) has entered the former necrotic zone of the cartilage. Gomori method. 144X.



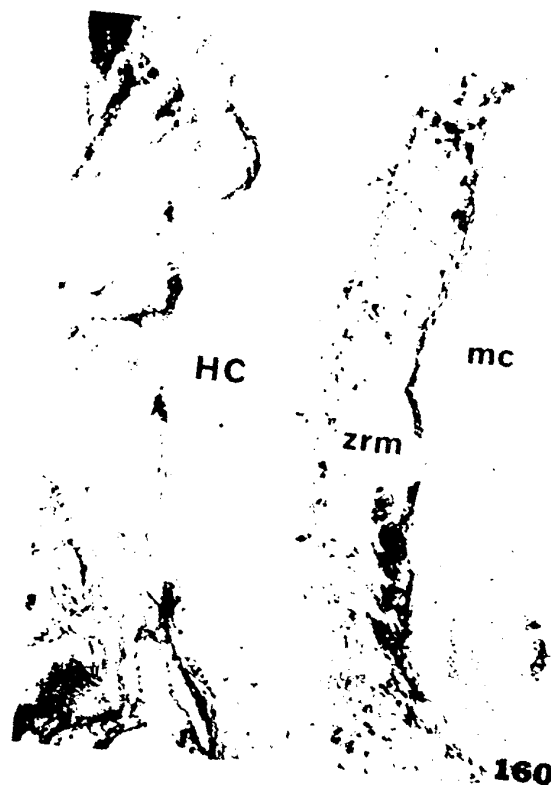
157



158



159



160

Figure 161

Control tibiotarsal growth plate (distal), 20 days incubation. The epiphyseal (EC) and early proliferative zone (PZ) cartilages remain AlkPase-negative, while activity rises from a cytoplasmic reaction in late proliferative cartilage to a full AlkPase-positive reaction for both cells and matrix in the hypertrophic zone (HC) of the growth plate. Gomori method. 144X.

Figure 162

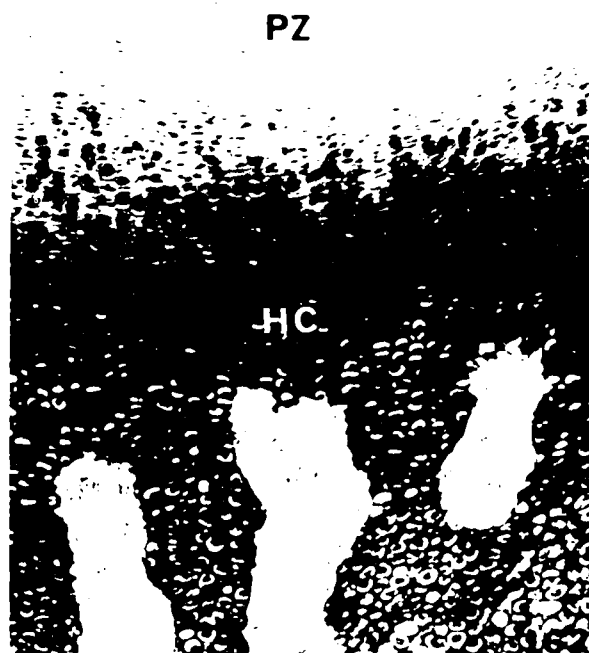
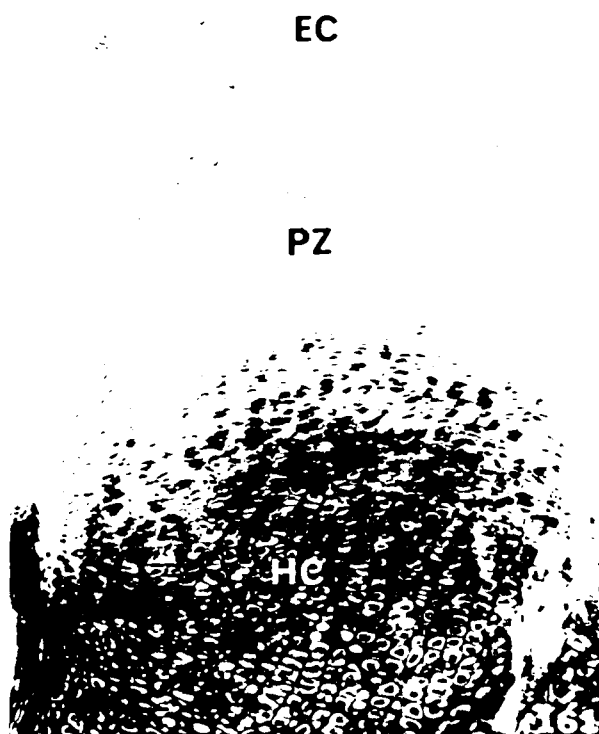
Insulin-treated tibiotarsal growth plate (proximal), 20 days incubation. The onset of AlkPase activity in the growth plate occurs at the same level as in fig. 161 (i.e. late proliferative zone, PZ), although the hypertrophic (HC) reaction appears much more intense. Note also the three large marrow channels entering deep into the growth plate. Gomori method. 144X.

Figure 163

Control tibiotarsus, 17 days incubation. Edge of growth plate from distal metaphysis, showing onset of AlkPase in the late proliferative zone, increasing in intensity towards the hypertrophic region. The dark line on the left is the AlkPase-positive periosteum which extends up to the level of the epiphyseal cartilage. Gomori method. 220X.

Figure 164

Insulin-treated tibiotarsus, 20 days incubation. Presence of a nodule of hypertrophying chondrocytes in the distal epiphysis, showing strong cellular and matrix AlkPase, suggesting early stages in the formation of a secondary center of ossification. See also fig. 112. Gomori method. 140X.



## II - RELATIONSHIP TO OTHER PATHOLOGIES

The question arises as to the relationship between the present insulin-induced pathologies and the conditions of:

- (1) Chondrodystrophy in chickens (Landauer and Dunn, 1925/26; Landauer, 1927; Hutt and Greenwood, 1929a; Lamoreux, 1942)
- (2) Achondroplasia in mammals (Brown and Pearce, 1945; Pearce and Brown, 1945; Crary and Sawin, 1963; Shepard et al, 1969)
- (3) Creeper condition in chickens (Landauer, 1931; Patten, 1937; Grüneberg, 1963; Elmer, 1968).

(1) Avian chondrodystrophy may fall into one of two categories: either sporadic, as described by Landauer and Dunn (1925/26), Hutt and Greenwood (1929a), for which the basis is not a simple Mendelian factor, or hereditary chondrodystrophy (Lamoreux, 1942) which is caused by an autosomal recessive mutation. In both cases the mortality is extremely high or total; sporadically occurring chondrodystrophics never hatch, while hereditary ones either commonly die before the 19th day of incubation or are unable to hatch without assistance.

The anatomical and histological features of both forms of chondrodystrophy are identical. These include shortened lower beak, together with curved upper mandibles to produce a "parrot beak", and shortened, thickened hindlimbs with bent long bones (especially the tibiotarsus) so that the plantar surfaces of the feet are rotated towards the body. Wing bones are less affected, and the head and cervical vertebrae appear normal. Among the non-skeletal anomalies is a retardation of feather growth. Histologically, affected bones are characterized by thickened epiphyses

and periosteal, irregular cartilage zonation with much reduced or absent proliferative region, and considerably less cartilage matrix than usual. Diaphyseal ossification is normal or advanced, and secondary centers of ossification may form precociously in the epiphyses (Landauer, 1927).

Patten (1937) compared glycine content of proteins from normal and chondrodystrophic chick embryos, and found decreased amounts of glycine in the latter group of embryos. This was particularly interesting because of the high glycine content of proteins from feathers and skeleton, both of which show abnormal differentiation in chondrodystrophy.

(2) Most studies of mammalian achondroplasia are based on work with rabbits. Its mode of inheritance, however, depends on the particular species of mammal: in rabbits it is transmitted as a simple Mendelian recessive, affected individuals being homozygous for the factor (Brown and Pearce, 1945); in dogs and humans it is inherited as a simple Mendelian dominant gene. As with sporadic chondrodystrophy in chickens, the lethality is absolute.

Physically, achondroplastic rabbit embryos are characterized by reduced size and stunting of the extremities, particularly the forelimbs. The shortened bones are always straight and "there is no suggestion of twisting or bowing" (Brown and Pearce, 1945). The abdomen is protuberant, the head is large in relation to the torso, and hindlimb muscles sometimes seem unusually prominent. Histologically, ossification of the diaphysis is retarded, the shafts remain cartilaginous, and a definitive marrow cavity fails to form (Pearce and Brown, 1945). Normal row formation is upset in the growth plate cartilage, and the amounts of cartilage matrix are reduced.



Crary and Sawin (1963) also examined rabbit achondroplasia and described the same general pathology as Brown and Pearce (1945). These authors also note that the metatarsals and phalanges of the forelimbs are more severely disturbed than those of the hindlimbs. They state that the disturbances of skeletogenesis can be traced "to a disturbance of mesenchyme or its precursor, probably chemical in nature, which results in retardation of growth and disorganization of cartilage cells".

Shepard et al (1969) conducted light and electron microscopic as well as histochemical studies of achondroplastic rabbit cartilage. They found increasing number of pyknotic cells towards the central region of the epiphyseal cartilage, and there was less cartilage matrix in the achondroplastic dwarf embryos. Localizations of various dehydrogenase enzymes, acid and alkaline phosphatases, as well as PAS-positive material revealed no differences between normal and achondroplastic cartilage. Ultrastructurally, a gradual degeneration sequence could be demonstrated between normal, intact chondrocytes subjacent to the perichondrium and the dead cells in the center of the cartilage mass. The chondrocytes appeared to shrink away from the surrounding matrix, cytoplasmic organelles became ill-defined, and the nuclei of these cells became convoluted. No structural changes were seen in the cartilage matrix, although they recommend a more complete study of possible matrix alterations in achondroplasia.

(3) The third pathological condition which bears some resemblance to the insulin-induced deformities of the present study is that shown by Creeper chickens. Landauer (1931) has extensively studied the pathogenesis of the Creeper trait, which occurs as a semi-dominant gene (Grüneberg, 1963).

Homozygous individuals never hatch, and normally are dead by the 4th day of incubation (Elmer, 1968) as a result of abnormal development of the vitelline arteries (Landauer, 1932). Heterozygous embryos are fully viable and show a number of skeletal abnormalities. These include long bone shortening with torsion and bending (especially in the lower tibiotarsal diaphysis) and "curled toe paralysis", in which the foot is clawed towards the body as a result of shortening of tendons. Microscopically, irregularities of organization occur in the growth plate and epiphyseal cartilage: the proliferative zone is thinner and poorly defined, normal row formation in the growth plate is absent, and epiphyseal cells are smaller than normal. Curiously, the fibula often develops more fully than in normal embryos. Diaphyseal marrow formation is initially delayed, as is periosteal ossification. However, periosteal ossification in Creepers soon matches, then surpasses the rate of normal embryos. In his summary, Landauer (1931) states: "The histological abnormalities of the long bones of Creeper fowls in all essential points are very similar to, if not identical with, the characteristic symptoms of human chondrodystrophy".

Elmer (1968) examined the effects of embryo extract from Creeper sources on the growth of embryonic chick tibiotarsi in organ culture. He found that the Creeper embryo extract produced a shortening of the rudiments and led to a decreased total protein content as compared with tibiotarsi grown in the presence of embryo extract from normal sources. Creeper embryo extract increased the rate of incorporation of  $H^3$ -leucine into the growing explants, leading him to conclude that "the reduced growth rate . . . appears to be related to aberrant leucine metabolism".

Before one may compare these three pathologies to insulin-induced dwarfism and micromelia, it is necessary to first resolve a problem of semantics. Brown and Pearce (1945) described the condition which they observed in rabbits as "achondroplasia", yet Grüneberg (1963) categorizes these same anomalies as "chondrodystrophy". Similarly, while the original authors of the papers dealing with the inherited skeletal disorder in chick embryos called the condition "chondrodystrophy", Gruenwald (1956) prefers to name the same condition "achondroplasia", and states that there are six forms of achondroplasia in the chick. Landauer (1931) uses the term "chondrodystrophy" for the human skeletal deformities which are similar or identical to the avian Creeper condition, while Pearce and Brown (1945) state that rabbit achondroplasia is histologically similar or identical to the Creeper condition. Yet as has already been shown, the histological changes in rabbit achondroplasia and Creeper chicks differ on a number of major points, including bending of the shortened bones and rate of diaphyseal ossification. It would thus appear that the Creeper condition must be set apart from the other two pathologies.

The suggestion has been made of altered protein metabolism in Creeper chicks (Elmer, 1968) and in insulin-induced micromelia (De Bastiani and Lunardo, 1956b). This similarity in causative mechanisms would therefore lend credence to Landauer's (1947a) view that many of the insulin-induced abnormalities are phenocopies of the developmental disturbances in Creeper embryos. Erhard (1959) however, feels that there are too many histological differences between insulin-treated bones and Creeper bones to consider the former as phenocopies of the latter. He prefers to ascribe a close relationship between insulin micromelia and

chondrodystrophia malacica (a form of chondrodystrophy marked by softening of the epiphyses).

Using viability as a criterion, the deformities of the present material cannot be considered as either chondrodystrophy or achondroplasia, as embryos deformed by insulin were observed to hatch unassisted (fig. 31). It has also been shown that bending of insulin-treated long bones is extremely common, while it is not in rabbit achondroplasia (Brown and Pearce, 1945). Furthermore, diaphyseal ossification is retarded in achondroplastic dwarfs (Pearce and Brown, 1945), while it is accelerated in the present material.

This leaves the Creeper condition as primary suspect for similarity to insulin-induced pathologies, if one assumes that a teratologically-induced disorder must of necessity be a phenocopy of a hereditary condition. Yet even the Creeper condition does not match all of the characteristics that have been described in the present study. Gruneberg (1963) has shown that the growth rates of leg and wing bones are the same in normal and in Creeper embryos, which as has been shown (fig. 2) is certainly not the case for insulin-treated tibiotarsi, as compared with normal tibiotarsi.

Thus, it is futile to attempt to correlate insulin-induced deformities with any hereditary trait or sporadically occurring mutation. It is perfectly evident that any agent, be it teratogenic or hereditary, if it affects the skeletal system, will show at least some similarities to pathologies resulting from other agents. The effects of insulin are therefore unique and reproducible, as are the other pathologies which have been described.

### III - NATURE OF THE CARTILAGE DEGENERATION

Central to the analysis of the insulin-induced pathologies seen in the tibiotarsus is the cause of the cartilage necrosis. The majority opinion among previous workers in this field is that upsets of carbohydrate metabolism have led to the observed changes of normal structure. As has been shown in the present study, the only histochemically detectable change in the cartilage matrix has been in the reaction of the zone of reduced matrix with the alcian blue-alcian yellow staining technique (figs. 67, 68). The matrix of this zone takes up alcian yellow but is not coloured by alcian blue, suggesting an absence or paucity of sulphated compounds. There are two possible mechanisms which may account for this change:

1. The release of intracellularly synthesized sulphomucins at the plasmalemmas of chondrocytes is in some way retarded or halted.
2. The synthesis of sulphated compounds within the chondrocytes may be blocked. In view of the well established role of the Golgi complex in the sulphation of secretory polysaccharides in cartilage (Godman and Lane, 1966), this suggests structural and/or functional alterations of the Golgi complex. This point will be discussed shortly in relation to the hypothesis of increased lysosomal activity in cartilage from insulin-treated embryos.

Previous assessments of the glycogen content of chondrocytes from insulin-treated long bones have varied widely. Hay (1958) has reported increased glycogen, while Parhon et al (1956) and Erhard (1959) state that glycogen levels are decreased. On the other hand, De Bastiani and Lunardo

(1956a) report highly variable results, and Anderson et al (1959) could find no differences in glycogen content between chondrocytes from normal and from insulin-treated embryos. The present results indicate no consistent, appreciable differences between glycogen content of chondrocytes from normal and from insulin-treated tibiotarsi.

As regards glycosaminoglycuronoglycans (mucopolysaccharides), again there were no real changes between control and insulin-treated tibiotarsi, with the exception noted above for the zone of reduced matrix. The intensity of staining fell off with necrosis of the cartilage, as would be expected because of the reduced amounts of matrix ground substance, but there was no loss of metachromasia (toluidine blue), basophilia (hematoxylin, aldehyde fuchsin) or alcianophilia (alcian blue, alcian blue-alcian yellow).

Based on these findings, it is therefore reasonable to infer that the only major upsets in the carbohydrate histochemistry of the insulin-treated tibiotarsi is the degree of mucopolysaccharide sulphation in the zone of reduced matrix. Thus, the minority opinion of De Bastiani and Lunardo (1956b) that alterations in patterns of protein synthesis are responsible for many of the insulin-induced pathologies may well provide an alternate biochemical basis for the observed changes in structure.

It has been observed that the necrotic regions in the cartilage always conform to the contours of the epiphyses. Erhard (1959) also noted this, and proposed a scheme for explaining the necrosis of cartilage on the basis of impaired diffusion of nutrients through the cartilage matrix. In Erhard's zonation sequence, cells of the "Randzone" (normal subperichondral chondrocytes) obtain full nourishment since they

are closest to the subperiochondral blood supply, and are therefore able to produce normal amounts of matrix. As nutrient levels drop off with distance away from the perichondrium, cells receive just enough energy for cellular maintenance, but are unable to produce significant amounts of matrix (zone of reduced matrix or "Zwischenzone"). Still deeper towards the center of the cartilage mass, the cells are completely starved, since the reduced nutrients have been used by the more peripheral cells; this is the zone of necrosis or cell death ("Erweichungszone"). Erhard cites reduced levels of glycogen in the cartilage as evidence of reduced nourishment, but there was no clear evidence of reduced glycogen in the present study. Further, as has been demonstrated here, the chondrocytes need not necessarily pass through the transitional phase of a zone of reduced matrix, but may simply show a uniform progressive degeneration (e.g. fig. 55).

In rabbit achondroplasia there is a similar type of cartilage necrosis, and Shepard et al (1969) have offered two possible mechanisms to account for this cellular degeneration. Firstly, the central chondrocytes, being situated in an avascular environment may be able to survive by utilizing "a special alternate metabolic system . . . . The genetic lack of this compensatory system might be expressed only under these conditions and then could produce the specific pathology of achondroplasia". The second speculation of these authors is that there may be as yet undetermined changes in the nature of the cartilage matrix which disrupt cellular metabolism.

In view of the present findings, it is postulated that insulin has triggered a massive lysosomal autophagic sequence, resulting

in the observed cartilage necrosis. Of direct relevance to this hypothesis are the observations of Brandes et al (1964), who induced autophagy in carbon-starved Euglena gracilis. If one accepts the idea of impaired diffusion of nutrients to the central chondrocytes (and the shape of the necrotic cavity certainly suggests this), then the chondrocytes may have responded in an identical fashion to Euglena when it was deprived of a source of nourishment (carbon) in its medium. It is also of interest that glucagon, the other principal hormone produced by the pancreatic Islets of Langerhans, will induce formation of autophagic vacuoles in hepatic cells (Arstila and Trump, 1968). These latter authors state that "autophagocytosis represents a rather common sublethal reaction to a variety of injurious stimuli, such as deficiency states, hypoxia, excesses of certain vitamins or HORMONES (my capitals), and administration of toxic compounds, especially antimetabolites and certain carcinogenic agents".

The present hypothesis of insulin-induced, lysosome-mediated chondrocyte autophagy becomes even more attractive when one considers the well established role of insulin in altering the permeability of membranes (Krahl, 1961). Further to this point, Sledge (1966) has stated that "insulin modifies the permeability of the cell membrane and affects intracellular membranes causing a loss of compartmentalization and reduction of intracellular barriers".

Grillo (1961) has shown that insulin is not normally present in chick embryos before the 12th day of incubation, and Zwilling (1943a) has stated that the other hormones related to insulin activity are not present during the first seven to eight days of embryogenesis. Considering



the massive dose of insulin which has been given to the embryos in the present study, it is therefore quite reasonable to suggest that the lysosomal and/or cell membranes generally have been severely damaged, leading to cytolysis. As regards lysosomes, this would mean rupture of the single limiting membranes of the lysosomes and subsequent release of hydrolytic enzymes within the cells. If this were so, then the small dense spherules frequently seen in the center of the cartilage necrosis would qualify as dense or residual bodies, the end products of lysosomal autophagy.

In addition, there might be an overproduction of lysosomes by the Golgi apparatus. The depressed amounts of sulphated matrix seen in the zone of reduced matrix intimate that the Golgi complex may have shifted its major secretory product from matrix precursors to lysosomes.

In discussing insulin-induced aberrant skeletogenesis, Sledge (1966) has stated: "a direct or indirect effect on the lysosome might be suspected but thus far has not been investigated".

Ultimately, the answer to the nature of the cytologic changes almost certainly lies with ultrastructural investigations of lysosome activity, detection of changes in  $S^{35}$  uptake by chondrocytes, and the discharge of sulphated mucopolysaccharides into the extracellular matrix.

## SUMMARY

1. The morphological changes resulting from treatment of developing chick embryos with insulin have been anatomically, histologically and histochemically examined. Particular attention was given to tibiotarsal histogenesis.
2. For the stage at which the insulin was given, the chief anatomical effects on the embryo were generalized reduction of body size, a bilateral disproportionate shortening of the hindlimb bones (micromelia), and frequent angulation of the tibiotarsus.
3. Insulin treatment produced a significant reduction in the growth rate of tibiotarsi, as compared to control tibiotarsi, with some evidence of recovery to more normal rates of growth towards the end of incubation.
4. Histologically, the most striking finding was necrosis of cartilage cells and matrix at both ends of the tibiotarsus. This degenerative change was usually more pronounced proximally, and involved all the cartilage zones.
5. Organization of the growth plates of insulin-treated tibiotarsi, in those areas of intact cartilage, deviated from the normal condition. The proliferative zone was often compressed and poorly demarcated from adjacent zones, and the normal parallel row arrangement of chondrocytes was never achieved.
6. Frequently, normal joint formation was impaired by the extension

across the joint space of the above necroses of adjacent epiphyses, or by the presence of fibrous material extending across the joint space.

7. Periosteal ossification, cartilage resorption and formation of the definitive marrow cavity were initially delayed in insulin-treated tibiotarsi, but soon progressed more rapidly than in control tibiotarsi.

8. Hypertrophic cartilage from insulin-treated tibiotarsi was characterized by slightly smaller chondrocytes, higher cell densities, and reduced amounts of extracellular matrix. These deviations from normal values were all statistically significant.

9. No consistently significant increases or decreases were noted in chondrocyte glycogen content, nor were histochemical differences found for mucopolysaccharides of fully intact regions of cartilage. Where necrosis occurred, however, there was a distinct loss of sulphate in the cartilage matrix.

10. As regards ossification, the duration and extent of osteoid was identical in control and insulin-treated tibiotarsi. Calcification of cartilage matrix was precocious and more extensive in the latter group. In addition, ectopic calcification occurred in association with necrotic events in the cartilage.

11. Insulin-treated bones developed secondary centers of ossification in both proximal and distal epiphyses.

12. Mineralization of intramembranous bones in insulin-treated embryos appeared normal on the gross level.

13. A close association of alkaline phosphatase (AlkPase) with ossification was found in both normal and insulin-treated tibiotarsi. In addition, there was a close correlation of AlkPase activity in cells and matrix undergoing necrosis (insulin-treated tibiotarsi), and with events of secondary ossification.

14. The relationship of the present pathologies of insulin-treated tibiotarsi to hereditary skeletal disorders has been discussed, and it has been concluded that there are several close parallels to the insulin syndrome, but none are identical in all respects.

15. A hypothesis is forwarded of increased lysosomal-mediated autophagy of cartilage, and alterations in the activities of the Golgi complex.

## APPENDIX A

### MACROSCOPIC DEMONSTRATION OF CALCIFICATION

1. Free embryos from surrounding membranes, yolk, etc.
2. For larger embryos, skin and eviscerate before fixation.
3. Fix in 10% neutral phosphate-buffered formalin, prepared according to Thompson (1966) for 2-3 days.
4. Clear embryos in 2% KOH for 2-10 days (depending on size), until skeleton can be seen through the musculature. Ultraviolet light may be used to accelerate soft tissue maceration.
5. Transfer embryos to fresh 2% KOH, and add 0.1% aqueous alizarin red S (C.I. No. 58005) until the solution is wine-coloured. Leave embryos in this staining solution until the skeleton is coloured deep purple.
6. Place embryos in 25% glycerin in 2% KOH, and leave there until the stain diffuses out of the soft tissues.
7. Transfer to 50% glycerin in 2% KOH for 2-3 days, then to 75% glycerin in 2% KOH for an equal period of time.
8. Finally, place embryos in 100% glycerin for storage. Add a few crystals of thymol to prevent bacterial growth.

### RESULTS

Calcified tissues (bone and cartilage) are stained reddish-purple, while other tissues (such as uncalcified cartilage) are transparent or very slightly opaque.

APPENDIX BDIFFERENTIATION OF BONE AND CARTILAGE MATRIX

1. Fix tissues in Bouin's fluid, dehydrate through a graded series of ethanol, clear in toluene, and vacuum embed in 56.5°C. Tissuemat (Fisher Scientific Co.)
2. Section serially at 8 micra and mount on albumenized slides.
3. Deparaffinize sections in xylene and hydrate to distilled water through a graded series of ethanol.
4. Oxidize sections in equal parts of freshly mixed 0.5%  $\text{H}_2\text{SO}_4$  and 0.5%  $\text{KMnO}_4$  for 2 min.
5. Rinse in distilled water, then decolourize sections in 2% oxalic acid by inspection.
6. Wash in running water for 2 min.
7. Stain in aldehyde fuchsin (Halimi, 1952) for  $1\frac{1}{2}$  min.
8. Rinse twice in 95% ethanol.
9. Wash in running water for 4 min.
10. Stain with 0.5% aqueous phloxine (C.I. No. 45410) for 2 min.
11. Rinse in distilled water.
12. Immerse in 5% phosphotungstic acid for 1 min, then wash in running water for 3 min.
13. Stain with 0.1% aqueous fast green FCF (C.I. No. 42053) for 20 sec.
14. Rinse quickly in 95% and 100% ethanol, clear in xylene and mount in Permount (Fisher Scientific Co.)

117

APPENDIX B (cont'd)

RESULTS

Cartilage matrix and elastic fibers are stained intensely purple.

Bone matrix and collagen fibers are intense green.

Nuclei of all cells are coloured bright red.

## APPENDIX C

### MICROSCOPIC DEMONSTRATION OF CALCIFICATION

1. Fix tissues in 10% neutral phosphate-buffered formalin for 24 hours.
2. Wash overnight in running water to remove excess fixative.
3. Dehydrate through a graded series of ethanol from 50% - 100%, all of which have been neutralized with  $\text{MgCO}_3$  to prevent decalcification.
4. Clear tissues in toluene and embed in 61°C. Tissuemat under vacuum.
5. Section at 10 micra and mount on albumenized slides.
6. Deparaffinize sections in xylene and hydrate through neutralized graded ethanols to distilled water.
7. Immerse slides in 5%  $\text{AgNO}_3$  for 30 min, during which time they are exposed to the light from a 100 watt tungsten bulb.
8. Rinse twice in distilled water.
9. Immerse in 5% sodium thiosulphate for 5 min.
10. Rinse twice in distilled water.
11. Counterstain with solution of nuclear fast red, prepared according to Thompson (1966), for 5 min.
12. Rinse well in distilled water and dehydrate in 95% and 100% ethanol.
13. Clear in xylene and mount in Permount.

### RESULTS

Sites of localization of the anions of calcium stain brown or black.

Nuclei are bright red, while cytoplasm and uncalcified matrix stain pale pink.



APPENDIX DMETACHROMAS<sup>7</sup>A

1. Fix tissues in Bouin's fluid, dehydrate and clear as usual. Vacuum embed in 56.5°C. Tissuemat.
2. Section serially at 8 micra and mount on albumenized slides.
3. Deparaffinize in xylene and hydrate through graded ethanols to distilled water.
4. Stain for 2 min. in 0.5% aqueous toluidine blue O (C.I. No. 52040)
5. Immerse for 2 min. in a mixture composed of equal parts of 5% aqueous ammonium molybdate and 1% aqueous potassium ferrocyanide. Companion slides should omit this step to remove "false" metachromasia.
6. Wash in running water for 2 min.
7. Dehydrate in two changes of absolute acetone, 3 min. each change.
8. Clear in xylene and mount in Permount.

RESULTS

Tissue chromotropes containing free sulphate, phosphoryl or carboxyl anionic groups, and with a minimum surface density of electronegative charges, will be metachromatically stained purple or red, while other tissues not meeting these criteria will be orthochromatically coloured blue. Normal cartilage matrix, because of its high content of sulphated compounds, will exhibit metachromasia.

## APPENDIX E

### ACID MUCOPOLYSACCHARIDE DEMONSTRATION

#### I - Alcian Blue Method

1. Fix tissues in Bouin's fluid, and embed in Tissuemat as usual.
2. Section serially at 8 micra and mount on albumenized slides.
3. Deparaffinize in xylene and hydrate through graded ethanols to distilled water.
4. Wash in running distilled water for 10 min.
5. Stain with freshly-filtered solution of 1% alcian blue 8GX (C.I. No. 74240) in 3% acetic acid for 30 min.
6. Wash in running water for 10 min.
7. Counterstain with nuclear fast red solution (Thompson, 1966) for 5 min.
8. Rinse in running water, 95% and 100% ethanol.
9. Clear in xylene and mount in Permount.

#### RESULTS

Acid mucopolysaccharides are stained blue, nuclei are bright red and cytoplasm is pale pink.

#### II - Alcian Blue and Alcian Yellow Method (Ravetto, 1964)

1. Fix, embed, section, and bring to distilled water as above.
2. Stain for 30 min. in 0.5% alcian blue 8 GX in 0.5 N hydrochloric acid at pH=0.5 .
3. Wash for 10 seconds in 0.5 N hydrochloric acid.
4. Wash well in running water.

APPENDIX E (cont'd)

5. Stain for 30 min. in 0.5% alcian yellow GX (C.I. No. 14030) in 3% acetic acid at pH=2.5 .
6. Wash in running water for 2 min.
7. Counterstain in nuclear fast red solution for 5 min.
8. Rinse in running water, 95% and 100% ethanol.
9. Clear in xylene and mount in Permount.

RESULTS

Sulphated groups are coloured blue, while carboxyl groups are coloured yellow. Tissue sites containing acid mucopolysaccharides ( such as chondroitin sulphuric or mucoitin sulphuric acids ) which contain both carboxyl and sulphate groups are coloured blue-green. Nuclei are bright red and cytoplasm is pale pink.

## APPENDIX F

### PERIODIC ACID - SCHIFF FOR GLYCOGEN

#### Solutions

a. Schiff Reagent: Dissolve 1 gm basic fuchsin (C.I. No. 42510) in 100 ml distilled water at 90-95°C. Cool to 50-60°C. and filter through Whatman filter paper (No. 1). Cool to 25°C., then add 2 gm sodium bisulphite and 20 ml 1 N hydrochloric acid. Stopper tightly and store in the dark overnight at room temperature. Add 300 mg activated charcoal, shake for 1 min., then filter. The solution should be colourless or pale yellow. Store at 4°C., and discard when reagent turns pink.

b. Metanil Yellow Counterstain: Dissolve 1.25 gm of metanil yellow (C.I. No. 13065) in 500 ml distilled water. Add 1.25 ml of glacial acetic acid, filter, and store in brown bottle.

Note: This counterstain was found to be more satisfactory than the usually recommended one of hematoxylin (Davenport, 1960) or celestin blue-haemalum (Pearse, 1961), as these latter dyes tended to be somewhat capricious in their degree of "blueness", sometimes tending towards purple or red, thereby visually competing with the recoloured Schiff reagent.

#### Staining Procedure

1. Fix in Bouin's fluid, and vacuum embed as usual. Section at 8 micra.
2. Deparaffinize sections in xylene and hydrate through graded ethanols to distilled water.
3. To digest out glycogen from tissue sections, incubate in 0.05% malt

APPENDIX F (cont'd)

diastase in 0.02 M phosphate buffer at pH=6.0 for 45 min. at 37°C.

Undigested controls should be incubated for the same time and temperature in the phosphate buffer only.

4. Wash in running water for 25 min. to remove diastase.
5. Oxidize in 0.5% periodic acid for 5 min.
6. Rinse in distilled water.
7. Immerse in Schiff reagent for 30 min., in total darkness.
8. Pass sections through three 20 min. changes of sulphurous acid.

This step was originally included in the procedure of the founders of the P.A.S. method, but is considered unnecessary by both Pearse (1961) and Thompson (1966).

9. Wash in running water for 15 min. to enhance coloration.
10. Stain for 1 min. in the metanil yellow solution.
11. Rinse in distilled water and dehydrate through graded ethanols.
12. Clear in xylene and mount in Permount.

RESULTS

P.A.S.-positive substances (including glycogen) are stained pale red to magenta; other tissue components are stained yellow. The difference in staining between diastase-digested sections and undigested controls represents glycogen.

## APPENDIX G

### BEST CARMINE FOR GLYCOGEN

1. Fix tissues in 10% neutral phosphate-buffered formalin, and embed as for the von Kossa Method (Appendix C).
2. Deparaffinize serial 10 micra sections in xylene.
3. Pass sections through two 5 min. changes of 100% and 95% ethanol.
4. Wash in running water for 25 min.
5. To digest glycogen, incubate in 0.05% malt diastase in 0.02 M phosphate buffer at pH=6.0 for 60 min. at 37°C. Undigested controls are incubated for the same time and temperature in the phosphate buffer only.
6. Wash in running water for 25 min. to remove enzyme.
7. Stain in Harris' hematoxylin (prepared according to Thompson, 1966) for 4 min.
8. Blue in running water and differentiate in acid alcohol if necessary.
9. Immerse sections in Best Carmine working solution (Thompson, 1966) for 20 min.
10. Rinse briefly in three changes of absolute methanol.
11. Rinse in absolute ethanol.
12. Clear in xylene and mount in D.P.X. Mountant (British Drug Houses) or Permount.

### RESULTS

Glycogen is stained deep red and nuclei are blue or purple. Other tissue components are faint pink in colour.

APPENDIX HALKALINE PHOSPHATASE DEMONSTRATION

1. Fix tissues in 80% ethanol at 4°C for 24 hrs.
2. Dehydrate in 95% ethanol (1 hr) and 100% ethanol (30 min).
3. Clear in two 15 min changes of benzene.
4. For older tibiotarsi, infiltrate with 3% celloidin in ether-alcohol.
5. Embed in 52.5°C Tissuemat under vacuum. Total time in Tissuemat not to exceed 30 min.
6. Section serially at 8 micra, using the cellulose tape method of Palmgren (1954) where necessary.
7. Deparaffinize sections in xylene, remove celloidin (where used) with ether-alcohol, and hydrate to distilled water through 100%, 70% and 40% acetone.
8. Immerse all sections in a buffer mixture composed of 11 parts of 0.1 M citric acid and 9 parts of 0.1 M sodium citrate at pH=4.5 . This serves to remove preformed insoluble calcium salts which would otherwise react to give a positive test.
9. Rinse in distilled water.
10. Incubate sections in the appropriate incubation medium for 30 min at 37°C.

a. Test Substrate

2% sodium beta-glycerophosphate .....	50 ml	
2% sodium barbital .....	50 ml	
2% calcium chloride .....	10 ml	
2% magnesium sulphate .....	4 ml	
Distilled water .....	100 ml	pH=9.4

APPENDIX H (cont'd)b. Control Substrate

Same composition as test substrate, but minus the glycerophosphate.

11. Rinse twice in distilled water.
12. Immerse in 2% aqueous cobalt sulphate for 3 min.
13. Rinse thrice in distilled water.
14. Immerse in freshly made 1% aqueous ammonium sulphide for 2 min.
15. Rinse twice in distilled water.
16. Counterstain with nuclear fast red solution for 5 min.
17. Rinse with distilled water, dehydrate through 95% and 100% ethanol.
18. Clear in xylene and mount in Permount.

RESULTS

Sites of alkaline phosphatase activity are demonstrated as black deposits of cobalt sulphide. Nuclei are red over a generally pale pink background.

Note: The acetone-based incubation medium of the modified Gomori method for alkaline phosphatase (Pearse, 1961) was found to be ineffective as a result of nonspecific precipitation while sections were incubating in the medium.



TABLE I (after Fisher, 1955)  
COMPOSITION AND PROPERTIES OF NPH INSULIN

Physical Form: crystalline suspension

Acidity: pH=7.2

Zinc content: 0.0012 mg/4 units

Protamine content: 0.02 mg/4 units

Glycerin content: 0.4 mg/4 units

NaCl content: 0.215 mg/4 units

Na<sub>2</sub>HPO<sub>4</sub> content: 0.1 mg/4 units

m-cresol content: 0.1 mg/4 units

TABLE 2  
DOSAGE AND TIMING STUDIES

Date: 23 Dec 66

Eggs incubated: 125

Injection Times: 120, 144 hrs

Eggs fertile: 107

Dosages: 0.05 ml of 0.9% NaCl  
2 units insulin in 0.05 ml  
4 units insulin in 0.05 ml

Fertility: 85.6%

<u>Injection Time</u>	<u>Treatment</u>	<u>Number</u>	<u>Dead</u>		<u>Normal</u>		<u>Micromelic</u>	
			#	%	#	%	#	%
120 hrs	NaCl	10	1	10.0	9	90.0	-	-
120 hrs	2 units insulin	20	10	50.0	8	40.0	2	10.0
120 hrs	4 units insulin	20	11	55.0	6	30.0	3	15.0
144 hrs	NaCl	10	1	10.0	9	90.0	-	-
144 hrs	2 units insulin	20	10	50.0	9	45.0	1	5.0
144 hrs	4 units insulin	27	14	51.9	3	11.1	10	37.0

TABLE 3  
DOSAGE AND TIMING STUDIES

<u>Date:</u> 18 Jan 67	<u>Eggs Incubated:</u> 88
<u>Injection Time:</u> 144 hrs	<u>Eggs Fertile:</u> 66
<u>Dosages:</u> 0.05 ml of 0.9% NaCl 4 units insulin in 0.05 ml	<u>Fertility:</u> 75.0%

TREATED (Insulin)

<u>DAY</u>	<u>NUMBER</u>	<u>DEAD</u>	<u>NORMAL</u>	<u>MICROMELIC</u>
8	5	2	-	3
9	5	3	1	1
10	7	5	-	2
11	11	8	-	3
12	8	4	1	3
13	9	6	-	3
20	10	6	4	-
<u>Totals -</u>	55	34	6	15
<u>Frequency % -</u>		61.8	10.9	27.3

CONTROL (NaCl)

<u>DAY</u>	<u>NUMBER</u>	<u>DEAD</u>	<u>ALIVE (normal)</u>
8	2	2	-
9	2	-	2
10	7	-	7
<u>Totals -</u>	11	2	9
<u>Frequency %</u>		18.2	81.8

TABLE 4  
DOSAGE AND TIMING STUDIES

Date: 19 Apr 67 Eggs Incubated: 162  
Injection Times: 120, 132, 144 hrs Eggs Fertile: 117  
Dosages: 0.05ml of 0.9% NaCl Fertility: 72.2%  
               4 units insulin in 0.05 ml

DOSAGE: 4 units insulin at 120 hrs

<u>DAY</u>	<u>NUMBER</u>	<u>DEAD</u>	<u>NORMAL</u>	<u>MICROMELIC</u>
8	9	4	1	4
9	10	5	1	4
10	31	26	2	3
<u>Totals</u> -	50	35	4	11
<u>Frequency %</u> -		70.0	8.0	22.0

DOSAGE: 4 units insulin at 144 hrs

<u>DAY</u>	<u>NUMBER</u>	<u>DEAD</u>	<u>NORMAL</u>	<u>MICROMELIC</u>
9	14	8	3	3
10	16	4	-	2
13	21	14	4	3
<u>Totals</u> -	41	26	7	8
<u>Frequency %</u> -		63.4	17.1	19.5

DOSAGE: NaCl at 132 hrs

<u>DAY</u>	<u>NUMBER</u>	<u>DEAD</u>	<u>ALIVE</u> (normal)
8	6	2	4
9	6	1	5
10	6	1	5
13	8	1	7
<u>Totals</u> -	26	5	21

TABLE 5DOSAGE AND TIMING STUDIESDate: 3 May 67Eggs Incubated: 133Injection Time: 120 hrsEggs Fertile: 100Dosages: 0.05 ml of 0.9% NaCl  
4 units insulin in 0.05 mlFertility: 75.2%TREATED (Insulin)

<u>DAY</u>	<u>NUMBER</u>	<u>DEAD</u>	<u>NORMAL</u>	<u>MICROMELIC</u>
8	1	-	-	1
9	7	4	2	1
10	3	1	1	1
11	4	3	-	1
12	18	9	4	5
16	26	19	4	3
19	23	16	6	1*
<u>Totals</u>	- 82	52	17	13
<u>Frequency %</u>	-	63.4	20.7	15.9

CONTROLS (NaCl)

<u>DAY</u>	<u>NUMBER</u>	<u>DEAD</u>	<u>ALIVE</u> (normal)
8	4	1	3
9	4	-	4
10	4	1	3
11	4	-	4
12	2	-	2
<u>Totals</u>	- 18	2	16
<u>Frequency %</u>	-	11.1	88.9

\* Specimen showed hyperen-  
cephaly in addition to  
micromelia (fig. 4)

TABLE 6RESULTS OF INJECTION AT PREFERRED DOSE AND TIMEDate: 21 Jun 67Eggs Fertile: 135Eggs Incubated: 179Fertility: 75.4%TREATED (4 units insulin at 132 hrs)

<u>DAY</u>	<u>NUMBER</u>	<u>DEAD</u>	<u>NORMAL</u>	<u>MICROMELIC</u>
8	2	-	-	2
9	10	4	4	2
10	2	-	-	2
11	8	4	1	3
12	11	7	1	3
13	18	12	2 *	4
15	26	20	2	4
20	23	13	4	6
<u>Totals</u> - 100		60	14	26
<u>Frequency %</u> -		60.0	14.0	26.0

\* One of these two embryos exhibited hyperencephaly of apparently spontaneous origin; the limbs appeared quite normal.

..... cont'd

TABLE 6 (cont'd)CONTROLS (0.9% NaCl at 132 hrs)

<u>DAY</u>	<u>NUMBER</u>	<u>DEAD</u>	<u>ALIVE</u> (normal)
8	2	-	2
9	2	-	2
10	4	1	3
11	3	1	2
12	4	1	3
13	5	1	4
15	3	-	3*
20	12	4	8
<u>Totals</u> -	35	8	27
<u>Frequency %</u> -		22.9	77.1

\* One of these embryos displayed exencephaly without any other apparent anatomical malformations, and is seen in fig. 3 .

TABLE 7RESULTS OF INJECTION AT PREFERRED DOSE AND TIMEDate: 8 Nov 67Eggs Fertile: 46Eggs Incubated: 64Fertility: 71.9%TREATED (4 units insulin at 132 hrs)

<u>DAY</u>	<u>NUMBER</u>	<u>DEAD</u>	<u>NORMAL</u>	<u>MICROMELIC</u>
9	2	1	-	1
10	1	-	-	1
11	2	1	-	1
12	23	21	-	2
13	3	2	-	1
<u>Totals</u> -	31	25	0	6
<u>Frequency %</u> -		80.6	0.0	19.4

CONTROLS (0.9% NaCl at 132 hrs)

<u>DAY</u>	<u>NUMBER</u>	<u>DEAD</u>	<u>ALIVE</u>
9	2	1	1
10	1	-	1
11	1	-	1
12	3	1	2
13	1	-	1
<u>Totals</u> -	8	2	6
<u>Frequency %</u> -		25.0	75.0

Note: Only 39 of the 46 fertile eggs were collected, due to incubator failure during the 14th day of incubation.



TABLE 8

RESULTS OF INJECTION AT PREFERRED DOSE AND TIMEDate: 18 Jan 68Eggs Fertile: 107Eggs Incubated: 120Fertility: 89.2%TREATED (4 units insulin at 132 hrs)

<u>DAY</u>	<u>NUMBER</u>	<u>DEAD</u>	<u>NORMAL</u>	<u>MICROMELIC</u>
8	12	6	1	5
9	1	-	-	1
10	4	2	1	1
14	5	4	-	1
15	6	5	-	1
16	18	14	3*	1
17	14	10	-	4
19	10	8	1	1
20	18	18**	-	-
<u>Totals</u> -	88	67	6	15
<u>Frequency %</u> -		76.1	6.8	17.1

\* These three embryos were all slightly smaller than normal embryos of the same age, but showed no evidence of skeletal abnormalities.

\*\* Two of these specimens had apparently died recently (judging by size) and were micromelic.

..... cont'd

TABLE 8 (cont'd)CONTROLS (0.9% NaCl at 132 hrs)

<u>DAY</u>	<u>NUMBER</u>	<u>DEAD</u>	<u>ALIVE</u>
8	3	1	2
9	1	-	1
11	1	-	1
14	1	-	1
15	2	1	1
16	1	-	1
17	4	2	2
20	6	5	1
<u>Totals</u> -	19	9	10
<u>Frequency %</u> -		47.4	52.6

Note: There appears to be an unusually high mortality rate for day 20 embryos of both treated and control groups, as compared to other batches. This may have been the result of some undetected environmental fluctuation during incubation.

TABLE 9

RESULTS OF INJECTION AT PREFERRED DOSE AND TIMEDate: 20 Feb 68Eggs Fertile: 50Eggs Incubated: 59Fertility: 84.7%TREATED (4 units insulin at 132 hrs)

<u>DAY</u>	<u>NUMBER</u>	<u>DEAD</u>	<u>NORMAL</u>	<u>MICROMELIC</u>
17	5	2	1	2
18	1	-	-	1
20	11	8*	1	2
24	25	24**	-	1 (fig. 31)
<u>Totals</u> -	42	34	2	6
<u>Frequency %</u> -		80.9	4.8	14.3

CONTROLS (0.9% NaCl at 132 hrs)

<u>DAY</u>	<u>NUMBER</u>	<u>DEAD</u>	<u>ALIVE</u>
17	3	1	2
18	2	1	1
19	1	-	1
20	2	1	1
<u>Totals</u> -	8	3	5
<u>Frequency %</u> -		37.5	62.5

\* Three of these embryos had died between days 17 and 20.

\*\* These embryos all failed to hatch, and were of varying ages from approximately days 10 to 20.

TABLE 10RESULTS OF INJECTION AT PREFERRED DOSE AND TIMEDate: 23 May 68Eggs Fertile: 44Eggs Incubated: 51Fertility: 86.3%TREATED (4 units insulin at 132 hrs)

<u>DAY</u>	<u>NUMBER</u>	<u>DEAD</u>	<u>NORMAL</u>	<u>MICROMELIC</u>
8	3	1	1*	1
9	3	-	2	1
12	1	-	-	1
13	8	7	-	1
15	4	1	-	3
18	1	-	-	1
20	13	10	2	1
<u>Totals</u> -	33	19	5	9
<u>Frequency %</u> -		57.6	15.1	27.3

\* This embryo was slightly dwarfed in overall body size, but did not display any of the micromelic features characteristic of insulin treatment.

..... cont'd

TABLE 10 (cont'd)CONTROLS (0.9% NaCl at 132 hrs)

<u>DAY</u>	<u>NUMBER</u>	<u>DEAD</u>	<u>ALIVE</u>
8	1	-	1
9	1	-	1
10	1	-	1
11	2	-	2
12	1	-	1
13	1	-	1
15	3	-	3
18	1	-	1
<u>Totals</u> - 11		0	11
<u>Frequency %</u> -		0.0	100.0

TABLE 11POOLED RESULTS OF ALL EGGS INJECTED AT 132 HOURSTREATED (4 units insulin in 0.05 ml)

<u>REFERENCE</u>	<u>NUMBER</u>	<u>DEAD</u>	<u>NORMAL</u>	<u>MICROMETIC</u>
Table 6	100	60	14	26
Table 7	31	25	0	6
Table 8	88	67	6	15
Table 9	42	34	2	6
Table 10	33	19	5	9
<u>Totals -</u>	294	205	27	62
<u>Frequency % -</u>		69.7	9.2	21.1

CONTROLS (0.05 ml of 0.9% NaCl)

<u>REFERENCE</u>	<u>NUMBER</u>	<u>DEAD</u>	<u>ALIVE</u>
Table 6	35	8	27
Table 7	8	2	6
Table 8	19	9	10
Table 9	8	3	5
Table 10	11	0	11
<u>Totals -</u>	81	22	59
<u>Frequency % -</u>		27.2	72.8

TABLE 12  
TIBIOTARSUS LENGTHS

TREATED EMBRYOS

<u>Day of Incubation</u>	<u>Measured Lengths (mm)</u>					<u>Mean Length (mm)</u>
8	1.9	2.3	2.3	2.4	2.5	2.28
9	3.0	3.5	4.0	4.0	4.9	3.88
10	3.0	3.2	3.5	3.8	4.5	3.60
11	3.2	3.3	3.8	4.8	4.9	4.00
12	4.8	5.2	5.5	5.7	6.1	5.46
13	3.9	5.5	5.6	5.7	6.5	5.44
15	4.6	5.0	5.4	8.5	8.6	6.42
17	6.9	7.4	9.5	10.0	10.9	8.94
20	12.2	13.0	13.0	15.7	16.6	14.10

CONTROL EMBRYOS

<u>Day of Incubation</u>	<u>Measured Lengths (mm)</u>					<u>Mean Length (mm)</u>
8	4.0	4.1	4.2	4.4	4.6	4.26
9	5.9	6.0	6.2	6.4	7.1	6.32
10	7.1	7.1	8.3	8.6	8.7	7.96
11	8.9	9.5	9.6	9.7	11.4	9.82
12	10.4	10.7	11.2	11.8	12.1	11.24
13	12.2	13.2	13.5	13.5	14.1	13.30
15	16.5	16.9	17.1	17.2	19.4	17.42
17	21.1	21.9	22.0	23.0	23.2	22.24
20	26.4	27.0	28.0	28.0	28.5	27.58

TABLE 14

CELL/MATRIX STUDIES: INSULIN-TREATED TIBIOTARSI

<u>Day of Incubation</u>	<u>Cells per 10,000 <math>\mu^2</math></u>	<u>Mean Cell Diameter (<math>\mu</math>)</u>	<u>Total Cell Area in 10,000 <math>\mu^2</math></u>	<u>Total Matrix Area in 10,000 <math>\mu^2</math></u>	<u>Amount of Matrix/Cell (<math>\mu^2</math>)</u>
8	29.3 (N=450) *	13.3 (N=40) *	4232	5768	215
9	21.0 (N=470)	15.7 (N=40)	4083	5917	283
10	23.8 (N=635)	16.1 (N=40)	4886	5114	221
11	25.4 (N=564)	16.5 (N=40)	5524	4476	178
12	22.1 (N=536)	16.5 (N=40)	4595	5405	268
13	21.8 (N=534)	16.5 (N=40)	4680	5320	249
15	25.7 (N=530)	15.8 (N=40)	4982	5018	196
17	16.8 (N=419)	19.9 (N=30)	5197	4803	292
20	20.2 (N=462)	17.9 (N=40)	4989	5011	276
<u>Mean Values:</u>					
	22.9	16.5	4796	5204	242

\* N = number of cells counted or measured



TABLE 13

CELL/MATRIX STUDIES: CONTROL TIBIOTARSI

<u>Day of Incubation</u>	<u>Cells per 10,000 <math>\mu^2</math></u>	<u>Mean Cell Diameter (<math>\mu</math>)</u>	<u>Total Cell Area in 10,000 <math>\mu^2</math></u>	<u>Total Matrix Area in 10,000 <math>\mu^2</math></u>	<u>Amount of Matrix/Cell (<math>\mu^2</math>)</u>
8	20.3 (N=579) *	15.8 (N=40) *	3939	6061	307
9	18.5 (N=445)	17.0 (N=40)	4175	5825	318
10	18.8 (N=474)	16.8 (N=40)	4202	5798	316
11	17.2 (N=433)	17.5 (N=40)	4142	5858	351
12	17.3 (N=437)	17.0 (N=40)	3968	6032	357
13	18.4 (N=441)	18.4 (N=40)	4014	5986	326
15	15.0 (N=400)	17.9 (N=40)	3754	6246	429
17	18.9 (N=454)	17.2 (N=40)	4350	5650	300
20	17.7 (N=468)	17.9 (N=40)	4320	5680	337
<u>Mean Values:</u>					
	18.0	17.3	4096	5904	338

\* N = number of cells counted or measured

TABLE 15  
COMPARISON OF MEAN VALUES FROM TABLES 13 AND 14

	<u>Control</u>	<u>Insulin-Treated</u>	<u>SE<sub>diff</sub></u>	<u>diff/SE<sub>diff</sub></u>
Cells/10,000 $\mu^2$	18.0	22.9	0.05	98.0
Mean Cell Diameter in $\mu$	17.3	16.5	0.093	8.6
Matrix/Cell ( $\mu^2$ )	338	242	18.7	5.1
Total Cell Area in 10,000 $\mu^2$	4096	4796		
Total Matrix Area in 10,000 $\mu^2$	5904	5204		

diff = difference between means

SE<sub>diff</sub> = standard error of the difference between means

## BIBLIOGRAPHY

- Altman, P.L. and Dittmer, D.S., comp. and ed. 1968. Metabolism. Biological Handbooks. Federation of American Societies for Experimental Biology. Bethesda, Maryland. 737 pp.
- Anderson, C.E., Crane, J.T. and Harper, H.A. 1959. Alterations in growth-cartilage in experimental dwarfism. I. Studies on insulin-dwarfed chicks. J. Bone Joint Surg. 41-A: 1094-1100.
- Arstila, A.U. and Trump, B.F. 1968. Studies on cellular autophagocytosis. The formation of autophagic vacuoles in the liver after glucagon administration. Amer. J. Path. 53: 687-733.
- Barbieri, M. and Bonetti, D. 1953. Condro-osteo-distrofia da trattamento insulinico nello sviluppo embrionale. Ricerche su embrioni di pollo. Minerva Ortopedica 4: 13-21.
- Barka, T. and Anderson, P.J. 1965. Histochemistry: Theory, Practice and Bibliography. Harper and Row, New York.
- Bélanger, L.F. and Hartnett, A. 1960. Persistent toluidine blue metachromasia. J. Histochem. Cytochem. 8: 75.
- Best, F. 1906. Über Karminfärbung des Glykogens und der Kerne. Zeitschr. Mikroskopie 23: 319-322.
- Brandes, D., Buetow, D.E., Bertini, F. and Malkoff, D.B. 1964. Role of lysosomes in cellular lytic processes. I. Effect of carbon starvation in Euglena gracilis. Exp. Molec. Path. 3: 583-609.
- Brinsmade, A., Büchner, F. and Rubsaamen, H. 1956. Missbildungen am Kaninchenembryo durch Insulininjektion beim Muttertier. Naturwiss 43: 259.
- Brown, W.H. and Pearce, L. 1945. Hereditary achondroplasia in the rabbit. I. Physical appearance and general features. J. Exp. Med. 82: 241-260

- Burdi, A.R. and Flecker, K. 1968. Differential staining of cartilage and bone in the intact chick embryonic skeleton in vitro. Stain Technol. 43: 47-48.
- Chen, J.M. 1954. The effect of insulin on embryonic limb-bones cultivated in vitro. J. Physiol. 125: 148-162.
- Chomette, G. 1955. Entwicklungsstörungen nach Insulinschock beim trächtigen Kaninchen. Beitr. pathol. Anat. 115: 439-451.
- Crary, D.D. and Sawin, P.B. 1963. Morphogenetic studies of the rabbit. XXXII. Qualitative skeletal variations induced by the ac gene (achondroplasia). Amer. J. Anat. 113: 9-23.
- Davenport, H.A. 1960. Histological and Histochemical Technics. W.B. Saunders, Philadelphia, Pennsylvania.
- Dawson, A.B. 1926. A note on the staining of the skeleton of cleared specimens with alizarin red S. Stain Technol. 1: 123-124.
- De Bastiani, G. and Lunardo, C. 1956a. Ricerche sul meccanismo di azione teratogena dell'insulina sulle ossa lunghe di embrioni di pollo. Clinica Ortopedica 8: 109-119.
- De Bastiani, G. and Lunardo, C. 1956b. Azione teratogena del metilandrosterndiolo raffrontata a quella insulinica nelle ossa lunghe di embrioni di pollo. Clinica Ortopedica 8: 128-133.
- Drury, R.A.B. and Wallington, E.A. 1967. Carleton's Histological Technique. 4th ed. Oxford U. Press, London. 432 pp.
- Duraiswami, P.K. 1950. Insulin-induced skeletal abnormalities in developing chickens. Brit. Med. J. II: 384-390.
- Duraiswami, P.K. 1952. Experimental causation of congenital skeletal defects and its significance in orthopaedic surgery. J. Bone Joint Surg. 34-B: 646-698.
- Duraiswami, P.K. 1955. Comparison of congenital defects induced in developing chickens by certain teratogenic agents with those caused by insulin. J. Bone Joint Surg. 37-A: 277-294.

- Elmer, W.A. 1968. Experimental analysis of the Creeper condition in chickens. Effect of embryo extract on elongation, protein content, and incorporation of amino acids by cartilaginous tibiotarsi. *Develop. Biol.* 18: 76-92.
- Erhard, R. 1959. Untersuchungen über die Insulinmikromelie am Hühnerembryo. *Roux' Arch. Entwickl.-Mech. Org.* 151: 381-429.
- Fell, H.B. 1925. The histogenesis of cartilage and bone in the long bones of the embryonic fowl. *J. Morph. Physiol.* 40: 417-459.
- Fell, H.B. and Canti, R.G. 1934. Experiments on the development in vitro of the avian knee-joint. *Proc. Roy. Soc. Lond. ser. B.* 116: 316-351.
- Fell, H.B. and Landauer, W. 1935. Experiments on skeletal growth and development in vitro in relation to the problem of avian phocomelia. *Proc. Roy. Soc. Lond. ser. B.* 118: 133-154.
- Fell, H.B. and Robison, R. 1934. The development of the calcifying mechanism in avian cartilage and osteoid tissue. *Biochem. J.* 28: 2243-2253.
- Fisher, A.M. 1955. Insulin preparations. *Can. Med. Assoc. J.* 73: 1-8.
- Follis, R.H. Jr. and Berthrong, M. 1949. Histochemical studies on cartilage and bone. I. The normal pattern. *Bull. John Hopkins Hosp.* 85: 281-297.
- Gendre, H. 1938. Le glycogène dans les cartilages en voie d'ossification. *Bull. Histol. appl.* 15: 165-178.
- Gibson, M.A. 1966. A technique for the demonstration of endochondral ossification. *Can. J. Zool.* 44: 496-498.
- Gitlin, D., Kumate, J. and Morales, C. 1965. On the transport of insulin across the human placenta. *Pediatrics* 35: 65-69.
- Glucksmann, A. 1942. The role of mechanical stresses in bone formation in vitro. *J. Anat.* 76: 231-239.

- Godman, G.C. and Lane, N. 1966. On the site of sulfation in the chondrocyte. *J. Cell Biol.* 21: 353-366.
- Gomori, G. 1952. Microscopic Histochemistry. U. of Chicago Press, Chicago, Illinois.
- Grillo, T.A.I. 1961. The ontogeny of insulin secretion in the chick embryo. *J. Endocrin.* 22: 285-292.
- Gruenwald, P. 1956. Environmental causes of abnormal embryonic development. *Clin. Orthop.* 8: 13-19.
- Grüneberg, H. 1963. The Pathology of Development. A study of inherited skeletal disorders in animals. J. Wiley and Sons, New York.
- Haardick, H. 1941. Wachstumsstufen in der Embryonalentwicklung des Hühnchens. *Biol. generalis (Wien)* 15: 31.
- Haines, R.W. 1942. The evolution of epiphyses and of endochondral bone. *Biol. Rev. Camb. Phil. Soc.* 17: 267-292.
- Halmi, N.S. 1952. Differentiation of two types of basophils in the adenohypophysis of the rat and the mouse. *Stain Technol.* 27: 61-64.
- Harris, H.A. 1932. Glycogen in cartilage. *Nature* 130: 996-997.
- Hay, M.F. 1958. The effect of growth hormone and insulin on limb-bone rudiments of the embryonic chick cultivated in vitro. *J. Physiol.* 144: 490-504.
- Henrichsen, E. 1956. Alkaline phosphatase and the calcification in tissue cultures. *Exp. Cell Res.* 11: 403-416.
- Henrichsen, E. 1958a. Bone formation and calcification in cartilage. *Acta orthop. Scand.* 27: 173-191.

- Henrichsen, E. 1958b. Alkaline phosphatase and calcification. Histochemical investigations on the relationship between alkaline phosphatase and calcification. Acta orthop. Scand. suppl. 34.
- Hotchkiss, R.D. 1948. A microchemical reaction resulting in the staining of polysaccharide structures in fixed tissue preparations. Arch. Biochem. 16: 131-141.
- Hutt, F.B. and Greenwood, A.W. 1929a. Studies in embryonic mortality in the fowl. II. Chondrodystrophy in the chick. Proc. Roy. Soc. Edin. 49: 131-144.
- Hutt, F.B. and Greenwood, A.W. 1929b. Studies in embryonic mortality in the fowl. III. Chick monsters in relation to embryonic mortality. Proc. Roy. Soc. Edin. 49: 145-155.
- Jeanloz, R.W. 1960. The nomenclature of mucopolysaccharides. Arthritis Rheum. 3: 233-237.
- Johnson, A. 1883. On the development of the pelvic girdle and skeleton of the hind limb in the chick. Quart. J. Micr. Sci. 23: 399-411.
- Josimovich, J.B. and Knobil, E. 1961. Placental transfer of I<sup>131</sup>-insulin in the rhesus monkey. Amer. J. Physiol. 200: 471-476.
- Keller, J.M. and Krohmer, J.S. 1968. Insulin transfer in the isolated human placenta. Obstet. Gynecol. 32: 77-80.
- Kóssa, J. von. 1901. Ueber die im Organismus künstlich erzeugbaren Verkalkungen. Beitr. pathol. Anat. 29: 163-202.
- Krahl, M.E. 1961. The Action of Insulin on Cells. Academic Press, New York.
- Lamoreux, W.F. 1942. Hereditary chondrodystrophy in the fowl. J. Heredity 33: 275-283.

- Landauer, W. 1927. Untersuchungen über chondrodystrophie. I. Allgemeine Erscheinungen und Skelett Chondrodystrophischer Hühnerembryonen. Roux' Arch. Entwickl.-Mech. Org. 110: 195-282.
- Landauer, W. 1931. Untersuchungen über das Krüperhuhn. II. Morphologie und Histologie des Skelets, insbesondere des Skelets der langen Extremitätenknochen. Zeitschr. Mikr. Anat. Forschung. 25: 115-180.
- Landauer, W. 1932. Studies on the Creeper fowl. III. The early development and lethal expression of homozygous Creeper embryos. J. Genetics 25: 367-394.
- Landauer, W. 1945. Rumplessness of chicken embryos produced by the injection of insulin and other chemicals. J. Exp. Zool. 98: 65-77.
- Landauer, W. 1947a. Insulin-induced abnormalities of beak, extremities and eyes in chickens. J. Exp. Zool. 105: 145-173.
- Landauer, W. 1947b. Potentiating effects of adrenal cortical extract on insulin-induced abnormalities of chick development. Endocrinology 41: 489-493.
- Landauer, W. 1948. The effect of nicotinamide and  $\alpha$ -ketoglutaric acid on the teratogenic action of insulin. J. Exp. Zool. 109: 283-290.
- Landauer, W. 1951. The effect of insulin on development of duck embryos. J. Exp. Zool. 117: 559-571.
- Landauer, W. 1952. Malformations of chicken embryos produced by boric acid and the probable role of riboflavin in their origin. J. Exp. Zool. 120: 469-508.
- Landauer, W. 1953. The effect of time of injection and of dosage on absolute and relative length of femur, tibiotarsus and tarsometatarsus in chicken embryos treated with insulin or pilocarpine. Growth 17: 87-109.



- Landauer, W. and Bliss, C.I. 1946. Insulin-induced rumplessness of chickens. III. The relationship of dosage and of developmental stage at time of injection to response. *J. Exp. Zool.* 102: 1-22.
- Landauer, W. and Clark, E.M. 1963. Interaction of insulin and chlorpromazine in teratogenesis. *Nature* 198: 215-216.
- Landauer, W. and Clark, E.M. 1964. Uncouplers of oxidative phosphorylation and teratogenic activity of insulin. *Nature* 204: 285-286.
- Landauer, W. and Dunn, L.C. 1925/26. Chondrodystrophia in chicken embryos. *Proc. Soc. Exp. Biol. Med.* 23: 562-566.
- Landauer, W. and Lang, E.H. 1946. Insulin-induced rumplessness of chickens. II. Experiments with inactivated and reactivated insulin. *J. Exp. Zool.* 101: 41-50.
- Landauer, W. and Rhodes, M.B. 1952. Further observations on the teratogenic nature of insulin and its modification by supplementary treatment. *J. Exp. Zool.* 119: 221-261.
- Lhotka, J.F. Jr. and Anderson, J.W. 1968. The dual histochemical approach for glycogen. Presented at the Third International Congress of Histochemistry and Cytochemistry. 18-22 August. New York, New York.
- Lichtenstein, H., Guest, G.M. and Warkany, J. 1951. Abnormalities in offspring of white rats given protamine zinc insulin during pregnancy. *Proc. Soc. Exp. Biol. Med.* 78: 398-402.
- Lillie, R.D. 1965. Histopathologic Technic and Practical Histochemistry. 3rd. ed. McGraw-Hill, New York.
- Lorch, I.J. 1946. Demonstration of phosphatase in decalcified bone. *Nature* 158: 269.
- Matukas, V.J. and Krikos, G.A. 1968. Evidence for changes in protein polysaccharide associated with the onset of calcification in cartilage. *J. Cell Biol.* 39: 43-48.

- McManus, J.F.A. 1946. Histological demonstration of mucin after periodic acid. *Nature* 158: 202.
- Palmgren, A. 1954. Tape for microsectioning of very large, hard or brittle specimens. *Nature* 174: 46.
- Pappas, A.M. 1968. Experimental congenital malformations of the motorskeletal system. *Clin. Orthop.* 59: 249-276.
- Parhon, C.I., Laurian, L., Bălăceanu, M. and Albu-Aderca, N. 1956. L'embryogénèse Dirigée. Note V. L'action de l'insuline sur le développement embryonnaire chez la poule (cataracte congénitale et achondroplasie). *Rev. Sci. Med.* I: 5-45.
- Patten, A.R. 1937. A comparison of the glycine content of the proteins of normal and chondrodystrophic chick embryos at different stages of development. *J. Nutrition* 13: 123-126.
- Pearce, L. and Brown, W.H. 1945. Hereditary achondroplasia in the rabbit. II. Pathologic aspects. *J. Exp. Med.* 82: 261-280.
- Pearse, A.G.E. 1961. Histochemistry. Theoretical and Applied. 2nd ed. J. & A. Churchill, London. 998 pp.
- Pritchard, J.J. 1952. A cytological and histochemical study of bone and cartilage formation in the rat. *J. Anat.* 86: 259-277.
- Quintarelli, G., Scott, J.E. and Dellovo, M.C. 1964. The chemical and histochemical properties of Alcian Blue. II. Dye binding of tissue polyanions. *Histochemie* 4: 86-98.
- Rang, M. (ed.) 1969. The Growth Plate and Its Disorders. E. & S. Livingstone, Edinburgh.
- Ravetto, C. 1964. Alcian blue-alcian yellow: a new method for the identification of different acidic groups. *J. Histochem. Cytochem.* 12: 44-45.
- Robison, R. 1923. The possible significance of hexosephosphoric esters in ossification. *Biochem. J.* 17: 286-293.

- Romanoff, A.L. 1960. The Avian Embryo. Structural and Functional Development. Macmillan, New York.
- Rouget, C. 1859. Des substances amyloides et de leur rôle dans la constitution des tissus des animaux. *J. Physiol. de l'Homme et des Animaux* 2: 308-325.
- Schajowicz, F. and Cabrini, R.L. 1958. Histochemical studies on glycogen in normal ossification and calcification. *J. Bone Joint Surg.* 40A: 1081-1092.
- Scott, H.R. 1952. Rapid staining of beta cell granules in pancreatic islets. *Stain Technol.* 27: 267-268.
- Sevastikoglou, J.A. 1963a. Insulin induced micromelia in chickens. I. Morphological study. *Acta orthop. Scand.* 33: 271-281.
- Sevastikoglou, J.A. 1963b. Insulin induced micromelia in chickens. II. Biochemical study. *Acta orthop. Scand.* 33: 282-290.
- Shepard, T.H., Fry, L.R. and Moffett, B.C. Jr. 1969. Microscopic studies of achondroplastic rabbit cartilage. *Teratology* 2: 13-22.
- Sledge, C.B. 1966. Some morphologic and experimental aspects of limb development. *Clin. Orthop.* 44: 241-264.
- Smithberg, M. and Runner, M.N. 1963. Teratogenic effects of hypoglycemic treatments in inbred strains of mice. *Amer. J. Anat.* 113: 479-489.
- Spicer, S.S., Horn, R.G. and Leppi, T.J. 1967. Histochemistry of connective tissue mucopolysaccharides. In *International Academy of Pathology, Monograph No. 7: The Connective Tissue.* ed. B.M. Wagner and D.E. Smith. pp. 251-303.
- Stanley, J. 1963. The Essence of Biometry. McGill U. Press, Montreal. 147 pp.

- Steedman, H.F. 1950. Alcian blue 8GS: a new stain for mucin. *Quart. J. Micr. Sci.* 91: 477-479.
- Thompson, S.W. 1966. Selected Histochemical and Histopathological Methods. Charles C. Thomas, Springfield, Illinois.
- Walker, B.E. 1961. The association of mucopolysaccharides with morphogenesis of the palate and other structures in mouse embryos. *J. Embryol. exp. Morph.* 9: 22-31.
- West, E.S., Todd, W.R., Mason, H.S. and Van Bruggen, J.T. 1966. Textbook of Biochemistry. 4th ed. Macmillan, New York. 1595 pp.
- Wickes, I.G. 1954. Foetal defects following insulin coma therapy in early pregnancy. *Brit. Med. J.* II: 1029-1030.
- Zwilling, E. 1948a. Insulin hypoglycemia in chick embryos. *Proc. Soc. Exp. Biol. Med.* 67: 192.
- Zwilling, E. 1948b. Association of hypoglycemia with insulin micromelia in chick embryos. *J. Exp. Zool.* 109: 197-214.
- Zwilling, E. 1949. Reversal of insulin-induced hypoglycemia in chick embryos by nicotinamide and  $\alpha$ -ketoglutaric acid. *Proc. Soc. Exp. Biol. Med.* 71: 609-612.
- Zwilling, E. 1951. Carbohydrate metabolism in insulin-treated chick embryos. *Arch. Biochem. Biophys.* 33: 228-242.
- Zwilling, E. 1959. Micromelia as a direct effect of insulin — evidence from in vitro and in vivo experiments. *J. Morph.* 104: 159-179.
- Zwilling, E. and DeBell, J.T. 1950. Micromelia and growth retardation as independant effects of sulfanilamide in chick embryos. *J. Exp. Zool.* 115: 59-81.